Scuola Normale Superiore

CLASSE DI SCIENZE MATEMATICHE, FISICHE E NATURALI
PhD program in Neuroscience

PhD Thesis:

Bidirectional Neuron-Glioma Interactions: Effects of Glioma Cells on Synaptic Activity and its Impact on Tumor Growth

Candidate: Elena Tantillo
Supervisors: Prof. Matteo Caleo
Dr. Chiara Maria Mazzanti

Index

Abstract

Gliomas grow in a neuronal environment, but the interactions between glioma cells and peritumoral neurons remain poorly understood. Understanding this complex relationship could add useful information to develop more effective therapeutic approaches for the treatment of this deadly disease. In recent years, the interaction between cancer cells and tumor microenvironment has emerged as one important regulator of tumor progression. Thus, my thesis aimed to investigate the crosstalk between neural peritumoral tissue and glioma cells; in particular, I assessed i) functional impairments of peritumoral tissue occurring during tumor progression and ii) the impact of neural activity on glioma proliferation.

To monitor longitudinal changes in network activity, I recorded visual evoked potentials (VEP) and local field potentials (LFP) after transplant of GL261 glioma cells (or PBS) in mouse visual cortex. Gliomas were injected in visual cortex to allow a detailed investigation of peritumoral neurons using several physiological parameters. Thanks to this analysis, I detected a progressive deterioration of VEP amplitudes along with tumor progression and changes in the LFP power spectra typical of focal epilepsy, with an increase of the power of delta band and the deterioration of alpha rhythm in glioma-bearing mice. To understand the molecular alterations that underlie these perturbed patterns of neuronal activity, I analysed the gene expression profile of microdissected peritumoral pyramidal neurons in the cortical superficial layers (i.e., II-III). The data were clear in indicating that glioma induces alterations in both pre- and post-synaptic markers, demonstrating that its progression shapes the network activity of peritumoral areas towards hyperexcitability. Indeed, I recorded the occurrence of seizures in a subset of glioma-bearing animals, finding alterations in the LFP power spectra just before the onset of ictal events.

To investigate how levels of cortical activity affects tumor cell proliferation, I inoculated GL261 glioma cells into the mouse neocortex and modulated neuronal activity by different methods. Second, I dissected the role of inhibitory and excitatory circuitries on tumor proliferation and I found that while the activation of excitatory networks exacerbate glioma proliferation (confirming the data in literature), inhibitory circuits decrease GL261 cell proliferation. Based on these data, I investigated whether a sensory stimulation of the visual cortex may also impact on tumor growth. I found that a reduction of visual cortical activity via Dark Rearing enhanced the density of proliferating glioma cells, while a Visual

Stimulation had the opposite effect. Intriguingly the effect was region-specific, as visual deprivation had no significant effect on glioma proliferation in motor cortex. I found that local blockade of neurotransmission via administration of the synaptic blocker botulinum neurotoxin A (BoNT/A) enhances glioma cell proliferation, underlying the importance of neural activity in controlling glioma progression. In addition, the stimulation with visual patterns combined with temozolomide treatment delayed the deterioration of visual responses induced by glioma growth. Altogether, these data demonstrate complex effects of different neuronal subtypes and afferent sensory input in the control of glioma proliferation.

Introduction

1.1. Gliomas

The treatment of gliomas represents one of the hardest challenge of our times for neuro-oncologists. Despite most neoplastic brain lesions derives from metastases of cancers outside the central nervous system (Gavrilovic and Posner, 2005), gliomas are among the most common primary brain tumors in adult and children (Ferlay et al., 2010; Ostrom et al., 2016), accounting for almost 30% of all primary brain tumors and 80% of all malignant ones (Weller et al., 2015). Although therapies are in continuous development, these tumors remain associated with high morbidity and mortality (Burnet et al., 2007). The name 'glioma' reflects the histomorphological resemblance of tumor cells with those of glial lineages in the normal brain, such as astrocytes and oligodendroglia, which has been regarded, for a long time, as the only proliferating cells in the mature brain (Jones et al., 2012). For the past century, the classification of brain tumors has been based largely on their histogenesis including cellularity, mitotic activity, nuclear atypia, vascularity and necrosis; thus, tumors have been classified according to their microscopic similarities with different putative cells of origin and their presumed levels of differentiation (Louis et al., 2016). Nowadays, the most used and known classification is the international classification published by the World Health Organization (WHO) with a specific aim: to establish a classification and grading of human tumours that is accepted and used worldwide (Louis et al., 2007).

The classical WHO classification grades brain tumors on a WHO consensus-derived scale of I to IV, according to their degree of malignancy as

judged by various histological features accompanied by genetic alterations (Louis et al., 2007). Grade I tumors are biologically benign and can be surgically removed; grade II tumors are low-grade malignancies that may follow long clinical courses, but early diffuse infiltration of the surrounding brain renders them incurable by surgery; grade III tumors exhibit increased anaplasia and proliferation over grade II tumors and are more rapidly fatal; grade IV tumors exhibit more advanced features of malignancy including vascular proliferation and necrosis and are recalcitrant to radio/chemotherapy (Furnari et al., 2007).

The most common gliomas affecting the cerebral hemispheres are classified in the “diffuse” type due to the ability to infiltrate through the brain parenchyma (Wesseling et al., 2011). Individual tumor cells can spread along white-matter tracts of the cerebrum, sometimes crossing the corpus callosum, entrapping neurons, clustering around small vessels or accumulate in the subpial space (Louis et al., 2007). Based on histopathological analysis, these gliomas are diagnosed as diffuse astrocytomas, with glioblastoma (GB) as its most malignant form, oligodendrogliomas or oligoastrocytomas, classified as II, III or IV WHO grades(Louis et al., 2007, 2016; Perry and Wesseling, 2016). Across the years, the WHO classification has undergone a substantial evolution breaking with the century-old principle of diagnosis, integrating genetic and molecular parameters in the classification methods which, in some cases, override the classical histological features (Louis et al., 2016; Wesseling and Capper, 2018). For instance, the detection of genetic mutations, as in isocitrate dehydrogenase 1 and 2 (IDH1/IDH2) (Yan et al., 2009), in association with the 1p/19q codeletion, determine a new method of classification (Wesseling and Capper, 2018). So, even if a tumour has the histological appearance of an astrocytoma, detection of

complete 1p/19q codeletion leads to the diagnosis of oligodendroglioma, IDH-mutant and 1p/19q-codeleted (Perry et al., 2016; Wood et al., 2019).

1.1.1. Glioblastoma (GB)

The 60-70% of all gliomas is represented by GB, the most lethal tumor of the CNS, classified as a WHO grade IV tumor due to its histopathological features (Louis et al., 2016). Glioblastoma presents significant intratumoral heterogeneity at cytopathological, transcriptional and genomic levels and this complexity has conspired to make GB one of the most difficult cancer to understand and to treat (Furnari et al., 2007). Typical histological features of GB include regions of necrosis, microvascular proliferation, abundant mitosis and pleiomorphic cells (Wen and Kesari, 2008). According to recent discoveries, GBs are now subdivided on the basis of the mutational state of isocitrate dehydrogenase (IDH) genes in: IDH wild type, which most frequently corresponds with the clinically defined primary or *de novo* GB; IDH mutant, which corresponds to the secondary GB; those not otherwise specified (NOS), for which the IDH status could not be determined (Louis et al., 2016; Verhaak et al., 2010). The 90% of GB are primary IDH-wildtype tumors with a rapid clinical presentation, while the remainder (about 10%) are mostly IDH-mutant tumors, typically arising from lower grade infiltrating astrocytomas (Wood et al., 2019). Although the molecular features of IDH-wildtype glioblastoma have been studied extensively, the prognosis remains poor (Ceccarelli et al., 2016; Ostrom et al., 2016). Some common mutations that represent frequent gene signatures in human GB used for clinical classification are those in TP53, PTEN, NF1, ERBB2, RB1, PIK3R1 and PIK3CA genes (McLendon et al., 2008). The mentioned

cancer-associated genes represents a core set of pathways that are commonly deregulated in glioblastoma, including growth factor signalling (receptor tyrosine kinase (RTK)/phosphatidylinositide 3-kinase (PI3K)/Ras), p53, and Rb signalling pathways. Moreover, amplification of EGFR (epidermal growth factor receptor) gene is frequent in primary glioblastomas as well as the methylation of the O6-methylguanine-DNA methyltransferase (MGMT) promoter that occurs in about 50% of glioblastoma cases (Louis et al., 2016; Shinojima et al., 2003). Other cellular processes deregulated in GB could be exploited for diagnostic and prognostic applications as the homeostatic pathways (Franceschi et al., 2018). Altogether, these alterations lead to aberrant signalling in proliferation, cell cycle regulation, senescence and apoptosis, underscoring the importance of such pathways in tumorigenesis (Brennan et al., 2013; McLendon et al., 2008). Different clinically relevant GB subtypes (proneural, neural, classical, and mesenchymal), are identified on the basis of the gene expression profiles together with somatic alterations (Brennan et al., 2013; Franceschi et al., 2015; Verhaak et al., 2010).

Despite the growing experimental investigation in this field and the improved therapeutic strategies (see **section 1.2**), GB remains essentially incurable, with an overall survival time ranging from 12 to 18 months, and a five-year relative survival following diagnosis of 6.8% (Ostrom et al., 2016, 2019). An important factor that limits the identification of an efficient GB treatment is the high cellular and genetic heterogeneity because the tumor cells that form GB mass, although belonging to the same patient, are not genetic phenocopies (Patel et al., 2014). Moreover, the cellular origin of gliomas remains a topic to debate. Although glioblastomass from human patients contain different types of driver mutations that may represent diverse subtypes, the contribution of the cell

of origin remain unknown. The cell of origin can be an important determinant of tumour phenotype and genotype in GB, and thus plays an important role in its malignant behaviour (Llaguno and Parada, 2016). In the past years, one hypothesis was that gliomas arise from neoplastic transformation and dedifferentiation of mature glial cells, astrocytes, oligodendrocytes, ependymal cells or their precursors (Martin-Villalba et al., 2008). Nowadays, the most accredited hypothesis places the origin of high-grade gliomas, in adult neural stem and progenitor cells (Llaguno and Parada, 2016). In particular, the subventricular zone (SVZ) of the lateral ventricles is identified as the likely neurogenic region it may give rise to the cells of origin of GB (Alcantara Llaguno et al., 2009). It has been demonstrated that astrocyte-like neural stem cells (NSCs) of the SVZ could carry driver mutations that stimulate the development of glioma, migrating from the SVZ to distant sites of the brain (Lee et al., 2018). To support this idea, more differentiated neuronal cells showed reduced abilities in forming a tumor mass, demonstrating that increasing lineage restriction is an impediment to glioma formation (Alcantara Llaguno et al., 2019). Altogether, these advances attempt to clarify dynamic changes of tumor composition for a more accurate classification and the setting up of specific treatments (Alcantara Llaguno et al., 2019).

1.2. Therapies

The standard of care of glioblastoma consists in maximal safe surgical resection followed by radiotherapy (RT) with concurrent and adjuvant chemotherapy (Temozolomide, TMZ). However, none all the accepted treatments are of real efficacy for the patients, due to the high rate of

recurrence, overall resistance and devastating neurological deterioration provoked by GB (Bahadur et al., 2019; Kim et al., 2015; Lin et al., 2015). Surgery alleviates symptoms of mass compression and provides material for diagnosis and molecular analysis, improving overall and progression-free survival (Brown et al., 2016). In addition, surgical excision provides an opportunity to apply some therapies during the procedure as implantation of chemotherapeutic agents and photodynamic therapy which have a promising outcome (Jain, 2018). However, the tumor removal does not eliminate the microscopic foci of neoplastic cells that invade the surrounding normal brain substance beyond the main tumor mass, provoking the 90% of recurrences within a two centimetre margin of the primary tumor site (Corso et al., 2017). Novel fluorescence-based technologies have incremented the tumor visualization. For instance, molecular-imaging techniques have been combined with GB targeting agents as Chlorotoxin (CTX)-based bioconjugates to improve tumor diagnosis and imaging (Cohen et al., 2018).

Moreover, fluorescence-guided surgery using 5-aminolevulinic acid allows a more precise resection of glioma mass and a better identification of tumor border, thus prolonging patients' survival(Munteanu et al., 2017; Stummer et al., 2006).

Unfortunately, the association with radiotherapy and chemotherapy cannot completely eradicate GB, since this would require unacceptably high radiation or chemotherapic doses that result in severe brain-neuron damage (Colman et al., 2006; Furnari et al., 2007). Thus, new therapeutic strategies are in continuous development, based on the combination of postoperative radiations with TMZ administration as a backbone on which to add new therapies summarized in the **Table 1** below (Laub et al., 2018; Reitman et al., 2018):

Table 1 ***Systemic therapy approved for recurrent high-grade Gliomas*** *(Laub et al., 2018)*

Systemic Therapy for Recurrent High-Grade Gliomas

Anaplastic Gliomas	Glioblastoma
Temozolomide	Bevacizumab
Lomustine or carmustine	Bevacizumab + chemotherapy (irinotecan, carmustine/ lomustine, temozolomide, or carboplatin)
Combination PCV	Temozolomide
Bevacizumab	Lomustine or carmustine
Bevacizumab + chemotherapy (irinotecan, carmustine/ lomustine, temozolomide, or carboplatin)	Combination PCV
Irinotecan	Platinum-based regimens (carboplatin)
Platinum-based regimens	

Abbreviation: PCV: procarbazine lomustine/carmustine, and vincristine.

In the last years there has been an explosion of research on glioblastoma, with thousands of new clinical trials (Bahadur et al., 2019; Ozdemir-Kaynak et al., 2018); however, no one resulted enough effective in counteracting GB growth, producing a significant increase of patients' survival. Indeed, because of the extreme heterogeneity of these tumors, finding effective therapies is still very challenging.

The majority of clinical trials are focused on systemic therapies, as opposed to surgical or radiotherapeutic treatments (Cihoric et al., 2017). Whereas targeted drug therapies are focused on the abnormal molecular and cytogenic pathways that affect tumor growth, invasion, angiogenesis and cell death (Roy et al., 2015), other clinical strategies are focused on immunotherapies, such as switching check-point inhibitors (i.e., pembrolizumab and nivolumab) (Reardon et al., 2017). In addition, other clinical trials are examining the role of vaccines, such as dendritic cell or anti-EGFR (O'Rourke et al., 2017), or the use of electrical tumor treating fields (TTF) to inhibit the formation of mitotic spindle (McClelland et al., 2018; Stupp et al., 2017; Wick et al., 2018).

Although the histological analysis remains essential in the diagnosis of gliomas, the methylation status of MGMT promoter has been recently identified as a potential determinant of chemotherapic treatment failure in glioblastoma (Wick et al., 2014). Indeed, while high levels of MGMT activity in cancer cells create a resistant phenotype by blunting the therapeutic effect of chemotherapy, the epigenetic silencing of the MGMT gene is associated with a diminished DNA-repair activity (Morandi et al., 2010; Wick et al., 2018).

Despite all studies lead on discovering new therapeutic targets or aimed at creating novel therapeutic approaches, the majority of the current proposed treatments have not reported significant improvements in the overall survival or in preventing recurrences for GB patients (Laub et al., 2018). This devastating scenario strongly indicates a lack of knowledge in the biology of gliomas, prompting scientists to go further the classical treatments, investigating peritumoral tissues as the tumoral invasion front into the neighbouring, healthy tissue (D'Alessio et al., 2019). Thus, scientists must now focus on elucidating the biomolecular characterization of tumor-adjacent tissue, in order to not only

optimizing surgical resection, but also to better defining the role of peritumoral tissue in gliomas progression, identifying new therapeutic targets (D'Alessio et al., 2019).

1.3. Tumor microenvironment

For long time, cancer research has focused mainly on understanding the biology of glioma cells, investigating the aberrant pathways that guide tumor onset and progression. Nowadays, the idea that the interaction between glioma cells and the local environment is crucial in driving tumor growth has strengthened (Hanahan and Coussens, 2012). Understanding microenvironmental determinants that contribute to the growth of glioma growth is therefore at the centre of current scientific research, with the aim of discovering new targets and strategies to prevent the high burden of morbidity and mortality by improving patients' survival and quality of life (Johung and Monje, 2017).

The features of the tumor microenvironment (TME) are dynamically modified during glioma progression and the interaction of tumor cells with the main components of the TME (neurons, reactive astrocytes, microglia, oligodendrocytes, inflammatory cells, endothelial cells, pericytes and GB-associated stromal cells) seems to shape the progression of the disease (D'Alessio et al., 2019; Venkatesh et al., 2015). For instance, the enhancement of cerebrovascular and lymphatic networks remodelling (Hahn et al., 2019; Hanahan and Coussens, 2012; Hoelzinger et al., 2007; Mancino et al., 2011), together with the metabolic and biochemical alterations in peritumoral tissues, are regulated by different communication routes which include secreted

molecules, gap junctions, tunnelling nanotubes and extracellular vesicles (D'Alessio et al., 2019; Jung et al., 2019; Lane et al., 2019; Matarredona and Pastor, 2019; Osswald et al., 2015).

1.4. Neural activity shapes the tumor microenvironment

Increasing evidences show that neurons are active part of the tumor microenvironment, contributing, with their direct and indirect action, in shaping the interactions between different players of glioma development. However, complex interactions between various types of neurons make this mechanism difficult to understand (Deisseroth et al., 2004; Ge et al., 2007).

In a non-pathological condition, electrical activity influences the development of central and peripheral neural system (Gafarov, 2018). During the maturation of CNS, patterned waves of electrical activity influences neurodevelopment inducing calcium transients in all the parts of the nervous system (Corlew et al., 2004; Wong et al., 1995). Interestingly, other mechanisms are profoundly regulated by neurons also in the adult brain. For instance, excitatory neurons regulate proliferation and differentiation of stem cells in the subgranular zone of the dentate gyrus and neurogenesis in the subventricular zone (Deisseroth et al., 2004; Paez-Gonzalez et al., 2014). Moreover, neurons also regulate I) Schwann cell proliferation and survival in the peripheral nervous system (Maurel and Salzer, 2000) and II) glial precursor proliferation in myelin plasticity in the CNS, conditioning brain structure and function (Scholz et al., 2009; Takeuchi et al., 2010). Studies on oligodendrocyte precursor cells (OPC) demonstrate the suppression of cell proliferation by silencing the neural activity in the rat optic nerve, either via nerve transection or via tetrodotoxin (Barres and

Raff, 1993). Moreover, OPC, pre-OPC and neural precursor cells show a mitogenic response to optogenetically increased cortical activity and subsequent differentiation (Gibson et al., 2014). Altogether, these data strengthen the pivotal role of neurons in controlling glial precursor cells, a likely origin of gliomas, pointing out the possible influence of neural activity on tumor cells.

Actually, there are many robust evidences that neural activity affects glioma cell behaviour. The most relevant studies of the latest years have demonstrated that pyramidal cell activity promotes patient-derived high-grade glioma proliferation through activity-dependent secreted factors, in particular neuroligin-3 (NLGN3) (Venkatesh et al., 2015, 2017). The mitogenic effects are a consequence of the activation of the PI3K-mTor, SRC and RAS signalling pathways, leading to a potentially autocrine/paracrine loop of NLGN3 expression, that inversely correlates with overall survival of glioblastoma patients (Venkatesh et al., 2017). It has been also demonstrated that AMPA receptor activation promotes glioma growth, mainly through microenvironmental interactions such as neuron-to-glioma synaptic transmission (Venkatesh et al., 2019). Moreover, NLGN3 seems to be implicated in the formation of bona fide AMPA receptor-dependent synapses between glioma cells and peritumoral excitatory neurons, integrating high-grade gliomas in the neural network (Venkatesh et al., 2019). Several studies suggest also a probable pivotal role in regulation of glioma proliferation exerted by other neural secreted molecules, that are neurotransmitters and neurotrophins; however, the role of activity-dependent secretion has not been demonstrated yet, because of the difficulty in unravelling the source that secretes these fundamental factors, since both neural and glioma cells can produce them.

1.4.1. Neurotransmitters

Glioma growth is regulated by complex multifactorial interactions and it is affected by activity-dependent protein factors, as described above. Besides proteins as NLGN3, neurotransmitters are other possible candidates released by neurons to control tumor progression (Johung and Monje, 2017). Indeed, it is well known that glioma cells express functional neurotransmitter receptors, which could interfere with mitogenic pathways. For instance, adult GBs express the dopamine receptors DRD2 and DRD4, whose inhibition seems to be particularly effective in reducing glioma cell proliferation and survival (Caragher et al., 2019; Dolma et al., 2016). Moreover, human GB cells also express serotonin receptors, albeit it is not clear whether they have an impact on tumor cell proliferation (Mahé et al., 2004). In particular, a retrospective study made on GB patients showed that increasing serotonin levels through the administration of a selective serotonin reuptake inhibitor (SSRI) didn't produce a significant survival benefit (Caudill et al., 2011; Otto-Meyer et al., 2020).

1.4.1.1. Glutamate

One of the most characterized neurotransmitter is undoubtedly glutamate. Glutamate is one of the most important and abundant molecule of the CNS, but its extracellular levels must be maintained low to guarantee a normal brain function. Therefore, the scavenger role of glia and astrocytes is of paramount relevance to maintain this equilibrium (Bergles and Jahr, 1997; Robert and Sontheimer, 2014). Indeed, glial membranes are abundant of Na+-dependent transporters (i.e. EAAT1 or EAAT2), representing the 1% of total brain proteins and being necessary for the clearance of glutamate (Danbolt, 2001). In particular,

glioma cells have an almost complete absence of Na+-dependent glutamate uptake, due to the loss of EEAT2 protein production and to the mislocalization of EAAT1 to the nuclear membrane (Buckingham and Robel, 2013; Robert and Sontheimer, 2014; Ye et al., 1999). Furthermore, glioma cells extrude glutamate outside, predominantly through the overexpression of the cystine-glutamate antiporter (system xc-, SXC) that exchanges intracellular glutamate for extracellular cysteine and that is involved in the generation of antioxidant glutathione (de Groot and Sontheimer, 2011). The biochemical source of glutamate for glioma cells is not entirely known. Published data show that glutamate may be generated from glutamine via a glutaminase reaction or that it could be accumulated due to other metabolic impairments as the decreased conversion in α-ketoglutarate by GLUD2 enzyme (de Groot and Sontheimer, 2011; Franceschi et al., 2018). Glioma cells express ionotropic and metabotropic glutamate receptors (de Groot and Sontheimer, 2011) and the increased extracellular glutamate levels in proximity of the tumor mass (Behrens et al., 2000) promote survival, growth and migration through the activation of PI3K-Akt pathway via AMPA receptor activation (Ishiuchi et al., 2007). The high amount of glutamate acts in a paracrine/autocrine manner on tumor cells, facilitating their spread into the brain parenchyma and resulting to be excitotoxic for neurons in the tumor vicinity (de Groot and Sontheimer, 2011). Moreover, gliomas increase the neural excitability of peritumoral neurons, but the mechanism that links hyperactivity and a further cell proliferation is still lacking (Venkatesh and Monje, 2017).

1.4.1.2. GABA

The role of GABA neurotransmitter is far more complex. In a normal brain, GABA is not only the most important inhibitory neurotransmitter of the CNS, but it also controls stem cell proliferation in the subventricular zone, limiting the generation of new neuroblasts (Blanchart et al., 2017; Young and Bordey, 2009). It has been demonstrated that glioma cells express GABA receptors, but the effects of their activity is still under debate. Studies on patient-derived glioma cultures show that the expression of functional GABA A receptors is more correlated with low-grade gliomas and oligodendrogliomas than glioblastomas (Labrakakis et al., 1998), but other *in vitro* studies on human glioblastoma samples presume the opposite (D'Urso et al., 2012). In a p16 *Arf* $^{-/-}$ PDGFB murine glioma model has been identified an endogenous ionotropic signalling within tumor cells, demonstrating that glioma cells are able not only to express GABA A receptor subunits and to respond to it, but they can also release GABA, especially in tumor bulk (Blanchart et al., 2017). Furthermore, studies demonstrated that the endogenous neurotransmitter limits cell proliferation of both murine and patient-derived glioblastoma cells, prolonging the survival of glioma-bearing mice (Blanchart et al., 2017). As a matter of fact, it is supposed that GABA could have a role not in the initial steps of transformation, but once the tumor is established, as proved by experiments with muscimol and bicuculline on animal models (Blanchart et al., 2017). Moreover, phosphorylation of H2AX by chloride influx within cells through GABA A receptor activation seems to be essential for the inhibition of glioma growth. It has to be noticed that in high-grade gliomas GABA A receptors are likely downregulated, reducing the inhibitory effect of the peptide on tumor proliferation (Jung et al., 2019). Intriguingly, the effect of

GABA is more robust in the quiescent stem-like population of glioma cells, suggesting a possible strategy to maintain tumor-initiating cells quiescent (Blanchart et al., 2017). This is sustained also by the downregulation of miRNA 155 in glioblastoma, which reduces the expression of GABA A receptors and, when the miRNA production is regained, GB cells recover the response to the GABA neurotransmitter (D'Urso et al., 2012). Taken altogether, these studies point out the interesting, but still not completely answered, question regarding the influence that GABAergic interneurons may exert on glioma.

1.4.2. Neurotrophins

Neurotrophins are a family of proteins that are historically implicated in several vital functions as growth, survival, development and plasticity in both central and peripheral nervous systems (Sofroniew et al., 2001); their role is much broader than their name might suggest (Vega et al., 2003). The classical molecules belonging to this group are nerve growth factor (NGF), brain-derived neurotrophic factos (BDNF), neurotrophin-3 (NT3) and neurotrophin-4 (NT4). They bind the p75NT receptor and one of the tyrosine kinase receptors (Trk; i.e. TrkA for NGF, TrkB for BDNF and NT4, TrkC for NT3) (Park and Poo, 2013), activating trophic or pro apoptotic pathways depending on molecular context (Meeker and Williams, 2015).

The role of neurotrophins in cancer and especially in gliomas is still under debate, because it is not clear whether they exert a pro-mitogenic effect on glioma cells or a protective role for the tumor microenvironment (Garofalo et al., 2015; Venkatesh et al., 2015). It is known that in paediatric tumors such as neuroblastoma or medulloblastoma tumor cells express neurotrophin receptors

and the clinical significance is suggested to be predictive of a favourable outcome (Donovan et al., 1993; Eberhart et al., 2001; Nakagawara et al., 1993). Also in adult low-grade gliomas TrkA and TrkB are highly expressed, while their presence in GB is weak, suggesting that those receptors might be involved only in the early stages of the disease (Wadhwa et al., 2003).

NGF was the first neurotrophin discovered to be responsible for sympathetic and sensory nerve growth and survival (Cohen et al., 1954). It has been demonstrated that in a rat model of glioma the activation of the TrkA receptor through NGF treatment has an anti-mitotic effect on C6 glioma cells, reducing their proliferation and inducing the differentiation, although tumor cells lack to synthetize neurotrophin (Kimura et al., 2002; Rabin et al., 1998). Also in humans, a phase II clinical trial with administration of NGF on patients with childhood optic gliomas led to a statistically significant improvement in electrophysiological parameters used to evaluate vision respect to placebo-treated patients (Falsini et al., 2016). Conversely, on human glioblastoma cell lines, NGF seems to improve tumor proliferation via Notch1 signalling (Park et al., 2018).

The role of BDNF in gliomas is more controversial. BDNF is a peptide secreted in an activity-dependent manner (Hong et al., 2008). *In vitro* studies demonstrate that neurotrophin stimulates high grade glioma cell proliferation, through the binding with its receptor TrkB (Xiong et al., 2013) and its release increases with neural activity (Venkatesh et al., 2015). On the other end, evidences suggests that BDNF overexpression in the hypothalamus has immune-augmenting properties, eliciting an increased anti-tumor immune response and reducing the activity of several proteins that would normally confer resistance to chemotherapeutic agents (Radin and Patel, 2017). Moreover,

glioma-bearing mice reared in an enriched environment (EE) showed increased level of BDNF together with significantly reduced tumor growth (Garofalo et al., 2015).

1.5. Neural alterations induced by glioma

Emerging researches suggest that glioma cells exert a powerful influence on neural tissues. Deficits in neurocognitive functioning frequently occur in glioma patients and heavily affect their quality of life (Aaronson et al., 2011; Seano et al., 2019). The impact of tumor mass on neurons could provoke mechanical compression on brain structures but also cell-death through tumor-released excitotoxins and disturbance in synaptic transmission, inducing a direct neuronal damage in the region of insurgence and disturbing the functional brain networks (van Kessel et al., 2017).

1.5.1. Tumor-associated epilepsy

Tumor-associated epilepsy (TAE) is among the most common comorbid condition in patients with gliomas, heavily affecting their quality of life (Beaumont and Whittle, 2000; Fisher et al., 2014; Taphoorn et al., 2010). Approximately 30-50% of patients with brain tumors manifest seizure as initial symptom of disease progression (van Breemen et al., 2007). Surprisingly, patients with low grade tumors are more prone to develop TAE with an incidence of the 80-90% (van Breemen et al., 2007; You et al., 2012a), whereas in high grade gliomas are less frequent (30-62%) but may be more difficult to control and occur predominantly during the onset of the disease (Armstrong et al., 2016). TAE often manifest as

focal seizures with secondary generalization and, despite its major clinical and social impact, the pathophysiological causes are poorly understood. Due to the complex heterogeneity of perturbed mechanisms, this kind of epilepsy is often refractory to antiepileptic treatments (Cowie and Cunningham, 2014; You et al., 2012a).

An important aspect that determines the insurgence of seizures is the glioma localization in the brain. As a matter of fact, the proximity to the cortical grey matter is a fundamental factor: tumors localized closely to the cortex or with limbic and perilimbic cortical localization are highly epileptogenic, whereas tumors located in the inner parts of the brain are less likely to manifest seizures (Berntsson et al., 2009; Cowie and Cunningham, 2014). In addition, epileptiform activity originates outside the tumor mass but within 1-2 mm from the tumor border for animal models (Köhling et al., 2006) and within 3 mm for human patients (Patt et al., 2000). Moreover, the tumor itself might generate action potentials through astrocytic tumor cell activity, which could also represent a source of epileptic activity (Bordey and Sontheimer, 1998).

The development of seizures is a complex phenomenon that involves multifactorial mechanisms in the peritumoral tissues as metabolic and pH changes, disruption of the BBB, immunological and inflammatory changes, ionic change (e.g. Mg2+ and Fe3+), hypoxia, acidosis and metabolic impairments that could affect neural morphology and function (Armstrong et al., 2016; Cowie and Cunningham, 2014; You et al., 2012a). Besides, the alterations in the balance between excitatory and inhibitory networks certainly play a pivotal role in the generation of seizures (MacKenzie et al., 2017; Nelson and Turrigiano, 1998; You et al., 2012a).

1.5.2. The hyper-activation of excitatory networks

As described in the **section 1.4.1.1**, glioma extrudes high amounts of glutamate in the extracellular space of the peritumoral area (Behrens et al., 2000; Buckingham et al., 2011), resulting in excitotoxicity, tumor invasion and hyperexcitability of neural tissues (Marcus et al., 2010; Robert and Sontheimer, 2014; Rzeski et al., 2001; Sontheimer, 2008a; Vanhoutte and Hermans, 2008). As a consequence, the elevated quantity of glutamate in peritumoral tissue can over-activatiate NMDA and AMPA receptors (Savaskan et al., 2008). The prolonged activation of NMDA receptors provokes a sustained influx of Ca2+ into the cell, mediating excitotoxicity and affecting the inhibitory function of GABA B receptors (Terunuma et al., 2010). The reduction of neuronal cell density creates room for tumor expansion (Buckingham et al., 2011) and the over-activation of AMPA receptors boosts neural excitability (Savaskan et al., 2008). Taken altogether, all these studies highlight that the glutamate-driven NMDA and AMPS activation is now considered to be one of the main causes of peritumoral cortical hyperexcitability (Buckingham and Robel, 2013; Campbell et al., 2012). Indeed, targeting glutamate receptors with talampanel (antagonist of AMPA receptors) and memantine (antagonist NMDA receptors) are currently tested in clinical trials with encouraging results (Huberfeld and Vecht, 2016).

However, it is worth noticing that glutamate release *per se*, although necessary, is insufficient to drive peritumoral epilepsy and that other concomitant dysregulations are necessary in order to establish long-lasting hyperexcitation (Campbell et al., 2015).

For instance, the chloride (Cl-) homeostasis of pyramidal neurons is heavily affected, with the downregulation of KCC2 (K-Cl cotransporter 2) and the

upregulation of NKCC1 (Na-K-Cl cotransporter 1). The high amount of intracellular chloride caused by the defective extrusion through KCC2 and the increased influx by NKCC1, lead to GABA-mediated depolarization, reversing chloride potential and leading to an excitatory action of gamma-aminobutyric acid (GABA) receptor activation on pyramidal neurons (Campbell et al., 2015; Conti et al., 2011; Di Angelantonio et al., 2014; Huberfeld and Vecht, 2016; Jung et al., 2019; Pallud et al., 2014). The excitatory role of GABA in peritumoral tissues is also supported by some studies on temporal lobe epilepsy, where it was found that stimulating parvalbumin interneurons (PV) could produce differential effects with respect to their distance to the epileptic focus. Indeed, activating PV cells close to the epileptic focus fails to block ictal generation, enhancing synchrony and promoting ictal generation; on the contrary, the stimulation of PV cells distant from the epileptic focus lead to an anti-epileptic effect (Sessolo et al., 2015). In addition, the reduction of KCC2 by a prolonged glutamate-activation of NMDA receptors, causes the degradation of GABA receptor subunits. Furthermore, pyramidal cells show a reduction in inhibitory synapses on the soma and axon initial segment, indicating an incorrect regulation of the circuits (Marco et al., 1997). Therefore, the decreased inhibition, the GABA possible switch to excitation and an altered expression of its receptors, could concur in neural hyperexcitability.

1.5.3. The degradation of inhibitory networks

In the tumor microenvironment, also inhibitory networks appear perturbed but the role of GABA connections in glioma environment is not completely understood. In particular, it has been reported that the peritumoral regions show

a significant loss of approximately 35% of GABAergic interneurons, together with a reduction in their firing rates and in synapses with pyramidal neurons (Campbell et al., 2015; Tewari et al., 2018; Yu et al., 2020) that leads peritumoral tissue to be hyper-excitable and more prone to seizures (Buckingham et al., 2011; Venkatesh et al., 2019).

During the latest years, it has been developed the concept that seizures occurring in peritumoral tissues are not only the result of a specific alteration of excitatory and inhibitory neurons. Indeed, studies showed that in TME the perineuronal nets (PNNs), that surround fast spiking interneurons acting as ionic buffering, neuroprotecting and stabilizing their synaptic activity, are degraded by glioma-released proteases. This results in increased membrane capacitance and, in turn, reduces the firing rate of the remained peritumoral inhibitory interneurons within 400 μm from tumor edge. In particular, the pro-seizure effect of PNN degradation seems to be due to the lacking role of electrostatic insulator affecting the physiological properties of fast-spiking interneurons (Tewari et al., 2018). All these events contribute to establish an unbalanced network, that leads peritumoral tissue to be hyper-excitable and more prone to seizures (Buckingham et al., 2011; Venkatesh et al., 2019).

1.6. Direct neuron-glioma interaction

As previously described, glioma cells interact with the local environment modifying it for their own advantage, through the secretion of specific factors that facilitate tumor progression. But the invasiveness of brain tumors can follow complex patterns: many gliomas cross the corpus callosum to form butterfly lesions, some remain confined to the white matter stopping abruptly at the gray-

white-matter junction, whereas others grow in the gray matter around neurons and blood vessels (satellitosis) (Louis, 2006; Wesseling et al., 2011). The neural satellitosis is a perfect example of direct interaction between glioma cells and neurons and this phenomenon has pioneered the study of the tumor connectivity with the brain microenvironment. Recently it has been discovered that many astrocytomas are able to directly interact with the surrounding environment, extending ultra-long membrane protrusions called tumor microtubes (TMs) that represent a route for glioma proliferation to invade the brain (Osswald et al., 2015). The presence of these structures is correlated with the worst prognosis in human gliomas and confers a resistance against all the available therapies (Weil et al., 2017). Studies in *drosophila* demonstrate that glioblastoma cells protrude TMs to enwrap neurons, depleting in them the Wingless-related integration site (WNT) pathway and causing neurodegeneration (Portela et al., 2019). Moreover, through TMs, glioma cells interact with peritumoral excitatory neurons forming functional bona fide AMPA-mediated synapses (Venkataramani et al., 2019), in which pro-mitotic peptides as NLGN3 are involved (Venkatesh et al., 2019).

However, despite the latest evidences demonstrating a tumor-supportive activity of excitatory neurons, an anti-proliferative interaction between peritumoral neurons and glioma cells has also been well-described (Liu et al., 2013). Interestingly, peritumoral neurons are capable of restrain glioma progression through the pivotal role of program death-ligand1 (PD-L1) protein, and indeed neuronal PD-L1 signalling in brain cells is important for GB patient survival (Liu et al., 2013). *In vitro* studies demonstrated that cortical neurons (but not glia) significantly inhibit GL261 cell proliferation, as assessed by 5-Bromo-2′-deoxyuridine (BrdU) incorporation (Liu et al., 2013). Specifically, high expression of PD-L1 by peritumoral neurons positively associates with GB patient survival,

demonstrating the existence of a PD-L1-dependent interaction between peritumoral neurons and tumor cells also *in vivo* (Liu et al., 2013).

Moreover, evidences demonstrate that the interaction between glioma cell lines and neurons lead to an upregulation of functional GABA A receptor expression in glioma cells, both *in vitro* and *in vivo* (Synowitz et al., 2001).

All these studies depict a very complex scenario, underlining the need to clarify the contribution of distinct neuronal cell types in tumor development.

1.7. Glioma models

Animal models represent a suitable tool to study the biology of tumors and to investigate the role of candidate pathways that might be involved in the development of this pathology. To create animal models of brain tumors we can take advantage of three different strategies: i) the infusion of tumor cells, ii) the delivery of oncogenic transgenes, or iii) the genome manipulation (Robertson et al., 2019). However, for a reliable prediction and validation of the effects of different therapeutic modalities, glioma models need to comply with specific and more strict demands than other models of cancer (Lenting et al., 2017). These demands are directly related to the combination of I) genetic heterogeneity of cell population, II) driver mutations within canonical cell-growth and survival pathways, III) the infiltration into the brain, IV) complex microenvironmental interactions that change tumor features and composition during its progression (Lenting et al., 2017; Quail and Joyce, 2017). Therefore, an ideal animal model of glioma should be sustainable *in vitro* but also be able, when *in vivo*, to mimic the complexity of the human pathology with a predictable and reproducible pattern (Peterson et al., 1994; Robertson et al., 2019).

In particular, the laboratory mouse is a suitable system that shares extensive molecular and physiological similarities to humans, such as angiogenesis and metastasis processes; so, they represent a powerful tool for studying cancer (Chen et al., 2012). More importantly, murine glioma models provide temporally and genetically controlled systems for studying the tumorigenic process, as well as response to treatment (Reilly and Jacks, 2001). Many different murine models are actually available. These models are designed to recreate a tumor with increasingly similar characteristics to the real pathology in humans or to reproduce an altered pathway known to be important in glioma development. Thanks to modern technologies such as the combination of magnetic resonance and ultramicroscopy, a detailed analysis of different biological features of some murine models has been done, pointing out differences in angiogenesis, grow pattern and intratumoral heterogeneity, allowing the researchers to choose the most suitable model for their studies (Breckwoldt et al., 2019). The nowadays principal used murine models are transgenic or created through glioma cells transplant.

1.7.1. Transgenic murine models

Transgenic mouse models offer an opportunity to develop and utilize an easily replenished, reproducible, spontaneously manipulated and accurate pre-clinical model of human cancers, which we can use to enhance our molecular knowledge and to test promising therapies (Miyai et al., 2017). The availability of modern techniques of genome sequencing have allowed the identification of driven mutations of gliomas. Consequently, a wide variety of genetically engineered mouse models (GEMMs) that incorporate genetic alterations found in

human patients has been developed (Kersten et al., 2017). . Especially, they represent a very powerful tool to investigate early initiation events of glioma formation and also to be used as preclinical models for testing new therapies (Llaguno and Parada, 2016).

In particular, GEMMs have been created by introducing genetic alterations in the germline and using breeding strategies that generate compound mutants with alterations in both oncogenes and tumour suppressors. Inevitably, mutations in some of the relevant genes are early lethal and therefore must be engineered using conditional tools (e.g. Cre-loxP recombination strategies) (Robertson et al., 2019). The general approach for the development of GEMMs involves loss of function of principal driven tumor suppressor genes, such as Cdkn2a (Ink4A/Arf), Nf1, Trp53, Pten, and Rb1 and/or the expression of driver oncogenes, such as mutant epidermal growth factor receptor (e.g., EGFR VIII) and Ras (K-Ras, H-Ras), Akt, and platelet-derived growth factor (PDGF) ligands (Kegelman et al., 2014).

The strategies to generate transgenic animal models are varied and one of the most popular approach that has contributed to our understanding of the potential cells of origin of GB is the RCAS-TVA system (Holland et al., 2000). Cells producing TVA, the receptor for subgroup A avian leukosis viruses, are susceptible to infection with replication-competent avian sarcoma-leukosis virus long terminal repeat with splice acceptor (RCAS) viral vectors (Wang et al., 2016). Holland et al. have developed transgenic mouse lines expressing the TVA in Nes- or Gfap expressing cells, presumed to be respectively progenitor cells and differentiated astrocytes and bred these with Cdkn2a-knockout mice (Holland et al., 1998). In addition, they have demonstrated that staminal cells were more susceptible to tumor initiation than Gfap-TVA cells, but differentiated astrocyte

populations derived from neural stem cells were not discernible (Holland et al., 2000). To address this problem, the model has been subsequently implemented combining the RCAS with lineage-restricted promoters (Jiang et al., 2017). With this system, a significant impact of differentiation state on tumour aggressiveness has been confirmed, with more restricted progenitors being less malignant (Jiang et al., 2017). Recently, the RCAS-TVA system has been combined with powerful techniques of genetic engineer as CRISP/Cas9 to deliver oncogenes or induce specific mutations in tumor suppressors (Oldrini et al., 2018). The limitation of this approach is the need of specific TVA-expressing mouse strains and the viral cargo length.

The complexity and heterogeneity of glioma pathogenesis, has led to design plasmid-based techniques as CRISPR- and PiggyBac-based approaches, that do not require mouse breeding or virus production and enable the delivery of larger cargo sizes (Pathania et al., 2017). In fact, they can deliver combinations of oncogenes and tumour suppressors in multiplex, directly *in vivo* and with high enough efficiency for tumour formation (Robertson et al., 2019).

However, viral vectors have been extensively used as engineering system for the generation of mouse models of interest in the study of brain tumors (Robertson et al., 2019). Moreover, the direct injection of adenovirus, retrovirus and lentivirus in the site of interest, allows a great spatial control of tumor initiation and reduces the amount of time required to generate germline colonies(Miyai et al., 2017). Viral vectors represent a very versatile and efficient system to obtain different subtypes and grades of glioma changing the expression of specific genes (i.e. PDGFB, EGFRvIII, activated p21–RAS, activated AKT), the lineage of the cell expressing specific receptors (GFAP, NES) and transgenic strains (null for Cdkn2a, Trp53 etc.) (Miyai et al., 2017). The

combination of genetic engineering tools together with viral techniques, conditional knock-out with cre-loop system and inducible promoters have produced a plethora of mouse models that develop gliomas with a range of histologic types, penetrance and latency and which recapitulate in varying degrees the pathological hallmarks of human gliomas (Llaguno and Parada, 2016). A glioma model that embraces diverse tools has been recently developed by Giachino et al. (Giachino et al., 2015) to study the tumor suppressor functions of Notch signalling. They have developed a mouse model expressing PDGF, thus activating receptor tyrosine kinase-PI3K-mTOR signalling in a Trp53-/- background, to identify tumor-initiating cells. A PDGF-IRES-Tomato retrovirus has been injected in the subventricular zone of mice carrying floxed Trp53, Hes5::CreERT2 allele and a Cre-reporter allele (Rosa-CAG::GFP) to lineage-trace cells. They also have exploited an inducible system to delete Trp53 in Hes5+ cells activating Cre recombinase by the administration of Tamoxifen. With this system, the formation of glioma has been induced in the subventricular zone and cells expressing both reporter genes have been identified as tumor initiating cells, marked in yellow (Giachino et al., 2015). Extensive evidences from this developing field suggest that formation of endogenous brain tumors, using viral vectors or plasmid systems to deliver oncogenes, is somewhat variable. The degree of penetrance, tumor latency and histopathological features are dependent not only on the species and age of animals, but also on the identity of specific genetic, on the vector system used to deliver them and on the anatomical location of genetic alterations (Candolfi et al., 2009).

1.7.2. Glioma cell transplant

The transplant of glioma cells is another strategy to induce gliomas in the brain of animal models, usually rats and mice. The unpredictable character of gliomas that develop in GEMMs has prompted researchers to create stable *in vitro* cell cultures that can initiate a tumor when injected in an adult rodent brain.

Grafting glioma cells offers the advantage to spatially and temporally control tumor initiation (Miyai et al., 2017). The use of bioluminescence in vivo is possible to monitor the growth of transplanted cancer cells longitudinally; this experiment requires a stable expression of the luciferase cassette in the transplanted cells and it is now widely used because of its simplicity and low-cost (Robertson et al., 2019).

The graft can be classified in xenograft, where implanted cells come from a different species, or syngeneic graft, in which glioma cells are from the same species as the recipient (Robertson et al., 2019). The former is usually done with stable human glioma lines or with patient-derived glioblastoma (PDX) cells that maintain histopathological properties and genomic characteristics of parental tumor *in situ* (Wainwright et al., 2017; Zeng et al., 2020). It has been found that PDX xenograft models contain heterogeneous sub-clones derived from a single tumor (Soeda et al., 2015), so the similarities with human gliomas render this model the most suitable to evaluate cell- and patient- specific drug responses. Xenograft models, however, require immune-deficient mice i.e. SCID, with impaired T and B cell lymphocyte development NOD-SCID, with the addition of the deficiency in natural killer cells, or athymic nude mice (Miyai et al., 2017). Alternatively, immune-humanized mice may be used whether the murine Ig-locus is exchanged for the human one (Morton et al., 2016). However, the lack of a

complete immune system makes xenograft models unable to be used for the study of immune-mediated responses. Moreover, the surrounding tumor microenvironment is not of the same origin of grafted cells and this may interfere with drug response (Miyai et al., 2017).

Syngeneic mouse models could overcome most of the xenograft limitations, providing a tool to model immune interactions (Robertson et al., 2019).

The possibility to graft tumor cells into syngeneic hosts give an important contribution for studying immunotherapy and immunosuppression in GB. Indeed, an efficient immune system plays a pivotal role in determining the efficiency of approaches as dendritic cell vaccination and immune checkpoint inhibition (Li et al., 2016; Tsiatas et al., 2016), hampered by the immune suppressive milieu in patients with glioma (Gielen et al., 2015). But also syngeneic models cannot fully recapitulate the intratumoral heterogeneity of human gliomas, not completely representing the genetic features of human GB cells (Lenting et al., 2017).

1.7.2.1. GL261 mouse model

One of the most used syngeneic mouse model of glioma is obtained by the intracerebral graft of murine GL261 cells. The GL261 mouse model has been generated in 1939 for the first time by Seligman and Sear by intracranial injection of the alkylating agent 3-methylcholantrene (Seligman and Shear, 1939). After, Ausman et al. transplanted tumor fragments subcutaneously and intracranially into C57BL/6 mice, with the latter resulting in a median survival of 24–25 days when implanted with $1x10^5$ tumor cells/10 µl (Ausman et al., 1970). Stable GL261 cell lines for transplantation has been then constituted in the mid-1990s (Szatmári et al., 2006).

For its histological features, GL261 tumor has been described like ependymoblastomas, but resembling GB phenotypes. They stain positively for the GB marker vimentin and harbour activating mutations of the K-ras oncogene as well as mutations of the p53 tumor suppressor gene, resulting in high expression of c-myc, as reported also in human gliomas (Candolfi et al., 2007; Gururaj et al., 2013; Sidransky et al., 1992; Trent et al., 1986). Furthermore, given the deficiency in PTEN, GL261 cells reproduce the dysregulation of PI3K pathway, as demonstrated by the detection of p-Akt *in vitro* and *in vivo* that is known to promote a tumor whose development is similar to human GB (Fresno Vara et al., 2004; Newcomb and Zagzag, 2009). Importantly, PTEN mutations up-regulate expression of PD-L1, a cell surface protein that can be expressed in GB tumors but not in normal physiologic states (Parsa et al., 2007) and that promotes immunosuppression by inducing T lymphocyte apoptosis (Dong et al., 2002).

In any event, the genetic features of GL261 are not completely accepted as a model of authentic GB, due to the presence of mutations not completely detected in the human pathology as those in K-ras (Miyai et al., 2017; Robertson et al., 2019). However, GL261 cells show interesting features of immunogenicity similar to the human counterpart, that make this murine model perhaps the most extensively used for preclinical testing of immunotherapeutic approaches for GB (Oh et al., 2014; Szatmári et al., 2006). These tumor cells are partially immunogenic, expressing high level of MHC I; however, the expression of molecules that activate the immune system as MHC II, B7-1, and B7-2, is low (Szatmári et al., 2006) as in GB cell lines, miming the escape from immune surveillance as in human GB (Anderson et al., 2007; Wu et al., 2007; Zagzag et al., 2005). Among the most relevant immunologic studies conducted in this model

there are i) the use of adoptive T cell transfer to restore and induce long-term immunity (Plautz et al., 1997) and ii) the use of antibodies to improve antitumor T cell activity via augmentation of costimulatory signalling (Kim et al., 2001). Gene therapy studies have also utilized the GL261 model, involving tumor modification for production of inflammatory cytokines (e.g. IL-2), to enhance tumor immunogenicity (Lichtor et al., 1995) as well as with IL-12-expressing DNA plasmids to slow tumor growth and stimulate a robust CTL response (Keke et al., 2004).

In summary, the structural characteristics of tumor development from GL261 cells recapitulate the main features of human GB. Hence, tumor formation

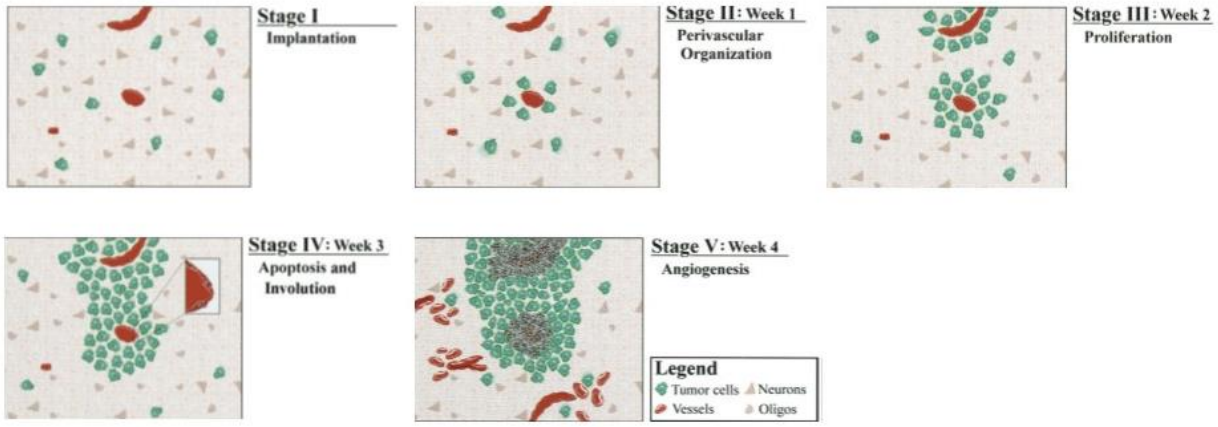

proceeds through five stages (**Figure 1**) over a four-week period after implantation: I) implantation; II) perivascular organization of tumor cells around blood vessels; III) proliferation near vasculature as mechanism of invasion; IV) hypoxia through blood vessel degeneration, which in turn promotes VEGF expression leading to angiogenesis; V) neovascularization towards necrotic regions to sustain tumor growth (Zagzag et al., 2000).

In the very early stages of neoplastic growth, just after implantation glioma cells are scattered in the neuropil, followed by early perivascular organization around existing cerebral vessels. This suggests an active homing of the tumor cells to the native cerebral vessels (Zagzag et al., 2000). In contrast, in the second phase there is formation of new blood vessels, mostly at the tumor periphery, which arise from existing vessels. This concept suggests that in richly

Figure 1 ***Five stages of GL261 growth in the brain.***

Stage I: GL261 cell graft. This is the initial phase just after tumor cell inoculation. The tumor cells are dispersed within the neuropil. Stage II: Perivascular Organization (Week 1). The tumor cells are concentrated around nutrient-rich native blood vessels. Stage III: Proliferation (Week 2). The tumor cells proliferate around the viable blood vessels. Stage IV: Apoptosis and Involution (Week 3). Apoptosis in vascular cells occurs and degeneration of the blood vessels becomes evident. The involution of the host vessels is likely to lead to hypoxia, which in turn will induce VEGF release, leading to angiogenesis. Inset: Apoptic bodies are seen in endothelial cells. Stage V: Angiogenesis (Week 4). Neovascularization occurs as blood vessels grow toward and vascularize the now necrosing tumor (central gray stippled area), providing a new source of nutrition (taken from Zagzag et al., 2000).

vascularized organs, as brain, tumors can obtain an efficient blood supply from a suitable native vascular bed (e.g., cerebral blood vessels) (Zagzag et al., 2000). Pre-existing vessels are able to temporarily provide essential blood supply for tumor progression, but failing to undergo angiogenesis, they involute. This leads in turn to tumor necrosis and, eventually, angiogenesis occurs (Zagzag et al., 2000).

The GL261 tumor mass presents also interesting histologic markers that recapitulate essentially all of the pathologic features of human glioblastomas, validating this model for preclinical studies. It presents areas of necrosis, initially focal zones around vasculatures and after, extensive regions with pseudopalisading cells surrounded by novel blood vessels. Tumor cell invasion

occurred both around vascular channels and as individual infiltrating tumor cells but they are not able to metastasize (Szatmári et al., 2006; Zagzag et al., 2000).

As a matter of fact, GL261 cells create a solid tumor mass (**Figure 2**), defined nodular, that exert the so called “mass-effect” on surrounding tissues, inducing compression, tissue deformation and tension. Moreover, with intravital multiphoton microscopy, it has been demonstrated that solid-stress induces a distortion of the morphology of peritumoral cells that is associated with neurological dysfunctions and neural loss (Seano et al., 2019). A detailed characterization of neural dysfunctions in GL261 mouse mode has been described by Vannini et al. (Vannini et al., 2016a, 2017). The authors report alterations in the morphology of peritumoral neurons, showing a shrunken dendritic arbor and a reduction of spine density. Implanting the tumor in the visual cortex, they exploited the visual system to detect physiological alterations due to glioma growth including i) enhanced spontaneous firing, ii) reduced visual responsiveness over a range of stimulus contrasts, iii) impaired response reliability and iv) increased size of receptive fields (Vannini et al., 2016a). After this study, through a battery of sensitive motor tests, the longitudinal progression of the tumor has been monitored when GL261 cells were implanted in the motor cortex, assessing the time course and the extent of dysfunction induced by glioma growth (Vannini et al., 2017). This characterization has allowed the identification of the appearance of the first symptoms associated with neuronal impairments 9-12 days after GL261 cells injection, while at day 22 glioma-bearing mice displayed a severe damage affecting all features of motor function, in parallel with a dramatic extension of the tumoral mass (Vannini et al., 2017). Altogether, these results pave the way for the use of GL261 mouse model in

preclinical experimentation of therapies designed to ameliorate the physiological status of peritumoral neural tissues.

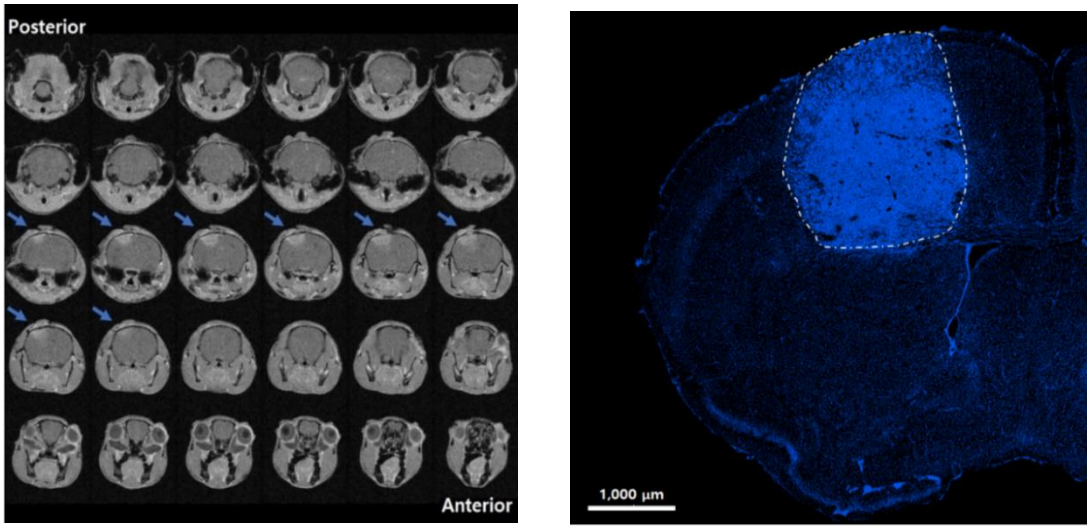

Figure 2 ***GL261 tumoral mass****. On the left, 7 Tesla (7T) magnetic resonance imaging (MRI) 14 days after GL261 inoculation; blue arrow indicates the tumor position. GL261 cells were implanted in the primary motor cortex. On the right, a representative image of the same tumour mass acquired from brain coronal section of GL261 glioma-bearing mouse stained with Hoechst (fluorescent stain of DNA, blue) 21 days after tumour induction. Image was captured with a microscope equipped with Apotome.2 using a 10× EC-PLAN-NEOFLUAR objective in ZENpro software. Scale bar is 1000 µm.*

Based on the extensive characterization of the GL261 glioma model here reported, it can be said that this model accurately represents the relevant biology of human GBs as mandated by the NCI Brain Tumor Progress Review Group. All the studies reported here confirm the relevance of this glioma model in the preclinical setting with respect to its histopathology as shown in the brains of both immunosuppressed and immunocompetent mice (Newcomb and Zagzag, 2009; Oh et al., 2014).

Aim of the thesis

High-grade gliomas infiltrate surrounding brain parenchyma during their development, establishing new interactions with the environment that can be exploited to sustain their own progression. Traditionally, brain tumor research has been focused on the study of the biology of glioma cells. However, in the recent years, the interaction between cancer cells and tumor microenvironment has emerged as one important regulator of tumor progression. An ample amount of

information has been published on how tumor cells might modulate peritumoral tissues and how tumor microenvironment might influence glioma expansion. Gliomas grow in a neuronal environment, and a role for pyramid neuron activity in tumor progression has been recently established (Venkataramani et al., 2019; Venkatesh et al., 2015, 2017). However, the impact of glioma growth on neuronal responses and plasticity is only partly understood. Similarly, the role of different neuronal subtypes in glioma progression remains to be established.

Therefore, the aim of this thesis is to shed light on fundamental missing links on the bidirectional interaction between neurons and glioma cells.

In the experimental setting we decided to employ the widely-used, well-accepted and characterized GL261 mouse model, already tested for molecular, functional and anatomical studies (Garofalo et al., 2017; Vannini et al., 2016a, 2017).

The first part of my thesis aimed at studying the longitudinal alterations that occur in peritumoral neurons during glioma growth. Specifically, I examined impairments of neural activity and network oscillations induced by tumor proliferation in the visual cortex. I also performed an electrophysiological monitoring of visual response to follow physiological impairments of neural circuits and the appearance of network hyperexcitability and seizures. Moreover, I also performed laser-capture microdissection of peritumoral neurons, followed by gene expression analysis to understand the molecular alterations induced by glioma in peritumoral excitatory neurons that contribute to the detected hyper-excitable phenotype.

In the second part of the thesis I focused my attention on the influence of neural activity on glioma proliferation. Recent studies have demonstrated an active role for neurons in controlling glioma progression, but the specific

contribution of different subsets of cortical neurons remains unexplored yet. To address this issue, I directly compared the effects on glioma cell proliferation of optogenetic stimulation of pyramidal cells vs. fast-spiking, GABAergic neurons in mice inoculated with GL261 cells into the motor cortex. Since both principal cells and fast-spiking interneurons are directly activated by sensory afferent input, I next placed tumors in the occipital cortex to test the impact of visual manipulation. Finally, I also tested an integration of current GB chemotherapy with a sensory stimulation to mitigate the progressive deterioration of peritumoral neural functionality during glioma progression.

Materials and Methods

2.1. Animals and Rearing

Adult (age > postnatal day 60) wild type C57BL/6J, Thy1-ChR2 (B6.Cg-Tg (Thy1-ChR2/EYFP, 18Cfng/J, Jackson Laboratories, USA) and PV-Cre (Tanahira et al., 2009) (B6;129P2-Pvalb tm1(cre)Arbr/J, Jackson Laboratories, USA) mice were used in the experiments. Animals were bred in our animal facility and housed in a 12 hours light/dark cycle, with food and water available *ad libitum*. All

experimental procedures were performed in conformity to the EU Council Directive 2010/63/EU and were approved by the Italian Ministry of Health (authorization number 260/2016 PR).

2.2. GL261 cells

The murine glioma GL261 cells were grown in complete Dulbecco's modified Eagle's medium (DMEM) containing 10% Newborn calf serum, 4.5 g/L glucose, 2 mM glutamine, 100 UI/ml penicillin and 100 mg/ml streptomycin at 37°C in 5% CO2 with media changes three times per week.

2.3. Glioma Induction

To induce the formation of glioma, mice under avertin anesthesia (intraperitoneal injection of 2,2,2-tribromoethanol solution; 250mg/kg body weight; Sigma Aldrich, USA) received a stereotaxically guided injection of 40,000 GL261 cells (20.000 cells/ul PBS solution) as described in (Vannini et al., 2016a, 2017). In C57BL/6J, Thy1-ChR2 and PV-Cre mice, cells were injected either into the primary visual cortex (2 mm lateral to the midline and in correspondence with lambda) (Vannini et al., 2016a) or into the motor cortex (Vannini et al., 2017) in correspondence with the forelimb representation (1,75 mm lateral to the midline and 0.5 mm anterior to bregma) (Alia et al., 2016; Allegra Mascaro et al., 2019). The GL261 cell solution was slowly infused with a Hamilton syringe guided by an automatized pump (KdScientific, USA) at a depth of 0.8–0.9 mm from the pial surface. Sham animals were subjected to the same procedure and infused with vehicle solution (PBS).

2.4. How glioma affects neural activity

2.4.1. Chronic electrode implantation

In order to longitudinally record the neural response of the visual cortex, in both C57BL/6J sham and glioma-bearing mice a chronic bipolar electrode was implanted 3 mm lateral to the midline and in correspondence with lambda at a depth of 750 µm from dura. The visual cortex was chosen as a recording site since it can be easily activated by photic stimuli and because of the availability of well-established parameters to evaluate its functionality. The electrode was positioned 1 mm lateral to the site of tumor injection (or PBS). It was formed by two twisted enamel-insulated nickel-chrome wires (120 µm), whose ends were spaced 800 µm, and by a ground electrode welded on a screw fixed in the cerebellum. All the wires were connected to a multipin socket. A portion of the skull overlying the occipital cortex was drilled on one side and the bipolar electrode was inserted; all the components were secured to the bone by acrylic dental cement (Cerri et al., 2016). During the surgery, a metal post was placed on the occipital bone of animals in order to allow the recording of visual evoked potentials (VEPs) in awake head-fixed mice (Frenkel et al., 2006).

2.4.2. Visual evoked potentials (VEPs) recordings

To measure the responsiveness of the visual cortex during tumor progression, we evaluated the components of visual evoked potentials (VEPs). VEPs were recorded in both sham (ctrl) and glioma-bearing mice (glioma). After

the recovery from the surgery and a period of habituation to the apparatus, awake head-fixed animals were subjected to recording sessions three times a week, from day 8 after tumor implantation (**Figure 3A**). Typical VEP responses consisted in an early negative wave and a late positive peak with latencies of approx. 60 and 110 ms, respectively (**Figure 3A**). Transient VEPs were recorded in response to two types of stimuli: i) abrupt reversal of a horizontal square wave grating (spatial frequency, 0.06 cycles/degree; 90% contrast, 1 Hz) and ii) flash (50% contrast, 1 Hz). They were generated by a computer on a monitor (Sony; 40 x 30 cm; mean luminance 15 cd/m2) by a VSG card (Cambridge Research Systems) and the display was positioned in front of the mouse's eyes (at a distance of 25 cm) to include the binocular visual field. Signals were amplified (10,000-fold), band pass filtered (0.5–100 Hz), and fed into a computer for storage and analysis. For each type of stimulus, at least 30 events were averaged. The response to a blank stimulus (0% contrast) was also recorded in each session to estimate noise. In every recording session were analysed: the peak-to-trough amplitude of VEP response (Pizzorusso et al., 2002; Porciatti et al., 1999; Restani et al., 2009; Vannini et al., 2016a) and the latency of the major components of the VEP (i.e. the first negative (N1) and the first positive (P1) peaks) (**Figure 3B, C**). Using the average of VEP amplitude of the first three recording sessions a baseline was defined for each type of stimulus. In addition, when the VEP amplitude of a glioma-bearing mouse resulted significantly decreased in two consecutive recording sessions respect to the baseline (Student's t-test, $p<0.05$), the animal was sacrificed together with a sham mouse (ctrl). Animals were deeply anesthetized with chloral hydrate and perfused transcardially with PBS (Sigma Aldrich, USA) followed by fixative (4% paraformaldehyde, 0.1 M sodium phosphate, pH 7.4). After, brains were gently

removed, cryoprotected by immersion in 30% sucrose and frozen in a powder of dry ice to preserve the RNA integrity. Tissues were stored at -80°C until the processing with the NeuN fast protocol (see **section 2.4.5**).

2.4.3. Local field potential (LFP) recordings

A group of glioma-bearing mice was specifically dedicated for the recording of local field potentials (LFPs) in freely moving conditions (for electrode implantation see **section 2.4.1**). Recording sessions were performed from day 8 after tumor implantation until the LFP was detectable (**Figure 10A**). All animals were recorded three times a week for 2 hours. Signals were amplified (10,000-fold), bandpass filtered (0.3–100 Hz), digitalized with a sampling rate *fs* = 200 Hz through a USB DAQ board (NI USB-6212 BNC, National Instruments, USA) and conveyed to a computer for storage and analysis. The analysis of epileptiform activity was performed using a custom-made application, based on LabView (National Instruments, USA), as described previously (Antonucci et al., 2009; Cerri et al., 2016; Mainardi et al., 2012; Vannini et al., 2016b). The program first identified epileptiform alterations and spikes in the EEG using a voltage threshold, which was set to 4.5 times the standard deviation of the EEG signal (determined during periods of baseline activity). Spikes were grouped in clusters when they were spaced by less than 1.5 sec and they were classified in: i) interictal events, that last less than 4 sec and ii) ictal events, lasting at least 4 sec (Mainardi et al., 2012). For each recording session, we determined the frequency and duration of clusters.

2.4.4. Spectral analysis

The power spectrum of the signals was estimated by using the Welch method of averaging modified periodograms (Kantz and Schreiber, 2003; Stine and Abarbanel, 1997) in a Matlab code.

To detect power spectra alterations between glioma-bearing and sham mice, we analysed the LFPs recorded with a blank stimulus during VEP recording sessions. We focused on estimating the power content of the standard neurophysiological spectral bands: δ = (0.5 − 4) Hz, θ = (4 − 8) Hz, α = (8 − 12) Hz, β = (12 − 30) Hz of the LFP signal (Buzsáki, 2009). In particular, we considered the relative power of a generic λ = δ, θ, α, β spectral band with respect to the total power of the signal as follows:

(1) $$P_{rel}(\lambda) = \frac{\sum f_{k\in\lambda} P(f_k)}{P_{tot}}$$

where fk is a frequency belonging to the λ spectral band, P(fk) is the corresponding power and Ptot is the total power of the LFP signal (Vallone et al., 2016).

To investigate in deeper details the alterations detected in the range 0.5-4 Hz between glioma-bearing and sham animals, the standard δ band was divided in two ranges: 0.5-1 Hz and 2-4 Hz (Lundstrom et al., 2019).

For all the analyses, at least three values were averaged. For each spectral band a baseline was established, averaging the relative power calculated in the first three recording sessions. To determine the alterations of power spectra induced by glioma progression, the difference between the averages of the last two recording sessions was done with respect to the baseline. A statistical

analysis was done (*Student's t-test,* GraphPad Prism 6) to compare the relative power of each spectral band between glioma-bearing and sham mice.

The relative power of standard spectral bands were analysed also on the LFP recordings of freely moving, glioma-bearing mice. In particular, we focused on the standard δ and α band intervals (respectively 0.5-4 Hz and 8-12 Hz) distinguishing the power spectra during the 5 seconds before each ictal event (pre-seizures) and for the entire duration of the seizure (during seizures), based on the results obtained by the analysis of epileptiform activity described in the **section 2.4.3.**

Only ictal events distant at least 10 seconds from each other were included in the analysis. For each recording session, a baseline was established with the average of the power spectra values of δ and α bands in LFPs without seizures and all the values were normalized on it. A statistical analysis through GraphPad Prism 6 using a *Student's t-test* was done to compare the power spectrum value of δ and α bands pre-seizures and during-seizures with the baseline.

2.4.5. Immunohistochemistry: NeuN fast protocol

Frozen brains of mice in which VEPs were recorded were also subjected to NeuN immunostaining analysis. All the steps of the immunohistochemistry were performed under RNase-free and sterile conditions to avoid RNA degradation and contamination. To further avoid RNA degradation, a fast immunostaining protocol was designed based on the protocols of Fink and co-workers (Fink et al., 2000, 2006).

SuperFrost Plus slides (Thermo Scientific, USA) were used to minimize tissue lost during the staining process. Slides were sterilized under UV for 1

hour before the use. Frozen brains were cut using a cryostat (Leica, Germany) to obtain coronal sections of 7 µm of thickness. A maximum of 3 brain slices were put in the same slide in order to perform the Laser Capture Microdissection in less than 2 hours for each slide. Cut tissues were immediately placed in a sterile box in dry ice or stored at -80°C until the use. Slides were kept at room temperature for 10 min before the beginning of the immunohistochemistry and incubated for 10 min with RNA*later* (Sigma Aldrich, USA) in PBS at room temperature (RT). Tissues were incubated for 30 min RT in a blocking solution (BSA 10%, Triton-X 1%, PBS) and 1 hour RT with guinea pig NeuN primary antibody (1:100, Synaptic Systems) in PBS. After 3 washes of 5 min in PBS, sections were incubated 1 hour with anti-guinea pig secondary antibody conjugated to AlexaFluor555 fluorophore (1:200, Thermo Fisher). After, slides were washed 2 times in PBS, incubated for 1 min with Hoechst, washed with ddH20 and left to dry (Buckanovich et al., 2006; Butler et al., 2016; Fink et al., 2000, 2006; Florell et al., 2001).

2.4.6. Laser Capture Microdissection (LCM)

Tissues were observed with a Zeiss Axio Observer microscope equipped with Zeiss AxioCam MRm camera (Carl Zeiss MicroImaging GmbH, Germany). For each brain section, the border of the tumor mass was identified with PALMRobo 4.5 Pro program (Zeiss) and, based on cellular morphology, pyramidal neurons of the layers 2/3 within 500 µm (Seano et al., 2019) from the tumor rim were selected. Targeted neurons were dissected through PALM RoboMover Automatic Laser Capture Microdissector (Zeiss) (**Figure 6A**). For each slide, dissected cells were collected in the adhesive cap of a collection

tube (**Figure 6B**). Immediately after LCM, every collection tube was places on dry ice or at -80°C until the RNA extraction. For each animal, at least 1500 pyramidal neurons were collected.

2.4.7. Gene expression analysis: Customized Real-Time PCR panel

2.4.7.1. RNA extraction (Maxwell)

To perform gene expression analysis on peritumoral pyramidal neurons, dissected cells were subjected to automatic RNA extraction using the Maxwell®16 Instrument (Promega) configured with the low elution volume (LEV) hardware. Maxwell® 16 Instrument is a magnetic particle-handling instrument that efficiently process liquid samples using paramagnetic particles with a result of few hundred nanograms of pure RNA suitable for amplification. The purification protocol was adapted to microdissected samples according to the company instructions. Hence, total RNA was isolated from the collected cells by incubation with 50 µl of lysis buffer PKD (Qiagen, Netherlands) and 10 µl of proteinase K solution (Promega, USA) at 56°C for 1 hour with the tube upside down. All samples were then centrifuged at maximum speed for 10 min and the RNA was purified using the Maxwell®16 LEV RNA FFPE Purification Kit (Promega, Madison, WI) following the extraction protocol (Negro et al., 2017). Samples were kept in dry ice and immediately processed.

The RNA was extracted also from half hemisphere of a wild type C57BL/6J mouse brain, frozen in nitrogen liquid to obtain RNA of good quality. The RNA of this sample was used as *inter-run calibrator*, which is a further normalizer necessary to improve the assessment of plate-to-plate variation and

to compare the expression of the same target genes in multiple experiments using relative quantification (Hellemans et al., 2008; Rieu and Powers, 2009). The RNA was extracted using the Maxwell® 16 LEV simplyRNA Tissue Kit (Promega, Madison, WI) according to the protocol and its quality and quantity were checked with the Agilent 2200 TapeStation instrument using the Agilent RNA Kit (Agilent Technologies, USA). The sample was considered of good quality, with the RIN (RNA Integrity Number) = 8.8 (Schroeder et al., 2006).

2.4.7.2. cDNA synthesis and Preamplification Reaction

The extracted RNA was then reverse transcribed into first strand cDNA using the iScript advanced cDNA synthesis kit (Bio-Rad Laboratories, USA), according to protocol instructions. Due to the small amount of input RNA and to the degradation of RNA caused by animal perfusion with 4% PFA, we chose to perform a quantitative analysis of gene expression through a custom-plate Real-Time PCR (Bio-Rad Laboratories, USA). To do that, undiluted cDNA was unbiased preamplified with a customized pool of PrimePCR Preamp assays (Bio-Rad Laboratories, USA), according to the manufacturer protocol (Okino et al., 2016). Preamp PCR was performed at 98°C for 3 min followed by 12 cycles of denaturation at 95°C for 15 sec and annealing/extension at 58°C for 4 min. The quality and quantity of the amplified fragments were checked with Agilent 2200 TapeStation instrument with the Agilent High Sensitivity D1000 Kit for fragmented DNA (Agilent technologies, USA).

The RNA of the *calibrator* was reverse transcribed in cDNA using nanoScript 2 Reverse Transcription kit (RT-nanoScript2, PrimerDesign Ltd, UK), according to the manufacturer instructions. The cDNA of the *calibrator*

was used in all the Real-Time PCR plates to compare all the analyzed samples.

2.4.7.3. Real-Time PCR and gene expression analysis

A quantitative Real-Time PCR was performed using 96-well custom plates (Bio-Rad Laboratories, USA) in which specific primers were lyophilized in each well. To assess a good comparison, every plate was designed to process the *calibrator* together with each sample at the same time. The analysed genes are reported in **Table 2**.

Gene Name	Protein
Gabra1	GABA(A) Receptor, A 1
Gabra5	GABA(A) Receptor, A 5
Grin2a	Glutamate Ionotropic Receptor NMDA Type Subunit 2A
Grin2b	Glutamate Ionotropic Receptor NMDA Type Subunit 2B
Slc32a1	VGAT
Slc17a7	VGlut1
Scn1a	Sodium Channel, Voltage Gated, Type I A Subunit
Snap25	Snap25
Vamp2	Vamp2
Dlgap4	SAP90/PSD-95-Associated Protein 4
Gephyrin	Gephyrin
Slc12a2	NKCC1
Slc12a5	KCC2
Cux1	Cux1
Foxp2	Foxp2
Bcl11b	CTIP2
Gria2	Glutamate Receptor Ionotropic, AMPA 2
β actin (reference gene)	β actin
Gapdh (reference gene)	Gapdh

Table 2 Panel of genes analysed for each sample and for the calibrator. The gene name and the corresponding codified protein are here indicated.

The quality of each sample and reaction was evaluated through PrimePCR experimental control assays, that are:

- Reverse Transcription Control assay
- Positive PCR control assay
- DNA Contamination control assay
- RNA Quality assay RQ1 and RQ2

Quantitative real-time PCR was performed using SsoAdvanced™ Universal SYBR® Green Supermix (Bio-Rad Laboratories, Hercules, CA), according to the manufacturer protocol.

The relative expression of target genes was calculated using the Livak (DDCt) method. For each sample, gene-expression values of layer specific genes were normalized on reference genes (i.e. GAPDH and β actin) and analyzed. Gene-expression values of the other genes, reported in Table 2, were normalized for reference genes and represented all together as an increase or decrease with respect to the *calibrator*.

2.5. How neural activity influences glioma growth

2.5.1. Thy1-ChR2 optogenetic stimulation

Thy1-ChR2 mice were used to dissect the role of excitatory circuits in glioma progression. These transgenic mice express the ChR2 gene, under the control of Thy1 promoter, mainly in deep cortical projection neurons (Arenkiel et

al., 2007; Spalletti et al., 2017; Wang et al., 2007). In these mice, GL261 cells were grafted in the motor cortex as described in the **section 2.3 .**The region around the site of the graft was thinned with the drill to facilitate the light penetration. After, a chamber of dental cement (Tetric EvoFlow, Ivoclar Vivadent, Switzerland) was created around the craniotomy and filled with a layer of agar (Sigma Aldrich, USA) and the silicone elastomer Kwik (World Precision Instrument, USA) to preserve the cortical surface. A metal post was placed on the occipital bone and fixed with dentistry cement (KERR, Dental Leader, Italy). Awake animals were subjected to a period of habituation to the apparatus before the stimulation sessions. After 13 days from tumor injection, a group of Thy1-ChR2 glioma-bearing mice (PYR STIM) was stimulated with an optogenetic fiber, according to the single stimulation protocol described in Venkatesh et al., 2015 (Venkatesh et al., 2015). The tip of the optic fiber was positioned stereotaxically over the dura mater surface (**Figure 14A)**. Animals were stimulated with cycles of 473 nm light pulses at 20 Hz for 30 s, followed by 90 s of recovery over a 30 min period. Optogenetic stimulation was done using the setup described in Spalletti et al., 2017 (Spalletti et al., 2017). The control group (CTRL) was let in a head-fixed position without fiber stimulation, in order to reproduce the same stress conditions of stimulated animals. Immediately before the beginning of the stimulation protocol, BrdU (5-Bromo-2′-deoxyuridine; Sigma Aldrich, USA) was intraperitoneally (i.p) administered (50 mg/kg) and 24 hours after animals were sacrificed to allow immunostaining analyses (see **section 2.5.7**).

2.5.2. AAV injection for ChR2 expression in Parvalbumin interneurons

PV-Cre mice were used to disentangle the role of inhibitory Parvalbumin (PV) interneurons on tumor proliferation. In order to allow expression of ChR2 in PV neurons, one week before GL261 graft, PV-Cre mice received two stereotaxically guided injections of 600 nl of an AAV virus (AAV1.EF1.dflox.hChR2(H134R)-mCherry.WPRE.hGH, Addgene, USA), one 500 µm anterior and one 500 µm posterior to the site of tumor injection into the motor cortex. The AAV sequence contains the channelrhodopsin-2 (ChR2) gene, which was inserted in parvalbumin interneurons through Cre-mediated recombination. In this thesis PV-Cre mice injected with the AAV will be indicated as PV-ChR2. The surgery was performed under avertin anesthesia (intraperitoneal injection of 2,2,2-tribromoethanol solution; 250 mg/kg body weight; Sigma Aldrich, USA).

2.5.3. PV-ChR2 optogenetic stimulation

After a week from virus injection, PV-ChR2 mice were injected with GL261 into the motor cortex. A portion of cranial bone anterior and posterior to the point of tumor injection was thinned with a drill and a chamber of dental cement (Tetric EvoFlow, Ivoclar Vivadent, Switzerland) was created around the craniotomy and filled with a layer of agar (Sigma Aldrich, USA) and the silicone elastomer Kwik (World Precision Instrument, USA) to preserve the cortical surface. A metal post was placed on the occipital bone and fixed with dentistry cement (KERR, Dental Leader, Italy) as previously described (Spalletti et al., 2017). Awake animals were subjected to a period of habituation to the apparatus before the stimulation sessions.

After 7 days from tumor injection, animals were randomized into two groups, to receive either real or mock (i.e. lights off) stimulation. A group of PV-ChR2 mice (PV STIM) was daily stimulated for a week with an optogenetic fiber positioned stereotaxically over the dura mater surface. Cycles of 15 min of 473 nm light pulses at 40 Hz for 3 s, followed by 90 s of recovery, were used to stimulate the anterior and posterior part of the craniotomy over a total period of 30 min. Optogenetic stimulation was done using the setup described in Spalletti et al., 2017 (Spalletti et al., 2017). The control group (CTRL) was let in a head-fixed position without fiber stimulation in order to reproduce the same stress conditions of stimulated animals. The day before the end of the protocol, BrdU (5-Bromo-2′-deoxyuridine; Sigma Aldrich, USA) was intraperitoneally administered (50 mg/kg) and animals were sacrificed 24 hours later for immunostaining analyses (see **section 2.5.7**).

2.5.4. Manipulation of visual afferent input

C57BL/6J mice bearing tumors in the primary visual cortex were subjected to different rearing conditions in order to physiologically manipulate the sensory-driven activity of the visual cortex, from day 11 to day 14 post glioma injection (**Figure 16A**). A group of animals was visually deprived through dark rearing (DR) in ventilated, completely light-tight shells (Gianfranceschi et al., 2003), while other mice were stimulated with square wave and sinusoidal gratings (visual stimulation, VS) for 8 hours/day; during the stimulation, animals were put in a Plexiglas cage surrounded by 4 LCD screens (one per side) with water and food available ad libitum and exposed to the visual stimulation protocol described below. For the visual stimulation, visual stimuli were generated by a VSG2:2 card

(Cambridge Research System, Cheshire, UK) and presented on the face of all the 4 LCD screens. The 8 hour protocol was composed by the repetition of two main modules of sinusoidal gratings of different spatial frequencies and contrasts: (i) a block of steady-state stimuli, consisting of gratings of increasing contrasts sinusoidally modulated at 2-6 Hz and (ii) a block of transient stimuli, i.e. gratings of increasing contrasts abruptly reversed at 1 Hz with a spatial frequency from 0.4 to 0.1 c/deg. Each block contained both horizontal and vertical gratings. The screen luminance was maintained at a low level (2 cd/m2) to minimize animals' stress.Animals with glioma into the primary visual cortex that were maintained into the normal light/dark cycle were called standard light (SL). BrdU (5-Bromo-2′-deoxyuridine; Sigma Aldrich, USA) was administered i.p. (50 mg/kg) at day 13 and then sacrificed 24h later in order to perform immunohistochemical analyses (see **section 2.5.7**).

2.5.4.1. TMZ administration

A dedicated group of glioma-bearing mice was subjected to VEP recordings with the same setup previously described (see **section 2.4.1** and **2.4.2**)**,** from day 8 after tumor implantation until the visual response was detectable, and VEP amplitude was quantified. From day 12 after tumor induction, a Temozolomide solution (2.5 mg/ml in saline, Sigma Aldrich, USA) was daily administered (40 mg/kg, ip) (Robinson et al., 2010)

During the treatment, animals were regularly weighed, monitored according with the Mouse Grimace Scale, MGS (Langford et al., 2010) and sacrificed when they lost more than 20% of weight. At the beginning of drug administration, animals were randomly allocated to either the TMZ or TMZ+VS group. The

TMZ+VS group received a daily administration of TMZ plus visual stimulation, according to the stimulation protocol described in **section 2.5.4.** VEP amplitudes were also compared with data already analysed of glioma-bearing mice without any treatment.

2.5.5. Botulinum Neurotoxin A injection

Botulinum Neurotoxin A (BoNT/A) was used to completely block synaptic transmission in the cortex. The stock solution of the toxin (50 nM) was diluted in a solution of 2% rat serum albumin in PBS (1:50) (Caleo et al., 2007; Costantin, 2005; Schiavo and Montecucco, 1995). Seven days after glioma graft, C57BL/6J mice with the tumor in the visual cortex received two stereotaxic injections of BoNT/A (1nM) or vehicle (2% rat serum albumin in PBS) (Restani et al., 2012a) under avertin anesthesia (intraperitoneal injection of 2,2,2-tribromoethanol solution; 250 mg/kg body weight; Sigma Aldrich, USA) (**Figure 17A**). Neurotoxin administration was made at the lateral and medial side of GL261 injection site (respectively 1.5 and 2.5 mm lateral to lambda) by means of a glass pipette (40 µm tip diameter) connected to an injector. At each site, 0.13 µl were slowly delivered at a depth of 800 µm. BrdU (5-Bromo-2′-deoxyuridine; Sigma Aldrich, USA) was administered i.p. (50 mg/kg) on day 13 and animals were sacrificed after 24h for immunohistochemical analysis.

2.5.6. Region-specific effect of dark rearing on glioma proliferation

To test the region specificity of the effects of DR, a group of C57BL/6J mice bearing tumors in the motor cortex was reared from day 11 to day 14 after glioma

implantation in complete darkness, as described above. BrdU (5-Bromo-2′-deoxyuridine; Sigma Aldrich, USA) was administered i.p. (50 mg/kg) on day 13 and animals were sacrificed 24h after for immunohistochemical analysis.

2.5.7. Immunohistochemistry

At the end of each protocol, animals were deeply anesthetized with chloral hydrate and perfused transcardially with PBS (Sigma Aldrich, USA) followed by fixative (4% paraformaldehyde, 0.1 M sodium phosphate, pH 7.4). Brains were gently removed, post-fixed for 1 h in the same fixative at 4°C, cryoprotected by immersion in 30% sucrose and cut using a sliding microtome (Leica, Germany) to obtain coronal sections of 50 µm of thickness. Sections were mounted on glass slides using VectaShield mounting medium (Vector Laboratories).

The detection of neural components infiltrating the tumor mass was performed in both C57BL/6J and Thy1-ChR2 mice. Those brain sections were stained for the axonal marker Tau (1:1000; SySy, Germany) and for the neural marker NeuN (1:1000, Millipore, Germany). Sections from Thy1-ChR2 glioma-bearing mice were also stained for the neural marker Parvalbumin (1:500; SySy, Germany).

In PV-ChR2 mice, we assessed colocalization of mCherry-ChR2 with parvalbumin. While mCherry staining was detectable in coronal sections without any amplification step, parvalbumin immunolabelling was performed using a primary guinea pig polyclonal antibody (1:500; SySy, Germany) as described in (Busti et al., 2020). Counts of double labelled cells were performed using Neurolucida software (Allegra et al., 2017).

For the evaluation of glioma cell proliferation, brain serial sections were stained with two markers of proliferation, Ki67 (1:400; Abcam, UK) and BrdU (1:500; Abcam, UK). Slices were incubated with fluorophore-conjugated secondary antibodies (Jackson Immunoresearch, USA) and with Hoechst dye (1:500; Bisbenzemide, Sigma Aldrich, USA) for nuclei visualization.

2.5.8. Image acquisition and data analysis

Fluorescent images were acquired using a Zeiss Axio Observer microscope equipped with Zeiss AxioCam MRm camera (Carl Zeiss MicroImaging GmbH, Germany). Images of the whole tumor were acquired for each slice through a 10x objective and obtained a single image using Zen Blue Edition software (Carl Zeiss MicroImaging GmbH, Germany). High magnifications of neural components were acquired also through a 20x objective.

2.5.8.1. Quantification of the density of cell proliferation

To minimize the variation between different immunostaining reactions and to normalize the data, we always processed a control group (i.e., reared in standard laboratory conditions) together with the experimental animals. Control animals were used to perform a preliminary analysis of the fluorescence intensity of the sample, setting the acquisition parameters for each channel (light intensity, exposition time), to avoid signal saturation at either end of the pixel intensity range (0 –255). The brightest focal plane along the z-axis was acquired and the resulting image was saved as eight-bit TIFFs. Signal quantification was

performed using Image J software (National Institute of Health, USA). Based on control animals, we set a threshold drawing four rectangles covering the most brightest proliferating cells in four different slices; their mean fluorescence intensity was calculated and used as threshold to discriminate Ki67 or BrdU positive pixels from the background. That was made for all the slices analysed. After, for each coronal slice the outline of the tumor mass was drawn and the density of proliferating cells was calculated as the fraction of area occupied by Ki67- or BrdU-positive pixels, with respect to total tumor area (Garofalo et al., 2015). Measurements of tumor proliferation were also normalized to the mean of the control group processed in the same immunohistochemical reaction. For comparison between different treatments, at least 3 animals per group were analysed. Statistical comparison were performed by cumulating the data obtained from all sections in the same experimental group. The average data obtained in each single animal was also reported.

2.5.8.2. Proliferation index

For the evaluation of proliferation index, high magnification images of the tumors previously analysed were taken with a 63x oil objective with the ApoTome 2 system (Carl Zeiss MicroImaging Gmbh, Germany), in two distinct regions of interest (ROI; 382 µm x 70 µm) at the border of tumor mass, one in the dorsal and one in the ventral part of the cerebral cortex (Figure 16H). The brightest focal plane along the z-axis was acquired and the resulting image was analysed. Cells labelled for Ki67 and/or Hoechst were counted using the Zen Blue Edition software (Carl Zeiss MicroImaging GmbH, Germany). The proliferation index was calculated as the proportion of Ki67-positive cells over the total sample of

Hoechst-labelled cells in the selected ROIs for each coronal slice. Statistical analyses were performed with GrahPad Prism 6. Differences between average VEPs amplitude and latency of glioma-bearing and shame-injected mice in visual cortex during tumor progression were analysed with Two Way analysis of variance (ANOVA) followed by Holm-Sidak test for multiple comparisons. For microdissections, a Student's t-test was applied to compare VEPs amplitude of glioma-bearing mice and the baseline. Differences between three or more groups were evaluated with One Way analysis of variance (ANOVA) followed by Dunnett's test for multiple comparisons. Normalized fractions of tumor area occupied by proliferating cells and proliferation index of two experimental groups was evaluated by *Student's t-test*. The comparison of the fraction of animals with a detectable VEP was performed using Kaplan-Meier (LogRank) statistics.

Results

3.1. Impact of glioma progression on neural activity

Many evidences have shown that glioma cells cause changes in neural peritumoral tissue. For instance, glioma cells influence neighbouring neurons by causing disabling peritumoral dysfunctions (van Kessel et al., 2017) and extruding high amount of glutamate, that results in excitotoxicity and tumor invasion (Marcus et al., 2010; Rzeski et al., 2001; Sontheimer, 2008a). Infiltrating glioma cells also perturb and impair the inhibitory cortical networks altering the chloride homeostasis and provoking a consequent switch of gamma-aminobutyric acid (GABA) towards excitation (Campbell et al., 2015; Conti et al., 2011; D'Urso et al., 2012; Pallud et al., 2014; Tewari et al., 2018).

In some cases, all these alterations can concur to promote the insurgence of comorbidity phenomena such as epileptic seizures (Armstrong et al., 2016; Buckingham and Robel, 2013). Although many studies are now focusing on the effects of glioma on neural networks (Yu et al., 2020), little is known about the molecular alterations that occur in peritumoral neurons caused by tumor progression. For this reason, the first part of my thesis aimed i) at clarifying the molecular changes on excitatory neurons provoked by glioma and ii) at revealing the electrophysiological alterations induced by tumor growth .

3.1.1. Progressive decay of visual response during tumor progression

Firstly, I investigated the effects of glioma growth on cortical neurons. To address this issue, I monitored the neural cortical activity of the visual cortex, where GL261 cells injection was performed, along with glioma progression. The visual cortex was chosen due to the presence of well-established parameters to evaluate its functionality and for the easy activation of neurons through visual stimuli presentation. As described in **section 2.4.1,** both sham and glioma-bearing animals were implanted with a bipolar electrode in order to allow longitudinal recordings of peritumoral tissue. The visual responsiveness to alternating gratings and flash stimuli was then recorded three times a week in head-fixed mice (**Figure 3 A**).

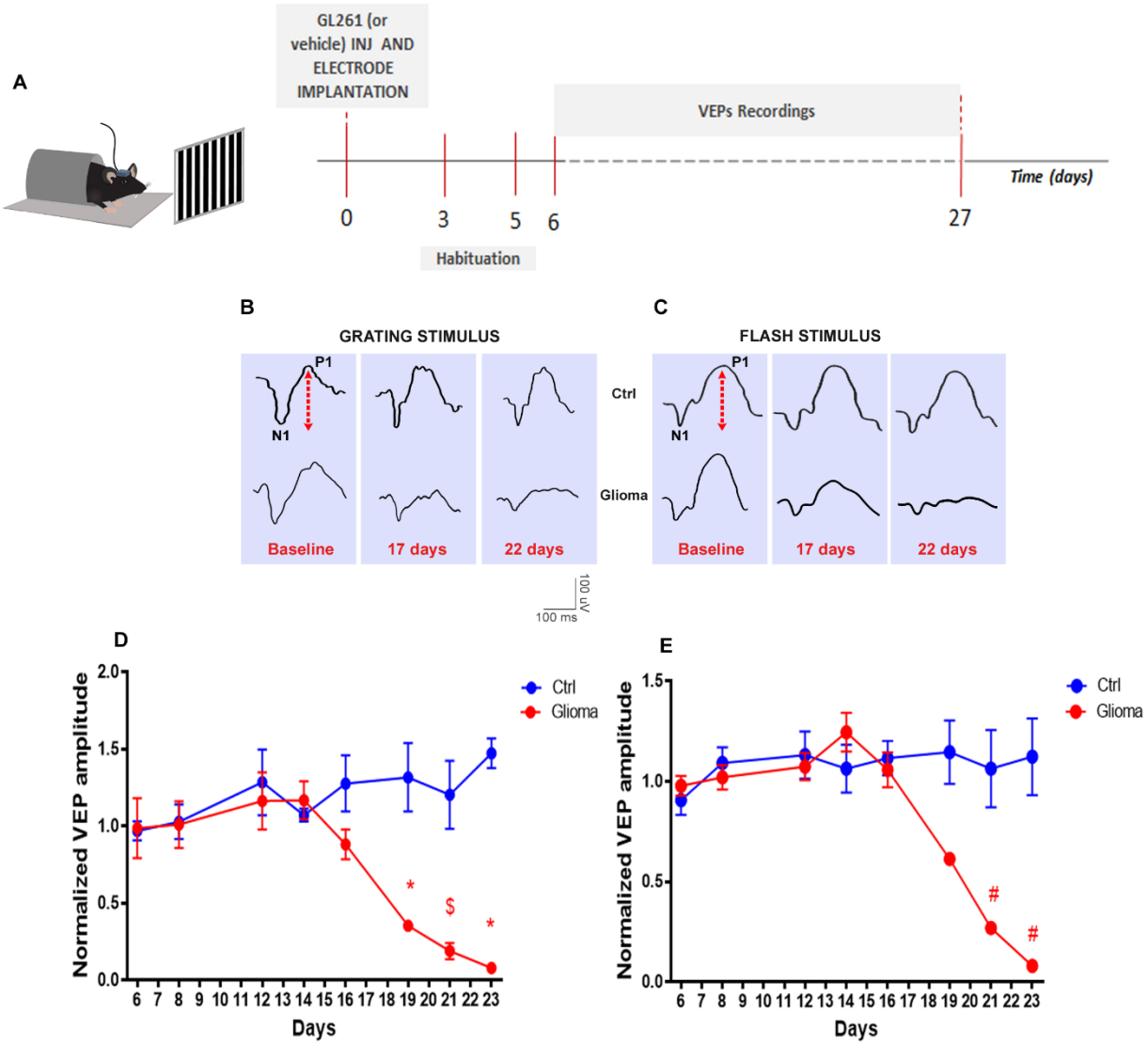

Figure 3 ***Deterioration of visual responsivity in glioma-bearing mice along with glioma progression***

A*) On the left, representative image of a head-fixed mouse during a VEP recording session. On the right, experimental protocol.* ***B****) Representative VEP waveforms in response to grating (left) and flash (right) stimuli are reported at day 12 (second recording session), 18 (early deterioration) and 23 (last recording sessions) after tumor (Glioma) or PBS (Ctrl) injection. During each recording session, the peak-to through amplitude of VEP (red arrows) was analysed. N1 indicates the first negative and P1 the first positive peak of VEP.* ***C, D****) Normalized average of VEP amplitude for glioma-bearing (red; n=6) and shame-injected (blue; n=5) mice. The mean ± sem is also shown for each timepoint. When not visible, error bars are within the symbol (Two Way ANOVA followed by Holm-Sidak test, $ p<0.05, * p<0.001, # p<0.0001)*

During each recording session the amplitude of Visual Evoked Potentials (VEPs) and the latency of the first two main components of VEP (i.e. N1 and P1 peaks) were analysed (**Figure 3B, C**). As a result, I found an initial progressive increase in VEP amplitude called stimulus-dependent response potentiation (SRP) in both experimental groups, likely indicative of the potentiation of thalamo-cortical synapses due to repetitive visual stimulation (Cooke and Bear, 2014). However, in glioma-bearing mice that increase was followed by a rapid decay and deterioration of visual responses that started from day 16 after tumor implantation. Also, a strongly dampened response was detected in glioma-bearing mice 23 days after cell transplant. On the contrary, sham animals showed a reliable and stable VEP responsivity in all the recording sessions (**Figure 3D, E**).

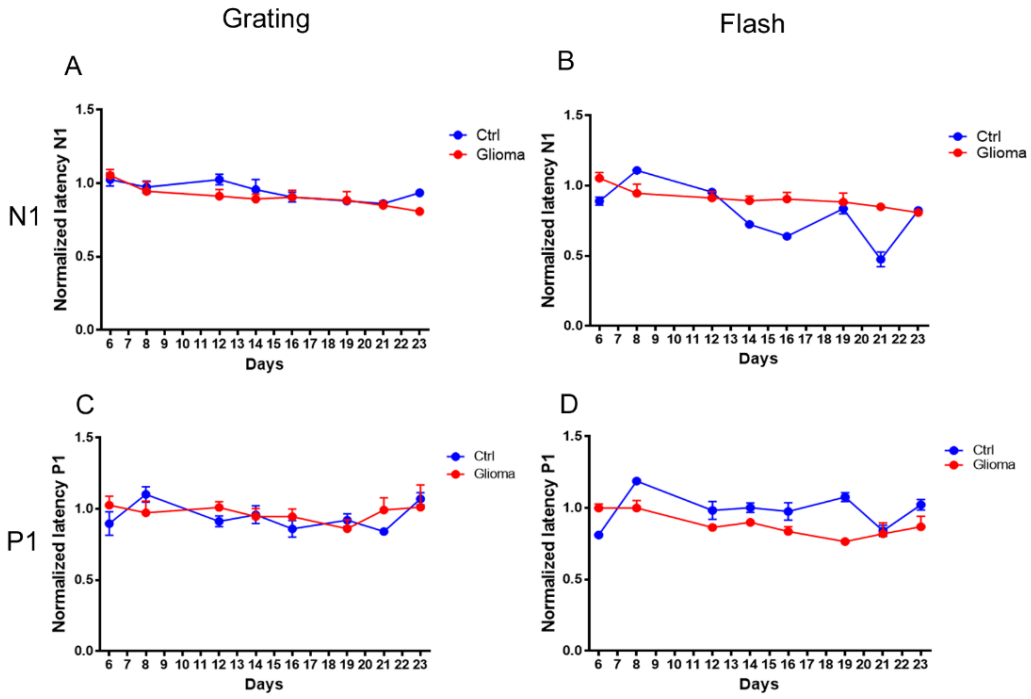

Figure 4 ***Glioma does not affect the latency of VEP response***

A-D*) Normalized amplitude of the first negative N1 (**A, B**) and the first positive P1 (**C, D**) peaks in response to grating (**A, C**) and flash (**B, D**) stimuli in glioma-bearing (red, n=6) and shame-injected (blue, n=5) animals. The mean ± sem is also shown for each value (Two Way ANOVA followed by Holm-Sidak test)*

I also evaluated the latency of VEP components, N1 and P1 (**Figure 4A-D**), for both type of visual stimuli. However, I failed to find any differences in this parameter, suggesting that it was not affected by tumor progression.

3.1.2. Spectral analysis of LFPs: enhancement of δ band and deterioration of α band during tumor growth

To detect whether glioma progression could affect ongoing brain oscillations, I analysed the LFPs recorded during blank stimuli (0% contrast). I firstly focused my attention on the alterations that occurred in the main neurophysiological spectral bands δ, θ, α and β (Buzsáki, 2009) (**Figure 5A**).

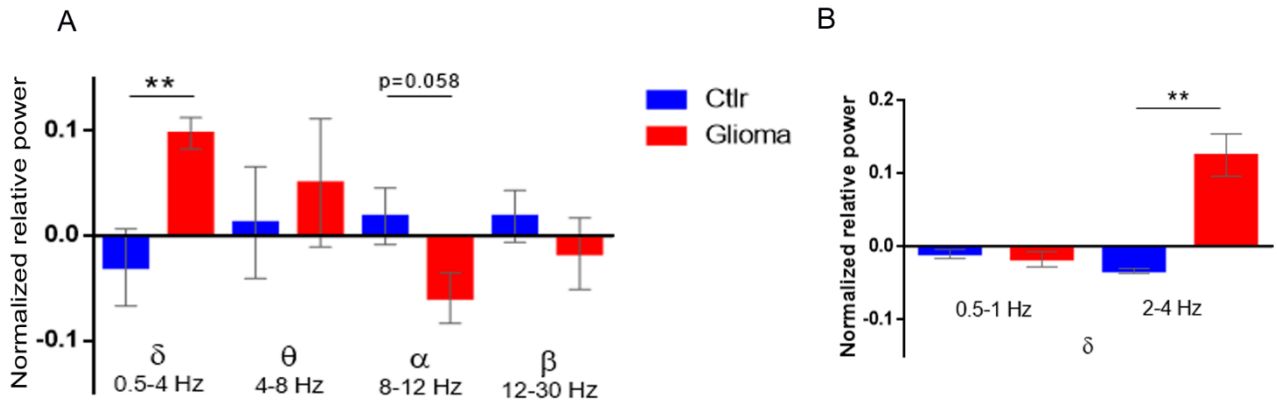

Figure 5 ***Enhancement of δ band and α rhythm degradation during tumor growth***

*Normalized relative power in glioma-bearing (red) and sham (blue) mice of the standard neurophysiological spectral bands (**A**) and of δ band in details (**B**). The histograms show the difference in relative power of the different spectral bands of the two last recording sessions with respect to the baseline (first three days of recordings). The mean ± s.e.m is shown for each group. (Student's t-test, **p<0.007).*

The progression of glioma mass caused a significant increase of the δ band power with respect to control animals, typical of focal epilepsy (Douw et al., 2010; Lundstrom et al., 2019; Schönherr et al., 2017) and a trend in α band deterioration. Moreover, I detected changes in the composition of peritumoral slow wave power (**Figure 5B**). In particular, glioma-bearing mice showed an increase especially in the "faster" δ band (2-4 Hz) during tumor progression, that might reflect a reduced inhibitory activity in the peritumoral region near the tumor mass (Lundstrom et al., 2019).

3.1.3. Molecular alterations in excitatory peritumoral neurons

After the electrophysiological characterization, I analysed the molecular features of peritumoral neural tissues to further investigate the alterations induced by glioma mass. After the monitoring of visual cortex activity through VEP analysis (as described in **section 2.4.2**), animals were sacrificed and brains cut and processed for the immunohistochemistry fast protocol (**Section 2.4.5**). Then, tumor mass was identified with Hoechst staining and neurons of each slices were marked with an anti-NeuN antibody (**Figure 6A**).

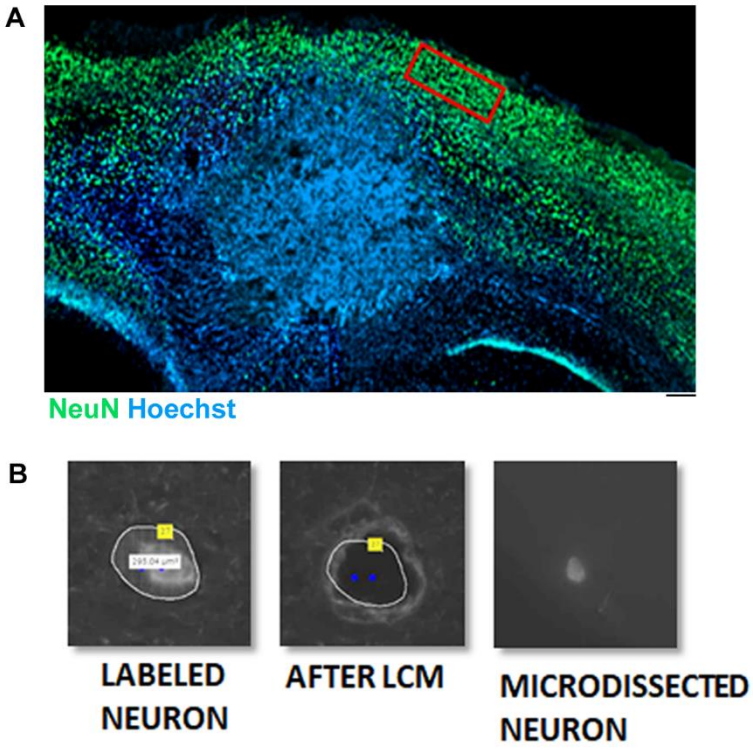

Figure 6 ***Laser Capture Microdissection***

A*) Representative tumor mass (blue) and peritumoral neurons (green) in the primary visual cortex. The red box indicates the ROI for the LCM. Scale bar, 100 µm.* ***B****) Representative images of LCM: labelled neurons were selected (left), removed by the laser (middle) and collected in the adhesive cap (right)*

For each brain slices, I used the Laser Capture Microdissection (LCM; see **section 2.4.6**) (**Figure 6B**) to only isolate the excitatory pyramidal neurons of layer 2/3. In this way, I was able to investigate which gene expression alterations were induced by tumor growth through a Real-Time PCR analysis on a customized panel of genes (**Table 2**). For each sample, I first checked the specificity of dissected neurons analysing two cell-type specific markers included in the panel: vGlut1 (Slc17a7 gene), as marker of excitatory neurons, and vGat (Slc32a1 gene), for inhibitory ones (Edwards, 2007).

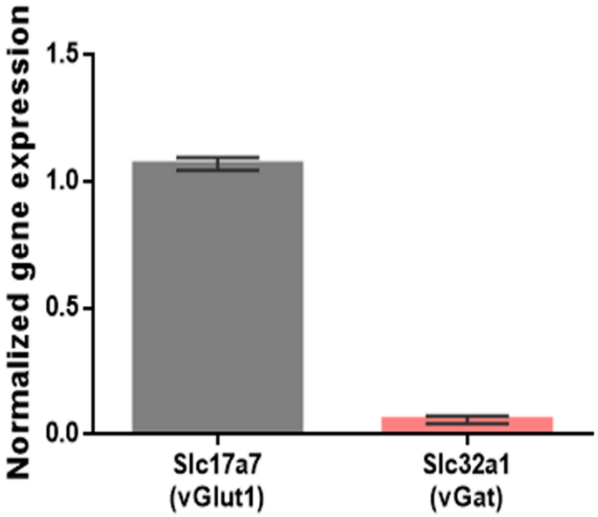

Figure 7 ***Dissected cells express excitatory neural markers***

Gene expression analysis of Slc17a7 and Slc32a1 in all samples detected by quantitative Real-Time PCR. Slc17a7 encoded for vGlut1 protein and it is specific for glutamatergic neurons; Slc32a1 encoded for the protein vGat specific for inhibitory neurons. Gene expression values were normalized on housekeeping GAPDH and β-actin mRNA. The mean ± s.e.m is also shown in grey for each gene.

Collected neurons showed a high expression of the gene encoding for vGlut1, which is specific for excitatory glutamatergic neurons; at the same time, a negligible expression of the marker for inhibitory circuits was detected (**Figure 7**). This result clearly indicated that collected cells were mainly excitatory neurons. I then checked the layer specificity of the LCM analyzing the gene expression of specific cortical layer markers (**Figure 8**). Gene-expression values were normalized for reference genes and expressed as an increase or decrease relative to the *inter-run calibrator* (see **section 2.4.7.1**) (Hellemans et al., 2008; Rieu and Powers, 2009).

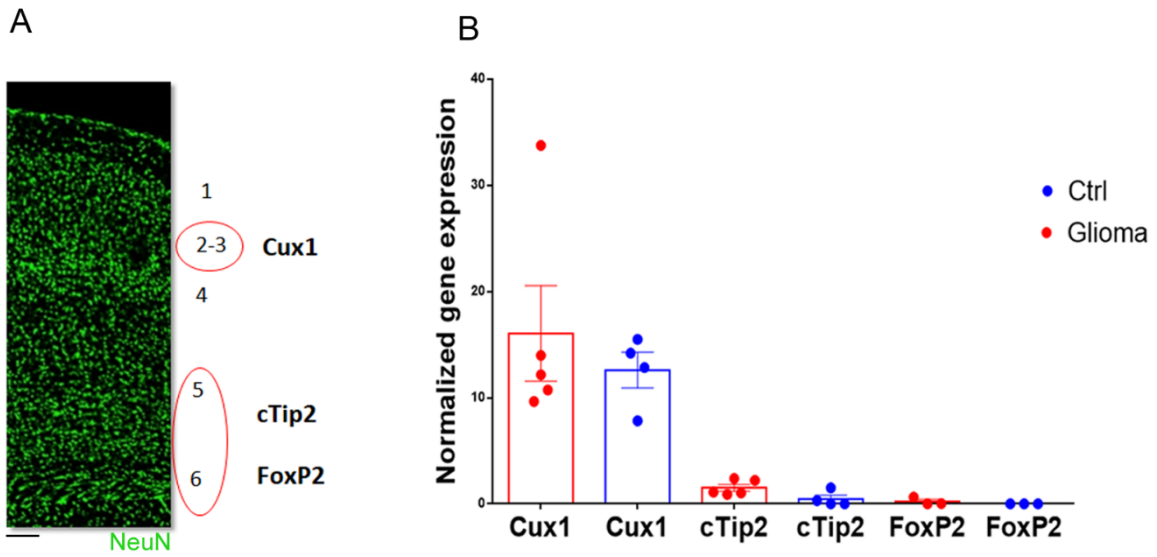

Figure 8 ***Layer specificity of microdissected neurons***

A*) On the left, representative immunostaining of a coronal section of primary visual cortex (neurons in green). On the right, layer organization of primary visual cortex and corresponding layer-specific genes included in the panel: Cux1 is a marker of the layer 2/3, cTip2 of the layers 5-6 and FoxP2 of the inner layer 6. Scale bar 100μm* ***B****) Gene expression analysis of layer specific markers detected by quantitative Real-Time PCR in neurons dissected from glioma-bearing (Glioma, red) and sham (Ctrl, blue) mice. Gene expression values were normalized on housekeeping GAPDH and β-actin mRNA and expressed as an increase or decrease relative to the calibrator. The mean ± s.e.m is also shown.*

The dissected neurons showed a high expression of Cux1 with respect to the markers of the deeper layers, confirming the layer specificity of the LCM for layers 2/3 (**Figure 8**). Next, an overall analysis of the gene expression of the panel was done in order to detect alterations induced by tumor growth, comparing glioma-bearing mice with controls (**Figure 9A, B**). Among all genes (**Figure 9A**), two targets were significantly altered during glioma progression: the Gabra1 gene, encoding for the GABA A receptor subunit α1, and the gene encoding for the pre-synaptic protein SNAP25. Both genes appeared down-regulated in peritumoral excitatory neurons of layers 2/3 in glioma-bearing mice (**Figure 9B**). These alterations might result because of an increased hyper

excitability of peritumoral tissues (Armstrong et al., 2016; Corradini et al., 2014; Köhling et al., 2006; Marco et al., 1997).

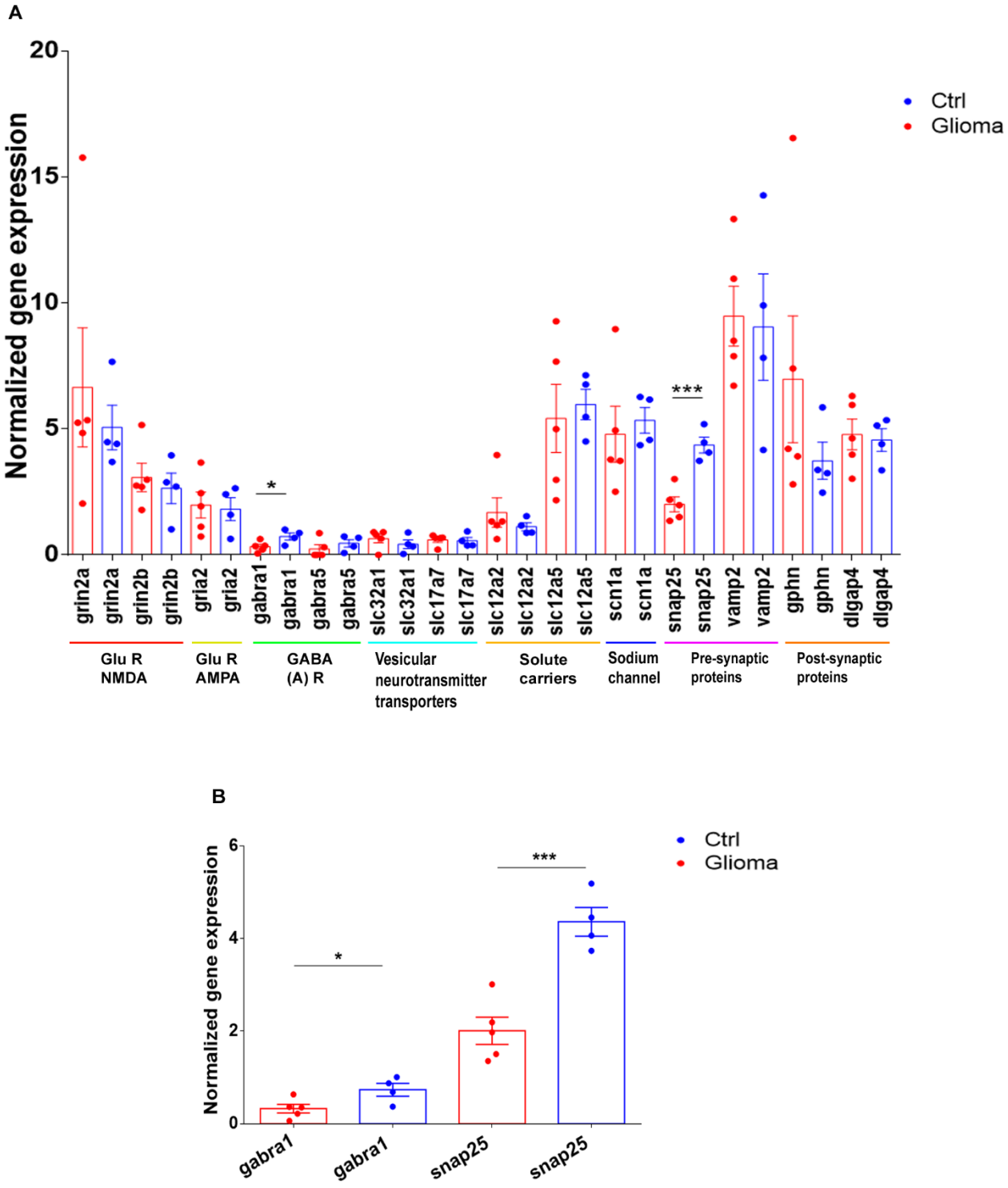

Figure 9 ***Pre and post synaptic alterations in peritumoral excitatory neurons***

A*) Expression analysis of a customized panel of genes detected by quantitative Real-Time PCR in dissected neurons from glioma-bearing (Glioma, red) and control (Ctrl, blue) mice. The coloured bars under the histogram represent a classification of genes: red= Glu R NMDA (Glutamate NMDA receptor subunit), yellow= Glu R AMPA (Glutamate AMPA receptor subunit), green= GABA A R (GABA A receptor subunit), ciano= Vesicular neurotransmitter transporters, ocra= solute carriers, blue= sodium channel, pink= pre-synaptic proteins, orange= post-synaptic proteins.* ***B****) Magnification of the genes with a significant alteration in the expression. Gene expression values were normalized on housekeeping GAPDH and β-actin mRNA and expressed as an increase or decrease relative to the calibrator. The mean ± s.e.m is also shown.*

3.1.4. LFP alterations in glioma-bearing mice

I also evaluated the presence of a hyper-excitable peritumoral tissue in glioma-bearing animals analysing LFPs recordings in freely moving mice (**Figure 10A**). In particular, I recorded ictal events in 80% of glioma-bearing mice. Frequency of seizures increased along with tumor progression reaching an average maximum number of 27 ictal events per hour (**Fig 10B**, **D**). Moreover, all glioma animals showed a significant interictal activity that augments during tumor progression, counting from 214 to 884 interictal events in a single recording session (**Fig 10C**, **E**).

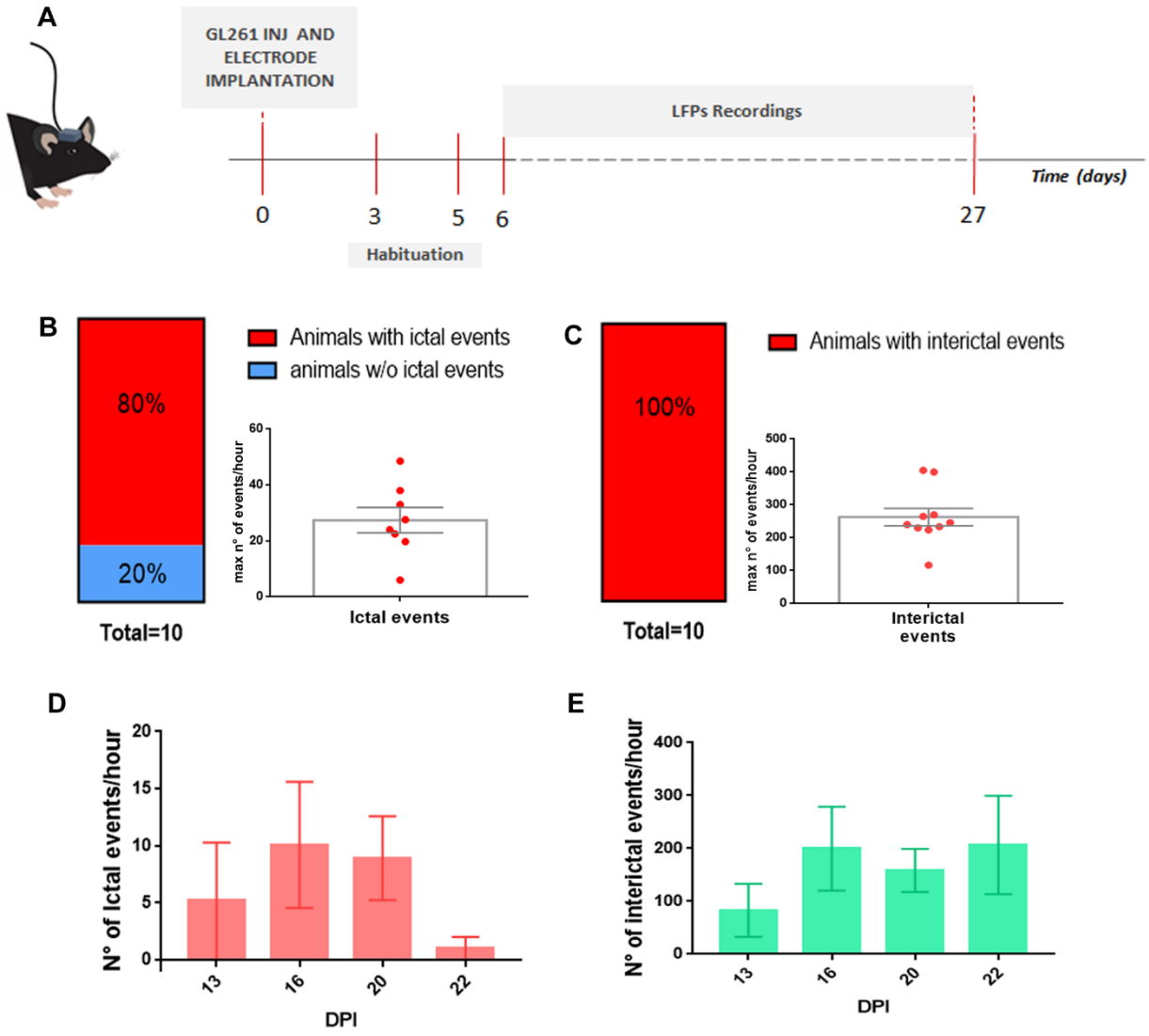

Figure 10 ***Glioma-bearing mice develop ictal and interictal activity during tumor growth***

A*) On the left, representative image of a freely moving glioma-bearing mouse during an EEG recording session. On the right, experimental protocol.* ***B****,* ***C****) On the left, fraction of glioma-bearing mice with and w/o ictal (****B****) and interictal (****C****) events (n total of animals=10) and on the right, quantification of ictal (****B****) and interictal (****C****) activity in the recording session with maximum number of events for each animal.* ***D****,* ***E****) Quantification of ictal (****D****) and interictal (****E****) events during tumor growth. (DPI=day post glioma injection). The mean ± s.e.m is also shown.*

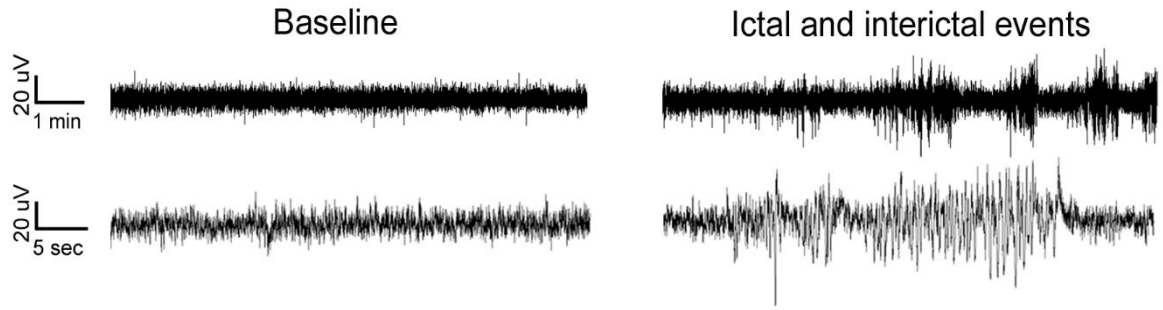

Figure 11 ***Altered LFPs during tumor progression***

Representative LFP recordings in glioma-bearing mice. Traces at the bottom represent a 60 sec epoch on an enlarged scale to better appreciate seizure-like events.

After, I analysed the LFP power spectra alterations for each glioma-bearing mouse in order to understand whether ictal and interictal events might be related to a modified oscillation of specific power bands (**Figure 12**). I focused my attention on the δ (0.5-4 Hz) andα (8-12Hz) bands, which we previously found being altered in glioma-bearing mice with respect to controls. I looked at the relative power 5 seconds before each ictal event and for all the duration of seizures and I found a significant increase of the δ band power and a strong decrease of the α band power with respect to baseline (i.e. LFPs without seizure-like events) (**Figure 12A-D**). Consistently, the 20% of glioma-bearing mice that didn't have any ictal activity in their LFPs also did not show any alteration in the power spectra of α and δ bands (**Figure 12A**, **C**).

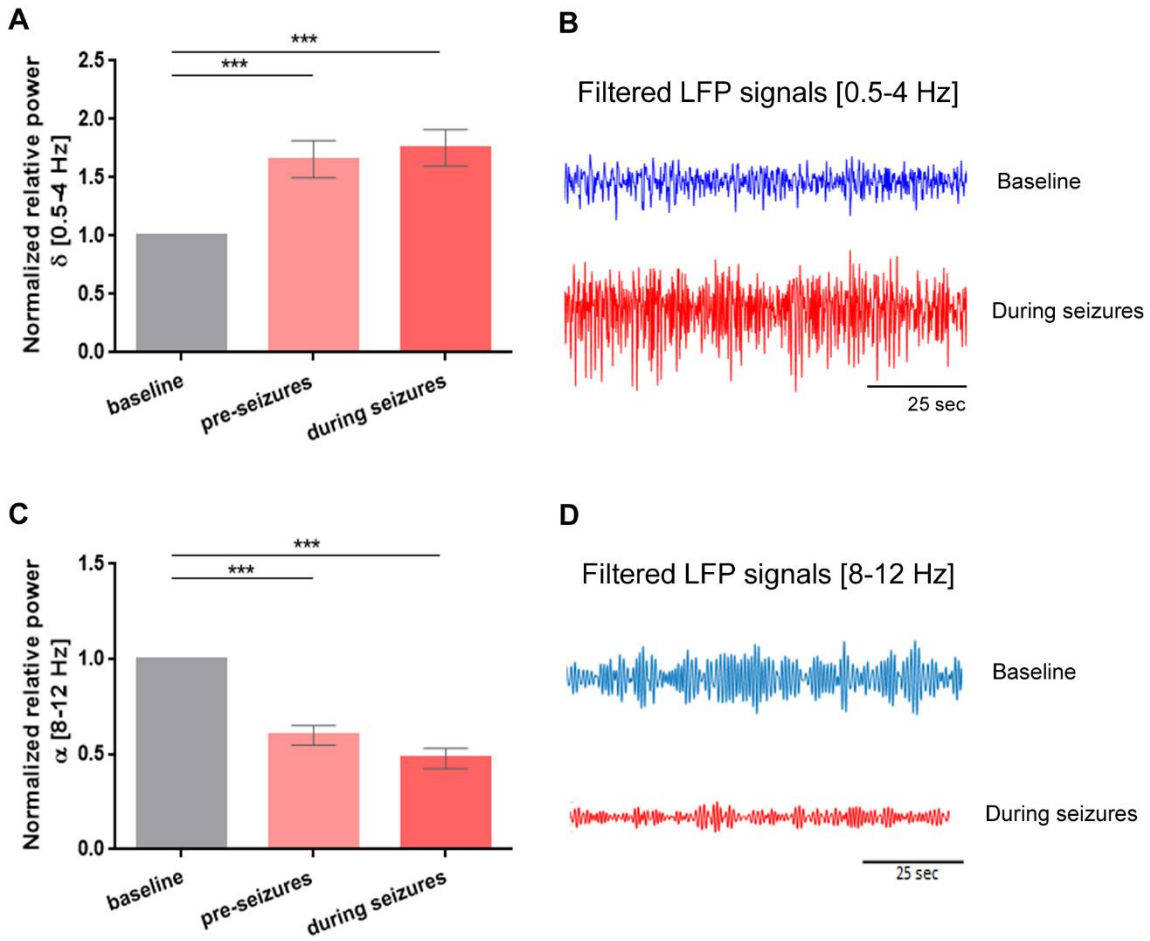

Figure 12 ***Altered δ and α bands in hyper-excitable peritumoral neurons***

A, ***C***) *Normalized relative power respect to the baseline of δ (**A**) and α (**C**)bands 5 seconds before ictal events (pre-seizures) and during ictal events (during seizures). The mean ± s.e.m is also shown. (Student's t-test, ***p<0.0008).* ***B***, ***D***) *representative LFP signal filtered for δ and α band frequencies during baseline and ictal-event.*

The enhancement in the relative power of δ band and the disruption of α band observed in glioma-bearing mice could be related with the deterioration of inhibitory circuits in the peritumoral tissues (Yu et al., 2020), that are known to be important regulators of δ and α oscillations (Gips et al., 2016; Klimesch, 2012; Righes Marafiga et al., 2020). Hence, the reported results introduce the relevance of an altered pattern of oscillations as a key indicator of peritumoral tissue hyper-excitability (Schönherr et al., 2017).

3.2. Impact of neural activity on glioma proliferation

The second part of my PhD thesis aims to contribute novel data on the role of neural activity in controlling glioma cell behaviour. Important studies of the latest years have pointed out that excitatory pyramidal neurons promote glioma proliferation (Venkatesh et al., 2015, 2017), suggesting that neuronal activity facilitates tumor progression through activity-dependent AMPA-mediated synapses that drive and increase tumor growth (Venkataramani et al., 2019; Venkatesh et al., 2019). However, while the excitatory system, guided by glutamate, seems to be exploited by tumor for its progression and sustenance (Sontheimer, 2008b; Venkatesh et al., 2015), the inhibitory system, guided by γ-aminobutyric acid (GABA), might have an opposite role (Blanchart et al., 2017; D'Urso et al., 2012; Tewari et al., 2018; Young and Bordey, 2009).

The experiments that will follow aimed at i) dissecting the contribution of specific neural cell types on tumor proliferation, by comparing the effects of optogenetic stimulation of pyramidal cells vs. fast-spiking, GABAergic interneurons and ii) studying the effect of visual afferent input on the proliferation of tumor mass placed in the occipital cortex.

3.2.1. Neuronal fibers infiltrate the glioma mass

I first evaluated the structural interactions between glioma cells and adjacent neurons. It is known that GL261 cells typically originate a nodular tumor that exert a compressive force on surrounding tissues (Seano et al., 2019), so I investigated whether some neural components could be present inside the solid tumor mass. GL261 cells were transplanted into the mouse visual cortex of C57BL/6J mice.

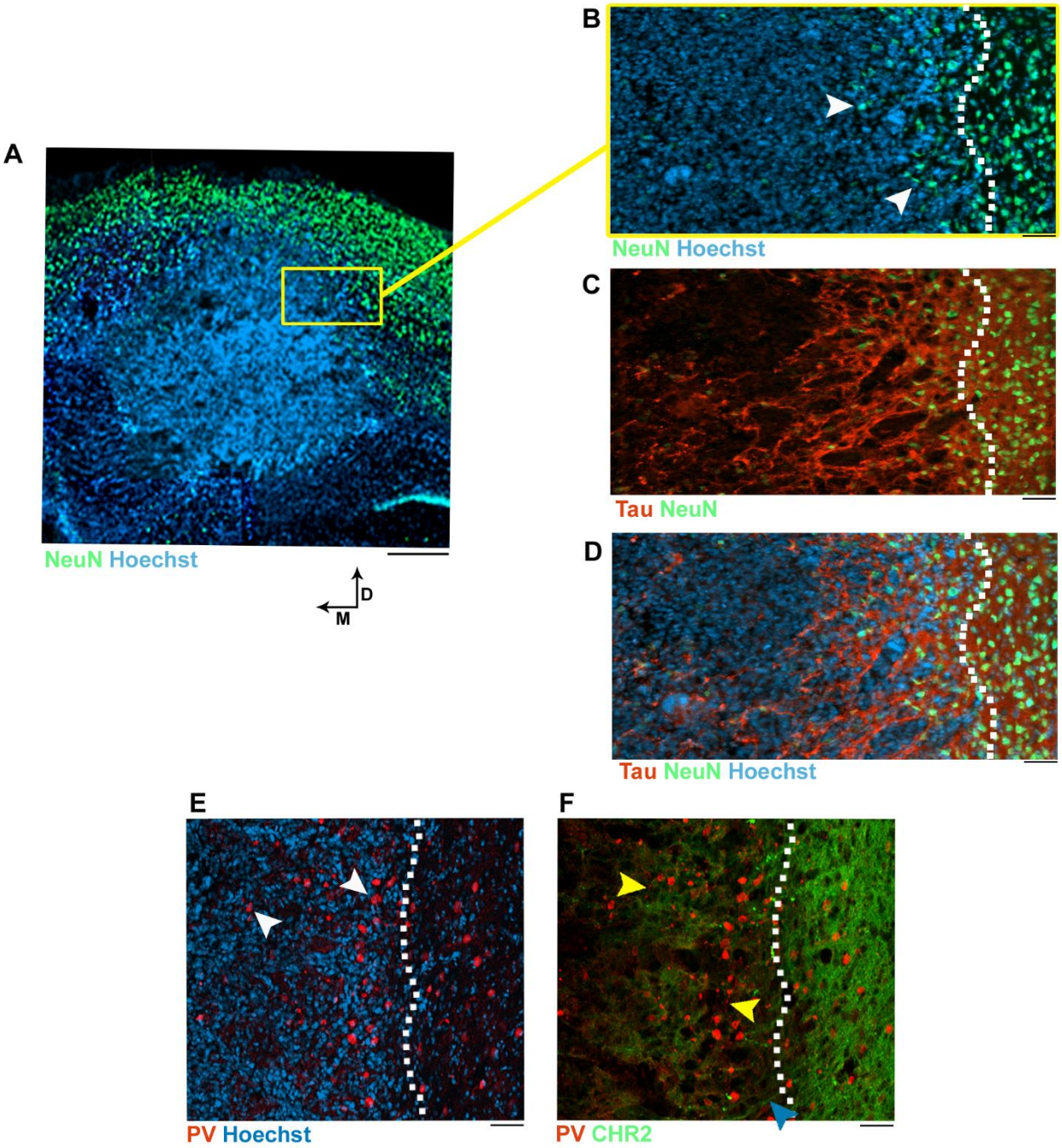

Figure 13 ***Neuronal processes penetrate the glioma mass***

A*) Representative tumor mass (Hoechst staining, blue) 14 days after GL261 cell transplant into the primary visual cortex. D, dorsal; M, medial. NeuN labelling is in green. Scale bar, 200 µm.* ***B-F****) High magnification images of a region at the border of the tumor mass. Dotted lines represent the presumptive tumor border. Scale bars, 100 µm.* ***B****) Neurons (in green; arrowheads) at the border of glioma mass (blue).* ***C****) Immunostaining for the axonal marker Tau (red) and NeuN (green) showing axonal fibers and neurons infiltrating the tumor.* ***D****) Triple labelling Tau (red)-NeuN (green)–Hoechst (blue).* ***E****) Parvalbumin (PV) interneurons (red, arrowheads) inside the glioma mass (blue).* ***F****) Triple staining with Hoechst dye (blue), PV (red) and EYFP (green). Note processes of Parvalbumin interneurons (indicated by yellow arrowheads) and excitatory neurons (cyan arrowhead) within the border of glioma.*

At day 14 after tumor graft, the tumor mass was clearly visible in the injected hemisphere (**Figure 13A**). Coronal brain sections were stained for the neural marker NeuN and the axonal marker Tau (**Figure 13B-D**).

I found a significant axonal staining within the glioma mass, indicating a physical interaction between glioma cells and neuronal processes (**Figure 13B-D**). Next, I investigated whether both inhibitory and excitatory neurons equally contribute to neural infiltration within the tumor mass (**Figure 13E-F**). In order to investigate the excitatory neurons, I took advantage of Thy1-ChR2-EYFP mice inoculated with GL261 cells into the visual cortex; Thy1-ChR2-EYFP mice express the light-gated cation channel channelrhodopsin-2 and enhance yellow fluorescent protein selectively in pyramidal neurons. Brain sections were also stained for parvalbumin (PV), a marker of fast-spiking, GABAergic interneurons (Deidda et al., 2015).The neuroanatomical analysis revealed processes and cell bodies of both parvalbumin and pyramidal neurons infiltrating within the tumor mass (**Figure 13E-F**).

3.2.2. Optogenetic stimulation of pyramidal, excitatory neurons promotes glioma growth

Previous studies have shown that activation of cortical excitatory neurons through a 20 Hz optogenetic stimulation increases glioma proliferation in transgenic immunodeficient mice bearing patient-derived orthotopic xenografts of pediatric cortical glioblastoma (Venkatesh et al., 2015, 2017).

Here, I repeated the single stimulation protocol previously employed by other authors (Venkatesh et al., 2015) (see **section 2.5.**1) in GL261-inoculated Thy1-ChR2-EYFP transgenic mice (**Figure 14B**) (Spalletti et al., 2017). Animals were injected with GL261 cells in the motor cortex and randomized to receive either real or sham (i.e. lights off) stimulation (**Figure 14A**). After this protocol, the proliferating cells were assessed in both experimental group by BrdU incorporation (**Figure 14C**).

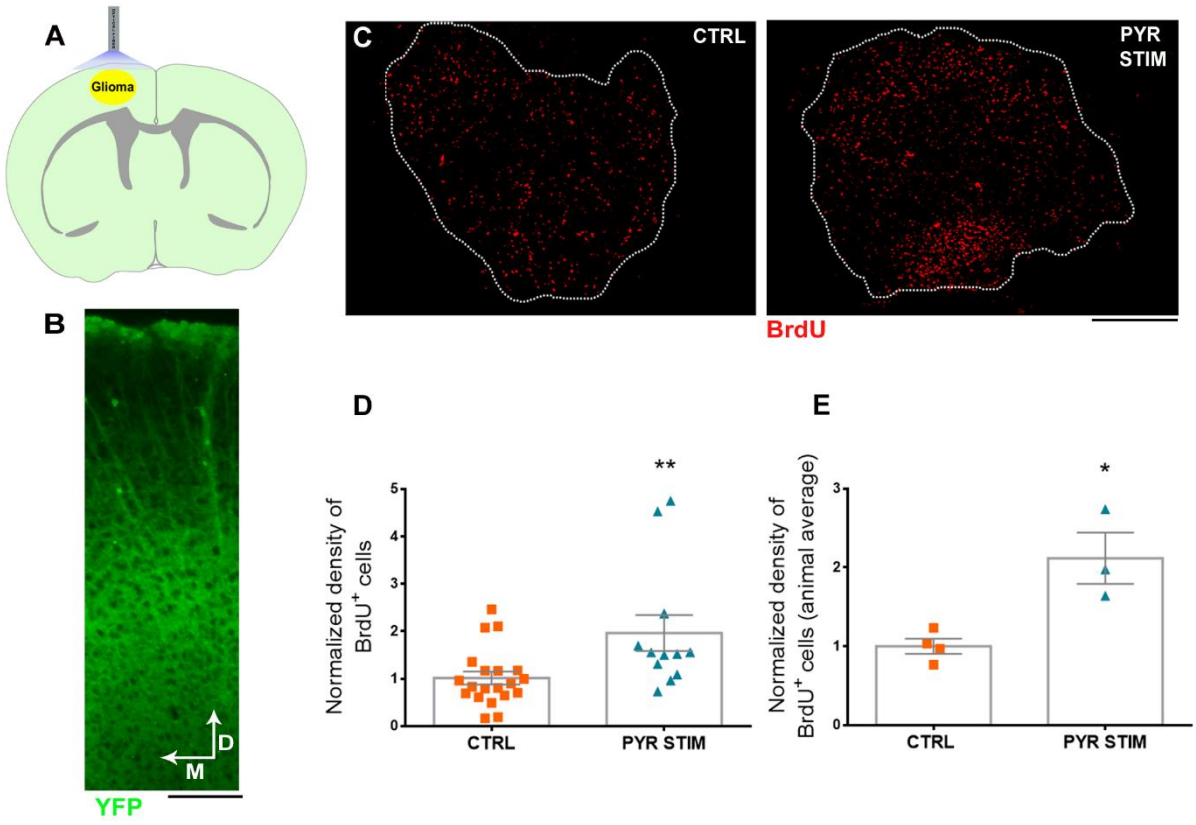

Figure 14 ***Optogenetic stimulation of neural activity promotes glioma proliferation.***

A*) Schematic brain section showing the location of the tumor in motor cortex and the optic fiber for optogenetic stimulation in vivo. The green shading indicates widespread expression of ChR2 in pyramidal neurons of the transgenic Thy1-ChR2-EYFP mouse.* ***B****) Coronal section through the motor cortex showing expression of ChR2-EYFP (green) mainly in layer V. Scale bar, 200 µm.* ***C****) Representative staining for BrdU (red) in the motor cortex, 14 days after GL261 injection. CTRL, control with sham stimulation; PYR STIM, mouse with optogenetic stimulation of pyramidal neurons. The dotted lines indicate tumor borders. Scale bar, 200 µm.* ***D, E****) Normalized fraction of tumor area occupied by BrdU-positive cells in control (CTRL; n=20 slices from 4 animals) and stimulated mice (PYR STIM; n=12 slices from 3 animals): data from single slices (****D****) and averaged per animal (****E****). The mean ± s.e.m is also shown in grey for each group (Student's t-test, **p=0.009 and *p=0.012, for D and E, respectively).*

Quantitative analysis of the density of BrdU-labelled cells showed that the 20 Hz optogenetic stimulation significantly increased tumor proliferation, either considering the single values from all the brain sections examined within each experimental group (**Figure 14D**, Student's t-test, p=0.009) and the animal average (**Figure 14E**, Student's t-test, p=0.012), confirming the proliferative effect described in literature (Venkatesh et al., 2015).

3.2.3. Optogenetic stimulation of Parvalbumin-positive, GABAergic interneurons restrains glioma proliferation

It is well known that GABA plays an important role in maintaining the balance of cortical circuits (Greenfield, 2013). Recent evidences have suggested that this neurotransmitter could exert a completely novel role, which is controlling glioma proliferation (Blanchart et al., 2017). Thus, I asked whether the selective stimulation of PV-positive, fast-spiking interneurons could have an impact on tumor growth. PV-cre mice (Cardin et al., 2009; Mariotti et al., 2018) received a

double injection of an AAV vector to allow the expression of ChR2 in PV interneurons (**Figure 15B**) surrounding the tumor mass. A week later, those mice were injected with GL261 cells in the motor cortex and randomized into two groups, to receive either real or sham (i.e. lights off) stimulation (**Figure 15A**). The neuroanatomical analysis indicated that over 80% of the PV cells were positive for mCherry in the transduced area (**Figure 15B**). Proliferating tumor cells were labelled by both Ki67 (**Figure 15C**) and BrdU immunolabeling.

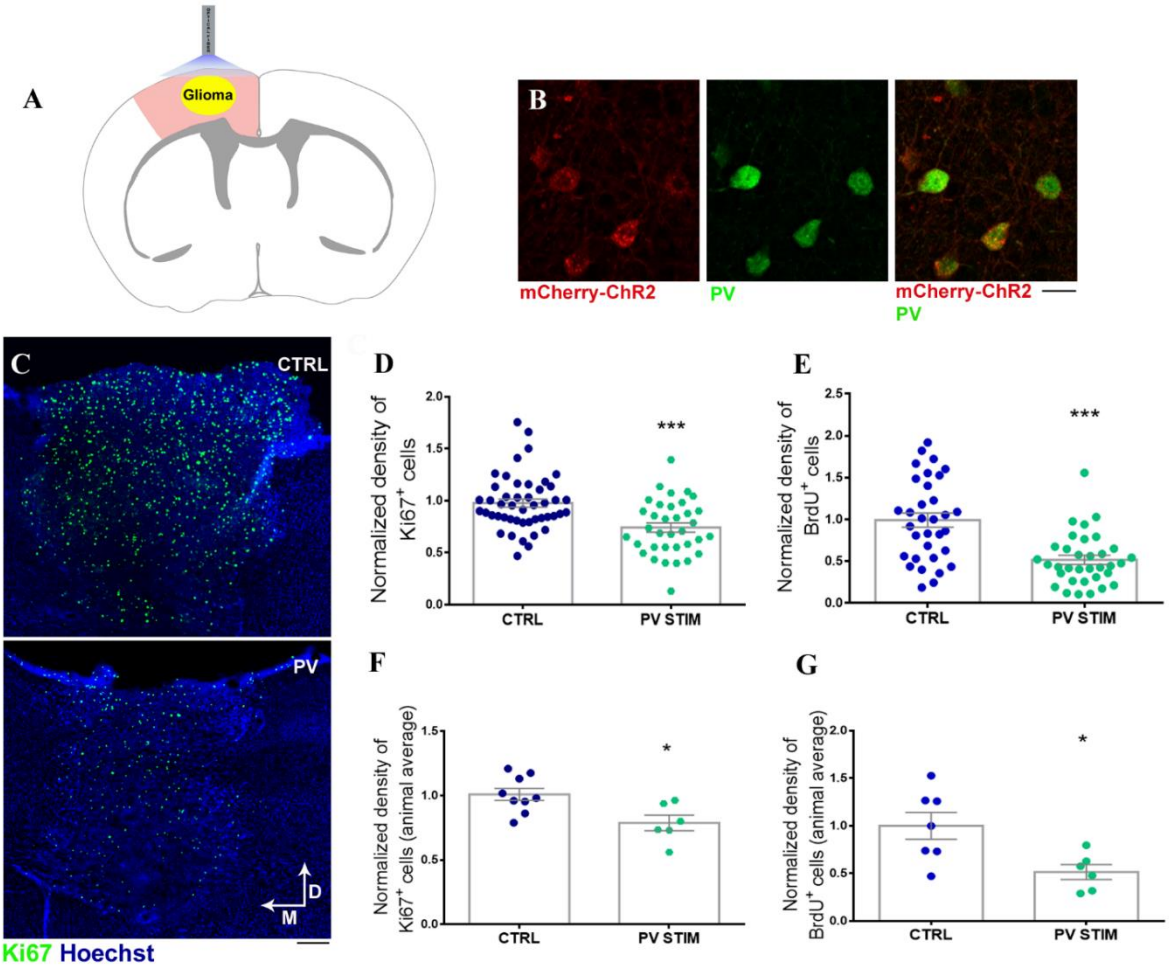

Figure 15 ***Optogenetic stimulation of Parvalbumin interneurons inhibits glioma proliferation.***

A*) Schematic cartoon illustrating the optogenetic stimulation of PV interneurons in a coronal section of the motor cortex. The red shading in the cortex indicates localized transduction of PV interneurons with the AAV vector.* ***B****) Representative images of a cortical section in a PV-Cre mouse transduced by AAV carrying mCherry-ChR2. The section is double labelled for mCherry (red) and Parvalbumin (green). Colocalization is shown in the panel at right. Scale bar, 50 µm.* ***C****) Representative images of proliferating Ki67-positive cells (green) within the glioma mass (blue) in the motor cortex of sham (CTRL, top) and stimulated (PV STIM, bottom) mouse 14 days after glioma injection. M, medial; D, dorsal. Scale bar, 100 µm.* ***D-G****) Normalized fraction of tumor area occupied by Ki67- (****D, F****) and BrdU- (****E, G****) positive cells in control (CTRL: Ki67, n=47 slices from 9 animals; BrdU, n=33 slices from 7 animals) and stimulated mice (PV STIM: Ki67, n=35 slices from 6 animals; BrdU, n=35 slices from 6 animals). Data from single slices (****D, E****) and averaged per animal (****F, G****). The mean ± s.e.m is also shown in grey for each group. (Student's t-test, ***p<0.001, *p=0.012 for F, *p=0.015 for G).*

The data clearly showed that 40 Hz optogenetic stimulation of PV

interneurons restrains tumor proliferation, considering either single slices (Student's t-test, ***p < 0.0001; **Figure 15D, E**) or the average value for each animal (Student's t-test, *p<0.05; **Figure 15F, G**).

Thus, a selective stimulation of fast-spiking interneurons reduces the density of proliferating cells in the tumour mass.

3.2.4. Afferent sensory input bidirectionally regulates tumor proliferation

Having established the distinct roles of pyramidal and GABAergic cells in the control of glioma growth, I next investigated the impact of a coordinated activation of excitatory and inhibitory neurons triggered by sensory experience. For this experiment, tumors were placed in the occipital cortex, as afferent sensory input can be easily downregulated via dark rearing (Gianfranceschi et al., 2003) or upregulated with controlled visual stimulation (Restani et al., 2009).

I implanted mice with GL261 cells in the visual cortex and all animals were maintained in a normal light/dark cycle until day 11. They were then randomized to remain in standard laboratory conditions (standard laboratory, SL), placed in total darkness (dark rearing, DR) or visually stimulated during the light period (visual stimulation, VS) by placing them daily for 8 hr in front of gratings of various contrasts as well as temporal and spatial frequencies (**Figure 16A**). Stainings for cell proliferation were conducted on day 14.

We found that dark rearing (DR) enhanced the density of proliferating cells in the tumor mass, whereas visual stimulation (VS) dampened it (**Figure 16B, D**). The statistical analysis demonstrated a bidirectional regulation of glioma proliferation by afferent sensory input. As in the previous experiments, I first performed the analysis by cumulating data from all the brain sections examined

within each experimental group (for Ki67 and BrdU: One-way ANOVA followed by Dunnett's test, DR vs SL $p<0.001$, VS vs SL $p<0.0025$; **Figure 16C, E**). Secondly, I performed the analysis on a per mouse basis, i.e. using the average densities measured in the animals reared in a specific condition (for Ki67 and BrdU: One-way ANOVA followed by Dunnett's test, DR vs SL $p<0.001$, VS vs SL $p<0.05$; **Figure 16F, G**). To further validate these results, I also calculated the proliferation index at the border of the tumor mass on all the analysed coronal slices, by counting the proportion of tumor cells expressing Ki67 over the total number of Hoechst-stained nuclei in each region of interest (**Figure 16H, I**). Also in this case, whereas cortical inhibition via light deprivation (DR) increased the number of dividing cells, visual stimulation (VS) reduced the proliferation index with respect to control glioma-bearing animals reared in standard light conditions (SL) (Student's t-test, DR vs SL $p<0.001$, VS vs SL $p<0.05$; **Figure 16L**). Altogether, these data provide solid evidence that afferent sensory input impact on tumor growth in the GL261 glioma model.

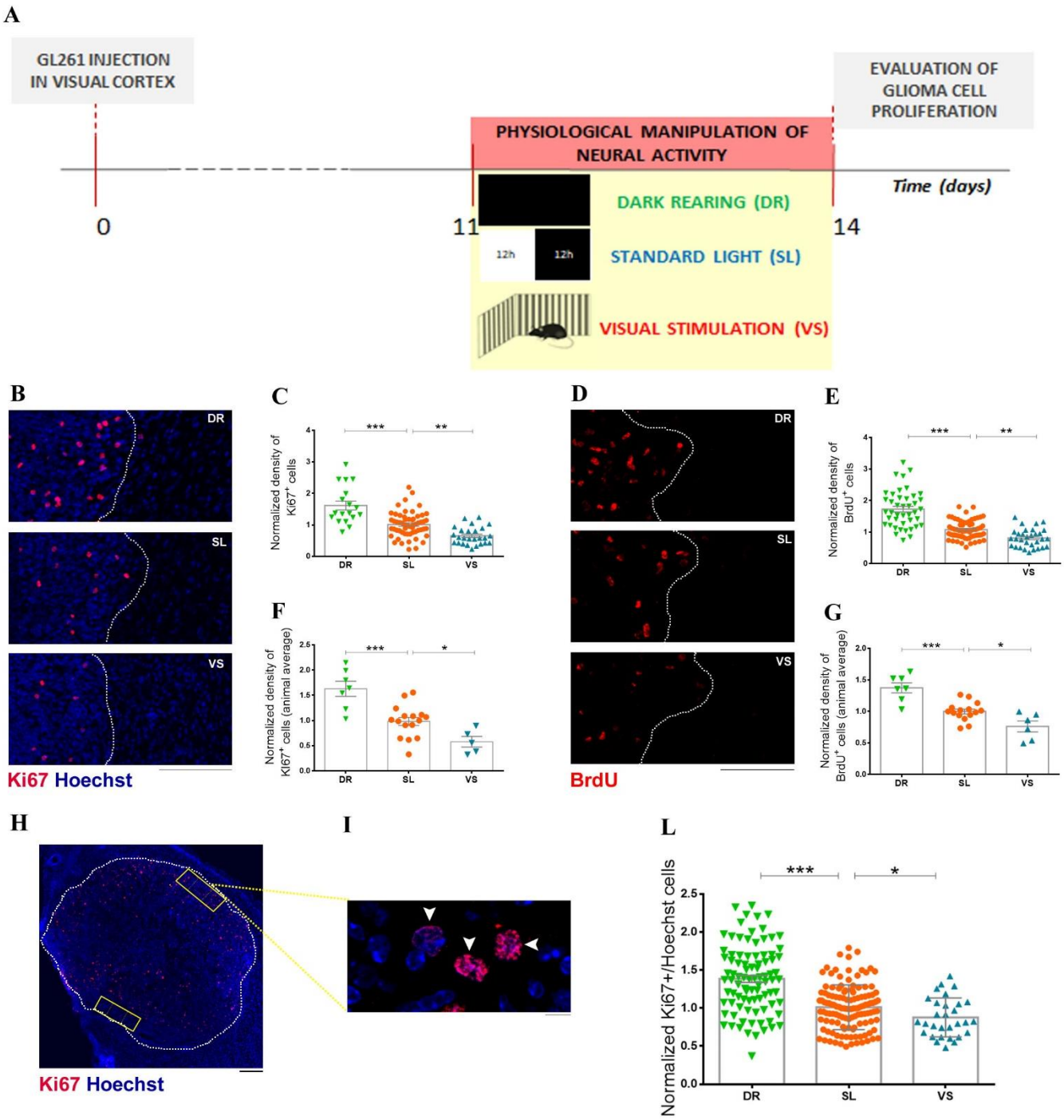
A
GL261 INJECTION IN VISUAL CORTEX
EVALUATION OF GLIOMA CELL PROLIFERATION
PHYSIOLOGICAL MANIPULATION OF NEURAL ACTIVITY
Time (days)
0
11
14
DARK REARING (DR)
12h
12h
STANDARD LIGHT (SL)
VISUAL STIMULATION (VS)
B
DR
SL
VS
Ki67 Hoechst
C
Normalized density of Ki67+ cells
***
**
DR
SL
VS
D
DR
SL
VS
BrdU
E
Normalized density of BrdU+ cells
***
**
DR
SL
VS
F
Normalized density of Ki67+ cells (animal average)
***
*
DR
SL
VS
G
Normalized density of BrdU+ cells (animal average)
***
*
DR
SL
VS
H
Ki67 Hoechst
I
L
Normalized Ki67+/Hoechst cells
***
*
DR
SL
VS

Figure 16 ***Manipulation of physiological activity bidirectionally impacts glioma cell proliferation***

A*)Experimental protocol.* ***B, D****) Representative immunostainings for Ki67 (****B****) and BrdU (****D****) (red) within the tumor mass in the visual cortex of glioma-bearing mice, 14 days after GL261 cell transplant. Dotted line represents tumor borders. DR, dark rearing; SL, standard light conditions; VS, visual stimulation. Scale bar, 200 µm.* ***C, E, F, G****) Normalized fraction of tumor area occupied by proliferating cells in the different experimental groups: data from single slices (****C,E****) and averaged per animal (****F,G****) (DR: Ki67, n=18 slices from 7 animals; BrdU, n=42 slices from 7 animals; SL: Ki67, n=58 slices from 16 animals; BrdU, n=63 slices from 15 animals; VS: Ki67, n=26 slices from 5 animals; BrdU, n=31 slices from 6 animals). The mean ± s.e.m is shown in grey for each group. (One-way ANOVA followed by Dunnett's test , *p < 0.05, **p < 0.025, ***p < 0.001).* ***H****) Representative immunostaining for Ki67 showing proliferating cells (red) at the border of tumor mass in the visual cortex. Blue: Hoechst counterstaining. Two ROI (regions of interest) for the cell count at the border of the tumor mass are indicated in yellow. Scale bar, 200 µm.* ***I****) High magnification of dividing (arrowhead) and non-dividing (blue) cells in a ROI. Scale bar, 10 µm.* ***L****) Proliferation index indicating the fraction of Ki67-positive cells with respect to all Hoechst-stained nuclei (DR, n=90 slices from 6 mice; SL, n=125 slices from 7 mice; VS, n=30 slices from 3 mice). The mean ± s.e.m is shown in grey for each group. (Student's t-test, *p < 0.05, ***p < 0.001).*

2.6.13. Blockade of synaptic transmission via BoNT/A enhances glioma cell proliferation

In previous experiments, I showed that a sensory deprivation (i.e. dark rearing, DR) enhanced glioma proliferation. To further exacerbate visual deprivation, I decided to completely block synaptic activity via Botulinum Neurotoxin A (BoNT/A). Mice were implanted with GL261 cells into the visual cortex and 7 days after the graft, they received injections of BoNT/A or vehicle (rat serum albumin, RSA) (**Figure 17A**). BoNT/A is a bacterial protease that exerts a long-lasting blockade of synaptic transmission at central level by cleaving SNAP-25 (synaptosomal-associated protein of 25 KDa), an essential component of the SNARE complex (Caleo et al., 2013, 2018; Ferrari et al., 2011; Restani et al., 2012b; Rossetto et al., 2006; Turton et al., 2002).

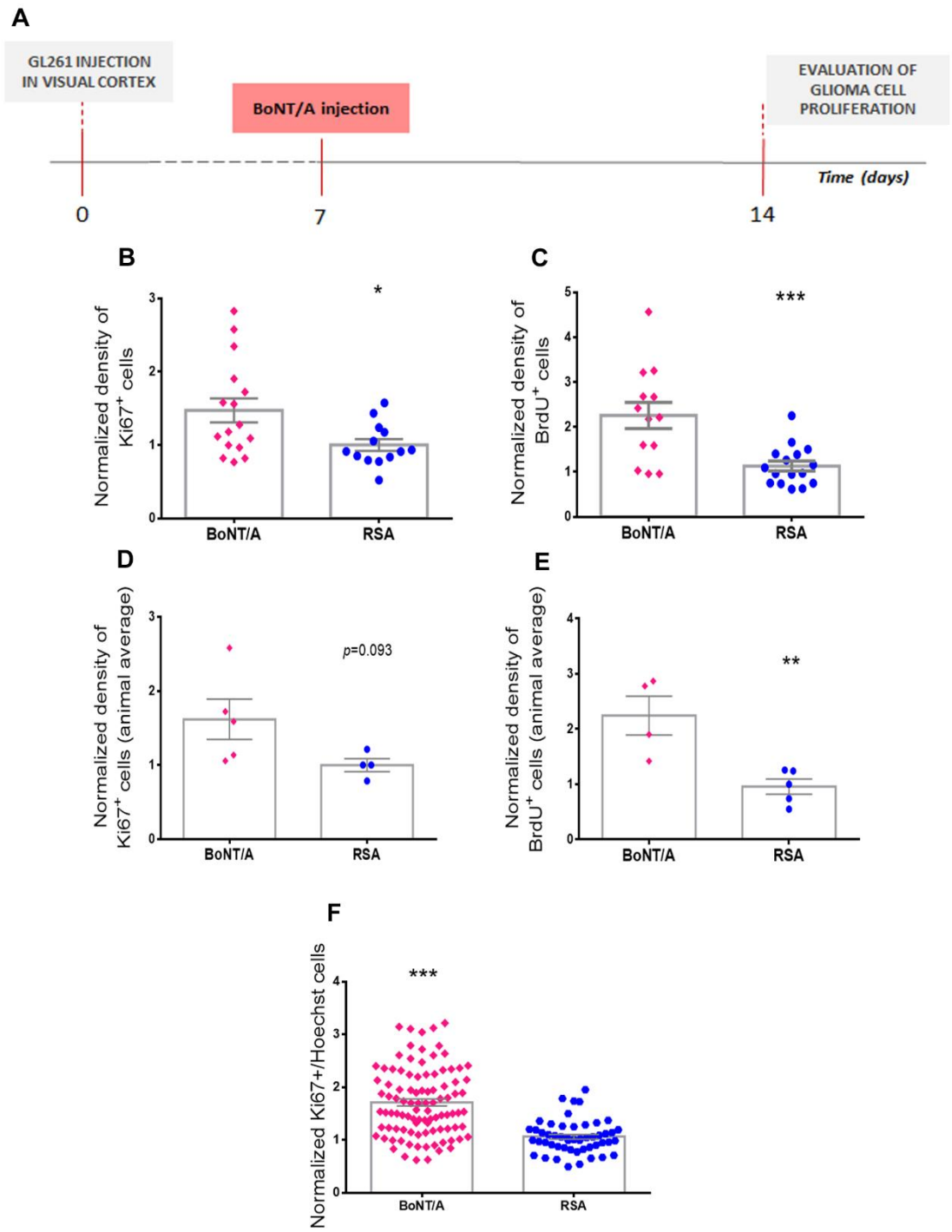

Figure 17 ***Blockade of cortical synaptic activity affects glioma cell proliferation***

A) *Experimental protocol.* ***B-E)*** *Normalized fraction of tumor area occupied by proliferating cells in the different experimental groups: (**B, C**) data from single slices (BoNT/A: Ki67, n=16 from 4 animals; BrdU, n=13 from 4 animals; RSA: Ki67, n=13 from 4 animals; BrdU, n=16 from 5 animals) (**D, E**) and averaged for animal.* ***F)*** *Proliferation index indicating the fraction of Ki67-positive cells with respect to all Hoechst-stained nuclei (BoNT/A, n=98 from 5 mice; RSA, n=51 from 4 mice). The mean ± s.e.m is shown in grey for each group. (Student's t-test , *p < 0.05, *p < 0.025, ***p < 0.001).*

I quantified the density of proliferating cells within the tumor area at day 14 by immunostaining for Ki67 and BrdU and I found that the disruption of cortical neurotransmission increased glioma proliferation considering either single slices (**Figure 17B, C**) and data averaged for animal (**Figure 17D, E**) (Student's *t*-test, *p=0.02, **p=0.009, ***p=0.0006). While the analysis of Ki67 positive cells on a single animal basis failed to reach statistical significance, there was an evident trend (p = 0.093). Indeed, the evaluation of the proliferation index (Figure 16**F**) confirmed these results, i.e. the enhancement of tumor proliferation following synaptic blockade.

2.6.14. The effects of sensory input on tumor proliferation are region-specific

The data reported above demonstrated that the manipulation of visual afferent input controls glioma cell proliferation. To determine whether these effects remain localized to the visual cortex, or involve secreted factors which may act at distance, animals implanted with GL261 glioma cells into the motor cortex were subjected to visual deprivation via dark rearing (**Figure 18A** from day 11 to day 14 after tumor injection. In this experimental setting, the tumor that develops in the motor area resulted unaffected by light deprivation **Figure 18B-E**, because had the same proliferation rate with respect to the one grown in glioma-bearing mice reared in standard light conditions (SL). The quantitative analysis showed no significant differences between deprived (DR) and standard light (SL) mice in the proliferation rates, considering both single slices (**Figure 18B, C**) and animal average (**Figure 18D, E**) measured via the density of both Ki67- (**Figure**

18B, D) and BrdU- (**Figure 18C, E**) positive cells (Student's t-test, p>0.05; **Figure 18B-E**).

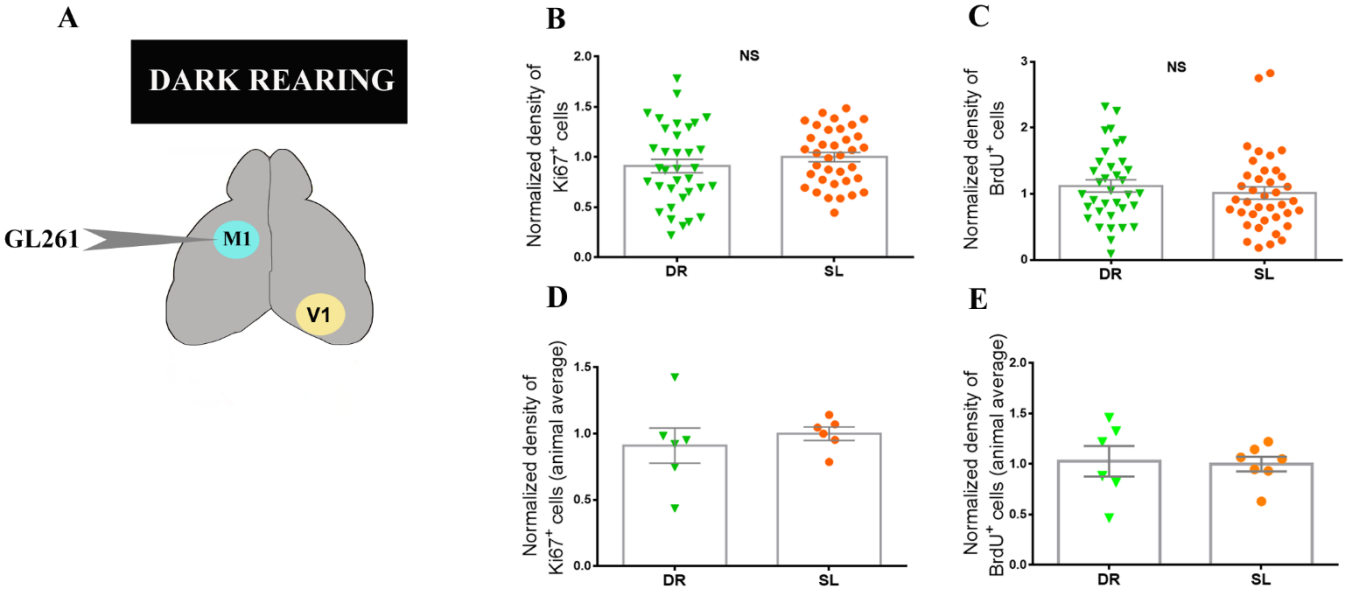

Figure 18 ***Dark rearing has no impact on tumor proliferation when glioma is located in motor cortex.***

A*) Schematic drawing of the experimental protocol: mice injected with GL261 cells in the motor cortex (M1) were reared in total darkness to inhibit visual cortex activity. V1, primary visual cortex* ***B, C****) Normalized fraction of tumor area occupied by proliferating Ki67+ (****B****) and BrdU+ (****C****) cells (Ki67: DR, n=35 slices from 7 animals; SL, n=36 slices from 6 animals; BrdU: DR, n=35 slices from 6 animals; SL, n=39 slices from 7 animals).* ***E****,* ***F****) Average values for each animal are reported. The mean ± s.e.m is shown in grey for each group (p > 0.05). NS, not significant.*

Taken altogether, these results indicate that the effect of visual manipulation on tumor proliferation is region-specific.

2.6.15. Sensory stimulation combined with temozolomide treatment delays the deterioration of visual responses induced by glioma growth

We next tested whether sensory stimulation can be exploited as an adjuvant to classical chemotherapy (i.e., temozolomide – TMZ) to delay neurological dysfunction in peritumoral neurons. As a readout of glioma growth, we used longitudinal measurements of visual evoked potentials (VEPs) in mice bearing

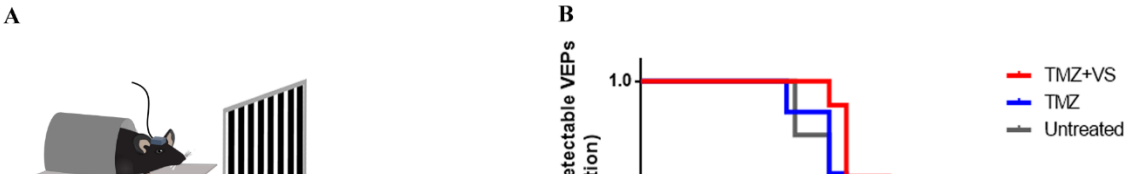

Figure 19 ***Visual stimulation combined with TMZ administration delays the impairment of cortical function due to glioma progression.***

A) *(Top) Schematic drawing of the experimental set-up for chronic VEP recordings in awake, head-restrained mice bearing GL261 cells in the visual cortex. (Bottom) Representative examples of VEP recordings at day 8 (left), 12 (middle) and 19 (right) following tumor inoculation. Note clear decrease of VEP amplitudes during tumor progression. N1, early negative peak; P1, positive peak.* ***B)*** *Fraction of animals with detectable VEPs in glioma-bearing animals that were left untreated (grey line, n = 6), administered with TMZ (blue line, n = 7), or given TMZ plus visual stimulation (TMZ+VS, red line, n = 9; **p=0.0023 with respect to untreated group).*

tumors in the occipital cortex.

Animals injected with GL261 cells into the visual cortex were implanted with a bipolar electrode (see **section 2.4.1**), to record VEPs from day 8 post injection (baseline recording) (**Figure 20A**).Glioma-bearing mice were either left untreated (n = 6) or given TMZ daily starting from day 12 after tumor inoculation (TMZ, n = 7). A subset of TMZ animals received also daily visual stimulation for 8 hours (TMZ+VS, n = 9). A progressive deterioration of the visual response was observed in all glioma-bearing mice (**Figure 20A**), consistent with the decay of VEP amplitude during glioma progression described in the **section 3.1.1**, but the

experimental groups showed different kinetics. Temozolomide monotherapy slightly protracted the time window of visual responsiveness, but the effect was not statistically significant (Log-rank test, p=0.17). The evaluation of VEP amplitudes demonstrated the maintenance of a detectable visual responsivity of peritumoral neurons in TMZ+VS group (Log-rank test, p=0.0023; **Figure 20B**). Thus, a therapy combining TMZ and visual stimulation delays the loss of neural responses in glioma-bearing mice.

Discussion

The results described in this thesis aim to provide novel evidences on the complex scenario of neuron-glioma interactions. This thesis is essentially divided in two main parts: the former is focused on the alterations that glioma growth causes on neurons, while the latter deals on the impact of cortical activity on tumor proliferation. Thanks to the longitudinal recordings of visual evoked potentials (VEPs), I monitored glioma progression and I demonstrated the effectiveness of a combination of sensory stimulation and TMZ delivery in slowing down glioma-induced neurological dysfunctions.

In all the experiments I employed intracortical transplants of GL261 cells, a widely used, well characterized, syngeneic and immunocompetent model of glioma (Oh et al., 2014). Moreover, these cells have already been employed in the lab for the study of glioma-induced neural dysfunctions (Vannini et al., 2016a, 2017). Limitations of this specific model include the fact that GL261 gliomas are not molecularly faithful to human GB (are driven by a set of mutations not observed in human GB) and typically grow as a large solid mass rather than a diffusely invasive cancer. Despite this growth pattern, I demonstrated robust

infiltration of neuronal processes within the tumor mass (**Figure 13**), which represent the structural basis for interactions between tumor cells and the neuronal microenvironment.

Effects of glioma progression on neural tissues

In the first part of the thesis, I aimed at investigating the functional and molecular impairments that occur in peritumoral neurons during glioma growth, making neuronal networks more excitable and prone to seizures. The ability of GL261 cells to induce alterations in visual function have already been reported by previous experiments of our group (Vannini et al., 2016a). It is known that life-threatening neurologic symptoms seen in patients with brain cancer get worse with the expansion of the tumor mass, resulting in morphological alterations of neurons (Seano et al., 2019); however, a detailed, longitudinal characterization of neural changes in the tumor microenvironment is still lacking in literature. Therefore, using a technique of chronic VEP recordings, I was able to longitudinally follow the activity of visual cortex in mice injected with GL261 (or PBS) in the same region (**Figure 3A**). The visual cortex was chosen as a recording site, since it can be easily activated by photic stimuli and because of the availability of well-established parameters that can be used to assess its functionality. After an initial phase of stimulus-dependent response potentiation (Cooke and Bear, 2014), the amplitude of neuronal response but not its latency progressively decayed along with tumor progression (**Figure 3B-E, Figure 4**). This result indicates that glioma growth do not impair axon myelinisation and conduction within the visual pathway (Walsh et al., 2005), but severely affects

axonal integrity and function of neurons in tumor-adjacent regions (You et al., 2012b).

Neurological damage is a hallmark of glioma pathogenesis and this include the disturbance of functional connectivity (Stoecklein et al., 2020). One reason is the impairment of the integrity of neuronal connections caused by glioma invasion into the brain. As demonstrated by a functional MRI study, altered connectivity throughout the brain was evident in patient affected by more aggressive forms of gliomas (Stoecklein et al., 2020). In my experiments, I detected spectral band alterations induced by tumor progression (**Figure 5**). These abnormal brain oscillations could be linked to the disruption of neural networks of brain regions connected to the site of the tumor, as recorded in humans (Stoecklein et al., 2020). In particular, looking at the difference in relative power of the spectral bands, I found a significant enhancement of δ band together with a trend of deterioration of α band in glioma-bearing mice. In physiological conditions, δ activity originates in cortical neurons (Tononi and Cirelli, 2012) with the function to synchronize their excitability state (Abel et al., 2013) and during wakefulness it is almost absent; however, it appears to be linked with a variety of neural disorders (Assenza et al., 2017). For instance, an increase in δ activity is detected either in patients with focal epilepsy and in patients with tumor-associated epilepsy, pathological conditions that share a common altered functional connectivity (Baayen et al., 2003; Douw et al., 2010; Lundstrom et al., 2019; Pellegrino et al., 2017). The data reported in this thesis showed that the increase in δ band is principally determined by the enhancement of 2-4 Hz oscillations, an hallmark shared with focal epilepsy patients (Lundstrom et al., 2019) (**Figure 5B**). This result may correlate with local synaptic strength, reinforced by the enhanced density of excitatory boutons detected in peritumoral

regions (Lundstrom et al., 2019; Yu et al., 2020). On the other hand, the α rhythm is generated in the thalamus but it is also prominently observed in cortical areas of the visual networks, where seems to play an inhibitory role (Haegens et al., 2011; Hanslmayr et al., 2005; Klimesch, 2012; Klimesch et al., 2007; Peterson and Voytek, 2017). Indeed, experiments on Rac1 cKO mice, model with a deficit of GABAergic interneurons, showed a decreased power in specific oscillations including α band (Kalemaki et al., 2018). The deterioration of α band is considered a peculiarity of diffuse cortical neuropathology and it has been found also in epileptic patients with a poor seizure control, whose EEG recordings are characterized by a shift of the α power band to lower frequencies (Abela et al., 2019). The cause of this phenomenon and its clinical relevance remain poorly understood but probably reflects cortical impairments that affect the correct cortico-thalamic communication (Abela et al., 2019; Bollimunta et al., 2011).

Thus, its decrease could reflect the degradation of inhibitory networks in proximity of the tumor, which alters the synchronization of the cortical firing (Kalemaki et al., 2018; Klimesch, 2012; Lorincz et al., 2009; Tewari et al., 2018). Altogether, these evidences indicate that glioma causes dysfunctions on excitatory and inhibitory neural circuits of the peritumoral areas in the GL261 mouse model which, thus, represents an interesting tool to reproduce brain network impairments attributable to a pro-epileptic condition.

Given these intriguingly results, I examined whether molecular changes in excitatory neurons could reflect their compromised functionality close to the tumor mass. I chose to analyse the expression of a specific panel of genes (**Table 2**) in the neural population that result to be mainly involved in phenomena of synaptic plasticity during adulthood (Maffei and Turrigiano, 2008), in both sham and glioma-bearing animals. Therefore, pyramidal neurons of the layer 2/3

(visually identified by NeuN immunostaining), were collected through LCM within the peritumoral region affected by glioma (Seano et al., 2019); healthy neurons were recovered from the primary visual cortex of sham animals (**Figure 6**). Every dissected sample expressed high levels of vGlut1 and Cux1 genes, indicating that the superficial excitatory neurons were collected (**Figure 7**). Among all the analysed genes, a significant decrease in expression was detected for GABRA1 and SNAP25, that respectively encode for the GABA A receptor subunit α 1, the main inhibitory subunit in the visual cortex (Fuchs et al., 2013; Heinen et al., 2004), and the protein SNAP25 of the SNARE complex, reflecting an impaired communication between pre- and post-synaptic neurons (**Figure 9**). The downregulation of GABRA1 gene may indicates a possible reduction of functional inhibitory GABAergic receptors and, consequently, excitatory circuits could be less susceptible to the regulation of/by inhibitory networks, increasing their firing rate. As indicated by patch-clamp experiments, peritumoral excitatory neurons of the layer 2/3 show a lowered excitability threshold (Buckingham et al., 2011) and a significant decrement of spontaneous inhibitory synaptic transmission (Campbell et al., 2015). Together with a reduction in inhibitory synapses on the soma, on axon initial segment and in tissues surrounding the tumor mass (Marco et al., 1997; Yu et al., 2020), the evidences clearly demonstrate a dampened GABA regulation. Moreover, it is well known that a variety of epileptic or seizure syndromes have been linked to genetic mutations of GABA A receptors, which compromise their function (Galanopoulou, 2008). In particular, mutations of the GABA A receptor subunit α1 are linked with genetic generalized and inherited epilepsies by impairing inhibitory network neurodevelopment (Fisher, 2004; Samarut et al., 2018).

All these mentioned studies suggest that the detected changes in the gene expression of GABRA1 gene could represent a key event in the cascade of impairments that lead to the imbalance between excitatory and inhibitory networks caused by glioma growth. Moreover, the downregulation of the SNAP25 gene could also be implicated in the establishment of a pro-epileptic phenotype of peritumoral excitatory neurons. SNAP25 is a protein that participates in the regulation of synaptic vesicle exocytosis through the formation of a complex with syntaxin and with the synaptic vesicle protein synaptobrevin/VAMP (Jahn and Scheller, 2006). It is already known that altered levels of SNAP-25 are involved in different psychiatric disorders, as the attention deficit hyperactivity disorder (ADHD) (Faraone et al., 2005); interestingly, a reduction in SNAP-25 levels is also linked with epileptic seizures, as confirmed by SNAP-25 heterozygous (SNAP-25+/−) mice (Corradini et al., 2014) and human epileptic patients (Rohena et al., 2013). Therefore, the present LCM result provides a novel evidence about the involvement of SNAP25 in tumor-associated epilepsy. Altogether, these molecular changes concur in leading to render peritumoral networks hyperexcitable and more prone to seizures.

To study in detail tumor-induced epilepsy, a group of glioma-bearing mice, grafted with tumor cells in the visual cortex, was dedicated to monitor the levels of cortical activity through continuous EEG recordings in freely moving conditions (**Figure 10A**). As hypothesized by Vannini and colleagues (Vannini et al., 2016a), 80% of glioma-bearing animals presented epileptic seizures, but the 100% of animals showed a marked hyperactivity in peritumoral tissues (**Figure 10B-E**). Analysing LFP traces, I also detected a conspicuous enhancement of slow oscillations and a degradation of α rhythm in proximity to seizures (**Figure 11**). Therefore, based on previous findings on altered brain oscillations, I further

examined the range of δ and α bands. I found that oscillations in the two frequency intervals are respectively increased and decreased not only during ictal events but also in the 5 seconds before the onset of each seizure, with respect to their levels in baseline conditions (**Figure 12**). Noteworthy, clinical studies on epileptic patients have shown an enhancement in δ oscillations in the post-ictal period, that was consistent with an overall increased number of neural units contributing to the spectral power (Miller et al., 2009). In addition, in focal epilepsy the activity in the 2–4 Hz band seems to be a relatively stronger modulator of high frequency activity near the seizure onset zone (SOZ) and may be related to a local desynchronization of the epileptogenic cortex together with a relative increase of excitatory drive (Lundstrom et al., 2019). Moreover, epileptic patients with a poor seizure control showed a shift of α band power towards theta frequencies, decreasing the overall α oscillations in the occipital regions not only during seizures but also in interictal LFPs intervals, suggesting that brain oscillation modifications could reflect seizure-promoting mechanisms (Abela et al., 2019).

Hence, an interesting parallelism can be made between previous studies on epileptic subjects and the main alterations demonstrated here in the peritumoral zone. In normal conditions, GABAergic inputs reduce network excitability and contribute essentially to the oscillatory patterning and synchronization of neural activity (Kuki et al., 2015). In particular, cortical parvalbumin interneurons contribute to maintain a correct brain oscillation and, together with somatostatin cells, regulate δ band frequencies in mice (Kuki et al., 2015; Righes Marafiga et al., 2020). In epilepsy, GABAergic connections contribute to reduce the seizure generalization and appear to control the ictal event spread (Sessolo et al., 2015). Noteworthy, the previously described deterioration of inhibitory networks in the

tumor microenvironment consists in the degradation of PNNs, loss of GABAergic interneurons and reduction of inhibitory synapses. Moreover, the imbalance between excitatory and inhibitory circuits and the cortical dysfunctions provoked by glioma growth could induce impairments in cortico-thalamic communication that reflect the degradation of α rhythm (Kalemaki et al., 2018; Peterson and Voytek, 2017). Therefore, the epileptiform activity observed in the peritumoral tissue could be triggered by both a loss of inhibition and by an increase in excitatory inputs of the region, provoking the recorded alterations in brain oscillations. The recorded impairments in proximity of ictal events suggest that they might be exploited as possible indicators of an epileptic phenotype or as biomarkers for seizure onset (Aich, 2014; Assenza et al., 2017). It also represents a possible target that might be modulated with non-invasive brain stimulations in order to restore a correct, physiological synchronism (Assenza et al., 2017; Peterson and Voytek, 2017) .

Effects of neural activity on glioma proliferation

The second part of the thesis provides significant evidences on the pivotal role of neural activity in controlling glioma proliferation. In particular, I dissected the relative contribution of pyramidal vs. fast-spiking GABAergic neurons in controlling glioma progression. I also tested the impact of afferent sensory input to glioma cell proliferation.

It is well known that the microenvironment is modulated by glioma cells to favour tumor progression with the induction of neural dysfunctions in peritumoral neurons, as previously described. On the other side, the most relevant literature of the latest years demonstrate that, in turn, also the activity of neural networks is

able to impact on tumor proliferation, via direct and indirect communication. Indeed, optogenetic stimulation of pyramidal neurons in the tumor-adjacent zone triggers calcium signals in glioma cells, increasing their proliferation and invasiveness (Venkataramani et al., 2019; Venkatesh et al., 2019). A pivotal role is played by high amount of glutamate released in the tumor microenvironment (TME) and by activity-dependent peptides as NLGN3 that stimulate glioma progression (de Groot and Sontheimer, 2011; Venkatesh et al., 2015). Moreover, NLG3 could be implicated in the formation of functional bonafide AMPA-mediated synapses between excitatory neurons and cancer cells (Venkataramani et al., 2019; Venkatesh et al., 2015, 2019).

In addition to principal cells, peritumoral cortical circuitry also comprises GABAergic interneurons. The largest class (40-50%) of GABAergic interneurons is represented by fast-spiking, parvalbumin-positive cells. They are distributed throughout all cortical layers, and form synapses on the soma and proximal dendrites of pyramidal cells and other interneurons (Lim et al., 2018). In the peritumoral zone, an overall loss of fast spiking interneurons and a reduction of their firing rates has been described (Tewari et al., 2018). This reduced firing is due to the degradation of perineuronal nets that surround these interneurons, and is critically involved in tumor-associated epileptic seizures (Tewari et al., 2018). So far, no data were available on the role for these GABAergic cells in tumor progression. To address this issue and disentangle the contribution of pyramidal and PV cells, I took advantages of two specific transgenic lines that allowed me to perform selective optogenetic stimulation in the tumor-adjacent zones of glioma-bearing mice. In this way I was able to compare the impact of the activity of two classes of principal neuronal cells on tumor proliferation. The GL261 mouse model produces a nodular tumor that grows as a large solid mass

rather than a diffusely invasive cancer (Seano et al., 2019). Therefore, it was mandatory to first demonstrate the interaction between the solid mass and neural fibers. Despite its growth pattern, I found a robust infiltration of neuronal processes within the GL261 tumor mass, which represented the structural basis for communication between tumor cells and the neuronal microenvironment (**Figure 13**). Recent studies have shown that solid tumors cause compression and dysfunction of nearby brain tissue (Seano et al., 2019). However, a direct molecular communication between peritumoral neurons and GL261 cells has also been described in the work of Liu and co-workers (Liu et al., 2013), where the authors suggested that peritumoral neurons restrain glioma progression through the pivotal role of PD-L1 protein; indeed, neuronal PD-L1 signalling in brain cells is an important marker of GB patient survival (Liu et al., 2013).

The optogenetic experiments were clear in indicating that pyramidal cell stimulation enhances cell proliferation of tumour mass, consistently with several previous reports (Venkatesh et al., 2015, 2017) (**Figure 14**). On the other hand, the selective stimulation of parvalbumin-positive interneurons elicited the opposite effect – i.e. a significant reduction of glioma cell proliferation (**Figure 15**). Thus, glutamatergic and GABAergic signalling appear to have inverse actions on tumor growth. Similar antagonistic effects of neurotransmitter systems have been described in other types of cancer such as breast cancer, where stimulation of parasympathetic (cholinergic) afferents reduces tumor growth and the stimulation of sympathetic (noradrenergic) nerves accelerates it (Kamiya et al., 2019). The effects of parvalbumin interneurons activation are consistent with the finding that human glioblastoma cells express functional GABA A receptors and that endogenous GABA released by tumor cells attenuates tumor growth (Blanchart et al., 2017). In addition, the present results indicate also that

peritumoral interneurons may represent a further source of GABA, supporting anti-proliferative effects. However, the high vulnerability of fast-spiking interneurons to glioma-induced excitotoxicity in the tumor-adjacent zone (Tewari et al., 2018) may trigger a vicious cycle with reduced GABA release, increased firing of pyramidal neurons and, consequently, enhanced tumor growth. A similar scenario is indicated by the recent work of Deneen and collaborators (Yu et al., 2020), where specific mutations harboured by transplanted glioma cells render tumours more aggressive and lethal. Gliomas driven by these variants shape synaptic connectivity in the peritumoral region, with enhanced density of excitatory boutons and decreased inhibitory synapses with a following heightened network hyperexcitability. All these data concur in indicating that glioma-derived factors may drive synaptic changes which result in aberrant activity patterns that lead to increased tumor growth.

Pyramidal neurons and fast-spiking interneurons are directly activated by sensory input via thalamocortical afferents (Sugiyama et al., 2008; Yu et al., 2016). Therefore, we wondered whether and how sensory stimulation affects glioma cell proliferation. To address this issue, we exploited glioma cell grafting in the visual cortex, a region where afferent activity can be easily modulated by photic stimuli (Deidda et al., 2015; Porciatti et al., 1999; Vannini et al., 2016a) . While high-grade gliomas in the visual cortex are rare, about 30-50% of the cortical mantle in humans is responsive to visual stimulation, making the results of this experiential modulation of sensory input potentially interesting in a translational perspective. Specifically, we employed either visual stimulation or dark rearing for three consecutive days to transiently enhance or reduce sensory input to the peritumoral areas (**Figure 16A**). The proliferation analyses indicated that dark rearing increases glioma cell proliferation, while stimulation with

gratings of different spatial and temporal frequencies has the opposite effect, counteracting tumor cell division (**Figure 16B-L**). I chose to employ short periods of visual stimulation/deprivation as activity in occipital areas is known to homeostatically rescale within one week to altered levels of visual input (Turrigiano, 2012). For example, in the case of chronic visual deprivation, pyramidal cell firing in the visual cortex is initially depressed during the first 2-3 days but then returns to baseline at one week due to homeostatic compensation (Hengen et al., 2016; Mrsic-Flogel et al., 2007). Activation of the cortical network by sensory stimuli results in a balanced and sequential activation of several classes of pyramidal cells and interneurons, in a layer-specific manner (Kerlin et al., 2010; Okun et al., 2015).

Can the impact of visual stimulation be explained based on a differential involvement of principal and GABAergic neurons? There are several possibilities to be considered. First, while pyramidal neurons show exquisite selectivity for properties of the visual stimulus (spatial and temporal frequency, contrast), fast-spiking interneurons (and other GABAergic cells) are broadly tuned for stimulus features (Kerlin et al., 2010). This means that during exposure to a specific grating, only a subset of pyramidal neurons are firing while GABAergic interneurons display a more global activation. Second, in the awake mouse, cortical responses to visual stimulation are precisely shunted by GABAergic inhibition, restricting the spatial spread and temporal persistence of pyramidal cell discharges (Haider et al., 2013). Third, parvalbumin-positive interneurons fire at much higher rates than cortical pyramids. Altogether, these data suggest that visual stimulation may trigger substantial GABA release that overcomes the effect of glutamatergic signalling.

After dark rearing, a substantial decrease of GABA-immunoreactive neurons has been found in primary visual cortex (Benevento et al., 1995). This reduction of GABAergic cells may remove a neurochemical brake to tumor growth, thus explaining the higher proliferation rates following visual deprivation. Moreover, I used BoNT/A (Rossetto et al., 2006; Schiavo et al., 2000) to completely block synaptic activity of the visual cortex around the tumor mass. This toxin specifically cleaves the SNAP-25 protein, an essential component of the neuroexocytosis machinery allowing a persistent “silencing” of specific brain regions after a single administration (Caleo and Restani, 2018). I detected an increase of glioma cell proliferation in glioma-bearing mice treated with BoNT/A, supporting the view that synaptic activity limits tumor progression (**Figure 17**). Importantly, the impact of visual input is region-specific, as shown by the lack of effect of dark rearing in mice with syngeneic glioma in the motor cortex (**Figure 18**).

One important goal of glioma therapies is the preservation of function in the peritumoral zone (Vannini et al., 2016a, 2017). For example, subjects with tumors in the occipital regions of the brain show several types of visual impairments that potently impact their quality of life (Sharrack et al., 2018). Based on our encouraging results of the counteracting effect cortical activity on tumor proliferation, the sensory stimulation might be used as a potential, adjuvant strategy to be implemented in the current glioma therapies in order to delay the neurological loss of function. Indeed, longitudinal monitoring of the decay of visual responses through chronic VEP recordings, showed that combining TMZ delivery with daily visual stimulation could be considered as an add-on of an already well-established therapy for GB. Glioma-bearing mice treated with a combination of TMZ and visual stimulation displayed a significant prolongation of

neural responsiveness, suggesting it as a possible strategy to delay the loss of sensory functions during glioma growth (**Figure 20**).

In summary, the data reported in the second part of this thesis highlight a key, and previously unrecognized, role for parvalbumin-positive GABAergic neurons in counteracting glioma cell proliferation. Moreover, I showed that levels of sensory afferent input bidirectionally modulate tumor proliferation. Drugs capable of stimulating GABAergic signalling may be tested to improve the efficacy of conventional anti-glioma treatments (Laub et al., 2018; Wick et al., 2018).

Conclusions

In conclusion, my results contribute to clarify the complex bidirectional interaction between glioma and the surrounding neural tissue. I demonstrated that glioma affects the neural activity of surrounding networks, deteriorating their functionality and leading to epileptogenic changes in gene expression (i.e. decrease of GABA-A and SNAP-25). As a consequence, this scenario can trigger a vicious loop that exacerbate glioma progression. In fact, the reduced GABA release and the activity of excitatory neurons can favour tumor progression. On the other hand, the stimulation of GABAergic interneurons in the surrounding tissues dampens tumor cell proliferation. Noteworthy, the anti-proliferative effect of GABA could overcome the effect of glutamatergic signalling, as demonstrated by sensory stimulation. Moreover, it was shown that a combination of sensory stimulation and chemotherapy produces a beneficial effect in preserving normal neural functions during the progression of this devastating disease.

Ongoing experiments

I am currently working on an experiment aimed to confirm the functional alterations of neural activity induced by the downregulation of GABRA1 in peritumoral excitatory neurons described in **section 3.1.3**. In particular, I am performing LFPs recordings in freely moving glioma-bearing and sham mice, injected in the visual cortex respectively with GL261 cells and PBS. The animals are treated with an intraperitoneal injection of DMCM (methyl-6,7-dimethoxy-4-ethyl-beta-carboline-3-carboxylate), a benzodiazepine inverse agonist (Alia et al., 2016) that acts as a negative allosteric modulator of GABA A receptors with high affinity for the alpha 1 subunit (Kulick et al., 2014; Puia et al., 1991). Given the reduced expression of the GABA-A alpha1 receptor in peritumoral neurons, I am testing the prediction that a subconvulsive dose of DMCM will trigger epileptiform activity in glioma-bearing mice but not in controls.

In order to verify whether gene expression alterations described in **section 3.1.3** are reflected also in their protein level, I will quantify peritumoral GABA A receptor alpha1 subunit and Snap25 protein through immunostaining in peritumoral tissues of glioma-bearing mice and in primary visual cortex of sham animals. I will analyse Gaba A receptor alpha1 subunit in proximity of the synaptic endings of Parvalbumin interneurons. I am also planning (collaboration with Michela Matteoli, Milan) to evaluate the alterations of GABA-A alpha1 and SNAP-25 expression in human peritumoral tissues. Moreover, regarding spectral band alterations described in **section 3.1.1** and **3.1.4**, I am also interested in modulating experimentally the alpha and delta rhythm to understand its involvement in triggering epileptic events.

Publications

During my PhD thesis, I have been working at the Fondazione Pisana per la Scienza (FPS)_ONLUS under the supervision of Dr. Mazzanti and at the CNR Neuroscience Institute under the supervisor Dr. Caleo. At FPS, I have participated to molecular studies in gliomas and other tumors. At CNR, I have performed *in vivo* experiments, carrying out all electrophysiological recordings, animal treatment, data analysis and neuroanatomical investigation.

A complete list of publication is reported below:

- DIFFERENTIAL ROLES OF PYRAMIDAL AND FAST-SPIKING, GABAERGIC NEURONS IN THE CONTROL OF GLIOMA CELL PROLIFERATION
  Tantillo E, Vannini E, Cerri C, Spalletti C, Colistra A, Mazzanti CM, Costa M, Caleo M. *Neurobiol Dis. 2020 Jul; 141*

- ANKRD44 GENE SILENCING: A PUTATIVE ROLE IN TRASTUZUMAB RESISTANCE IN HER2-LIKE BREAST CANCER

  La Ferla M, Lessi F, Aretini P, Pellegrini D, Franceschi S, **Tantillo E**, Menicagli M, Marchetti I, Scopelliti C, Civita P, De Angelis C, Diodati L, Bertolini I, Roncella M, Mc Donnel AL, Hochman J, Del Re M, Scatena C, Naccarato AG, Fontana A, Mazzanti CM. *Front. Oncol. 2019 jun 26;9;547*
- MITOCHONDRIAL ENZYME GLUD2 PLAYS A CRITICAL ROLE IN GLIOBLASTOMA PROGRESSION.

  Franceschi S, Corsinovi D, Lessi F, **Tantillo E**, Aretini P, Menicagli M, Scopelliti C, Civita P, Pasqualetti F, Naccarato AG, Ori M, Mazzanti CM. *EBioMedicine. 2018 Nov;37:56-67*
- BACTERIAL TOXINS AND TARGETED BRAIN THERAPY: NEW INSIGHTS FROM CYTOTOXIC NECROTIZING FACTOR 1 (CNF1).

  Tantillo E, Colistra A, Vannini E, Cerri C, Pancrazi L, Baroncelli L, Costa M, Caleo M. *Int J Mol Sci. 2018 May 31;19(6):1632.*
- MICRORNAS DISTRIBUTION IN DIFFERENT PHENOTYPES OF AORTIC STENOSIS.

  Fabiani I, Pugliese NR, Calogero E, Conte L, Mazzanti MC, Scatena C, Scopelliti C, **Tantillo E**, Passiatore M, Angelillis M, Naccarato GA, Di Stefano R, Petronio AS, Di Bello V. *Sci Rep. 2018 Jul 2;8(1):9953.*
- DEVELOPMENT OF A YEAST-BASED SYSTEM TO IDENTIFY NEW HBRAFV600E FUNCTIONAL INTERACTORS.

  Lubrano S, Comelli L, Piccirilli C, Marranci A, Dapporto F, **Tantillo E**, Gemignani F, Gutkind JS, Salvetti A, Chiorino G, Cozza G, Chiariello M, Galli A, Poliseno L, Cervelli T. *Oncogene. 2019 Feb;38(8):1355-1366.*
- LONGITUDINAL ALTERATIONS OF CORTICAL ACTIVITY DURING GLIOMA PROGRESSION IN A MOUSE MODEL

  Tantillo E, Cerri C, Mazzanti CM, Costa M, Caleo M. *Neuro-Oncology, Volume 19, Issue suppl_6, 6 November 2017, Pages vi250*
- LOSS OF C-KIT EXPRESSION IN THYROID CANCER CELLS.

  Franceschi S, Lessi F, Panebianco F, **Tantillo E**, La Ferla M, Menicagli M, Aretini P, Apollo A, Naccarato AG, Marchetti I, Mazzanti CM. *PLoS One. 2017 Mar 16;12(3):e0173913.*

References

Aaronson, N. K., Taphoorn, M. J. B., Heimans, J. J., Postma, T. J., Gundy, C. M., Beute, G. N., et al. (2011). Compromised health-related quality of life in patients with low-grade glioma. *J. Clin. Oncol.* doi:10.1200/JCO.2011.35.5750.

Abel, T., Havekes, R., Saletin, J. M., and Walker, M. P. (2013). Sleep, plasticity and memory from molecules to whole-brain networks. *Curr. Biol.* doi:10.1016/j.cub.2013.07.025.

Abela, E., Pawley, A. D., Tangwiriyasakul, C., Yaakub, S. N., Chowdhury, F. A., Elwes, R. D. C., et al. (2019). Slower alpha rhythm associates with poorer seizure control in epilepsy. *Ann. Clin. Transl. Neurol.* doi:10.1002/acn3.710.

Aich, T. K. (2014). Absent posterior alpha rhythm: An indirect indicator of seizure disorder? *Indian J. Psychiatry*. doi:10.4103/0019-5545.124715.

Alcantara Llaguno, S., Chen, J., Kwon, C. H., Jackson, E. L., Li, Y., Burns, D. K., et al. (2009). Malignant Astrocytomas Originate from Neural Stem/Progenitor Cells in a Somatic Tumor Suppressor Mouse Model. *Cancer Cell*. doi:10.1016/j.ccr.2008.12.006.

Alcantara Llaguno, S., Sun, D., Pedraza, A. M., Vera, E., Wang, Z., Burns, D. K., et al. (2019). Cell-of-origin susceptibility to glioblastoma formation declines with neural lineage restriction. *Nat. Neurosci.* doi:10.1038/s41593-018-0333-8.

Alia, C., Spalletti, C., Lai, S., Panarese, A., Micera, S., and Caleo, M. (2016). Reducing

GABA A-mediated inhibition improves forelimb motor function after focal cortical stroke in mice. *Sci. Rep.* 6, 1–15. doi:10.1038/srep37823.

Allegra, M., Spalletti, C., Vignoli, B., Azzimondi, S., Busti, I., Billuart, P., et al. (2017). Pharmacological rescue of adult hippocampal neurogenesis in a mouse model of X-linked intellectual disability. *Neurobiol. Dis.* doi:10.1016/j.nbd.2017.01.003.

Allegra Mascaro, A. L., Conti, E., Lai, S., Di Giovanna, A. P., Spalletti, C., Alia, C., et al. (2019). Combined Rehabilitation Promotes the Recovery of Structural and Functional Features of Healthy Neuronal Networks after Stroke. *Cell Rep.* 28, 3474-3485.e6. doi:10.1016/j.celrep.2019.08.062.

Anderson, R. C. E., Anderson, D. E., Elder, J. B., Brown, M. D., Mandigo, C. E., Parsa, A. T., et al. (2007). Lack of B7 expression, not human leukocyte antigen expression, facilitates immune evasion by human malignant gliomas. *Neurosurgery*. doi:10.1227/01.NEU.0000255460.91892.44.

Antonucci, F., Bozzi, Y., and Caleo, M. (2009). Intrahippocampal infusion of botulinum neurotoxin e (BoNT/E) reduces spontaneous recurrent seizures in a mouse model of mesial temporal lobe epilepsy. *Epilepsia* 50, 963–966. doi:10.1111/j.1528-1167.2008.01983.x.

Arenkiel, B. R., Peca, J., Davison, I. G., Feliciano, C., Deisseroth, K., Augustine, G. J. J., et al. (2007). In Vivo Light-Induced Activation of Neural Circuitry in Transgenic Mice Expressing Channelrhodopsin-2. *Neuron* 54, 205–218. doi:10.1016/j.neuron.2007.03.005.

Armstrong, T. S., Grant, R., Gilbert, M. R., Lee, J. W., and Norden, A. D. (2016). Epilepsy in glioma patients: Mechanisms, management, and impact of anticonvulsant therapy. *Neuro. Oncol.* 18, 779–789. doi:10.1093/neuonc/nov269.

Assenza, G., Fioravante, C., Lazzaro, di B., Ferreri, F., Florio, L., Guerra, A., et al. (2017). Oscillatory activities in neurological disorders of elderly: Biomarkers to target for neuromodulation. *Front. Aging Neurosci.* doi:10.3389/fnagi.2017.00189.

Ausman, J., Shapiro, W., and Rall, D. P. (1970). Studies on the chemotherapy of cxperimental brain tumors: development of an experimental model. *Cancer Res.*

Baayen, J. C., De Jongh, A., Stam, C. J., De Munck, J. C., Jonkman, J. J., Kasteleijn-Nolst Trenité, D. G. A., et al. (2003). Localization of Slow Wave Activity in Patients with Tumor-Associated Epilepsy. *Brain Topogr.* doi:10.1023/B:BRAT.0000006332.71345.b7.

Bahadur, S., Kumar Sahu, A., Baghel, P., and Saha, S. (2019). Current promising treatment strategy for glioblastoma multiform: A review. *Oncol. Rev.* doi:10.4081/oncol.2019.417.

Barres, B. A., and Raff, M. C. (1993). Proliferation of oligodendrocyte precursor cells depends on electrical activity in axons. *Nature*. doi:10.1038/361258a0.

Beaumont, A., and Whittle, I. R. (2000). The pathogenesis of tumour associated epilepsy. *Acta Neurochir. (Wien).* doi:10.1007/s007010050001.

Behrens, P. F., Langemann, H., Strohschein, R., Draeger, J., and Hennig, J. (2000). Extracellular glutamate and other metabolites in and around RG2 rat glioma: An intracerebral microdialysis study. *J. Neurooncol.* doi:10.1023/A:1006426917654.

Benevento, L. A., Bakkum, B. W., and Cohen, R. S. (1995). Gamma-aminobutyric acid and somatostatin immunoreactivity in the visual cortex of normal and dark-reared rats. *Brain Res.* doi:10.1016/0006-8993(95)00553-3.

Bergles, D. E., and Jahr, C. E. (1997). Synaptic activation of glutamate transporters in hippocampal astrocytes. *Neuron*. doi:10.1016/S0896-6273(00)80420-1.

Berntsson, S. G., Malmer, B., Bondy, M. L., Qu, M., and Smits, A. (2009). Tumor-associated epilepsy and glioma: Are there common genetic pathways? *Acta Oncol. (Madr).* doi:10.1080/02841860903104145.

Blanchart, A., Fernando, R., Häring, M., Assaife-Lopes, N., Romanov, R. A., Andäng, M., et al. (2017). Endogenous GAB AA receptor activity suppresses glioma growth. *Oncogene* 36, 777–786. doi:10.1038/onc.2016.245.

Bollimunta, A., Mo, J., Schroeder, C. E., and Ding, M. (2011). Neuronal mechanisms and attentional modulation of corticothalamic alpha oscillations. *J. Neurosci.* doi:10.1523/JNEUROSCI.5580-10.2011.

Bordey, A., and Sontheimer, H. (1998). Properties of human glial cells associated with epileptic seizure foci. in *Epilepsy Research* doi:10.1016/S0920-1211(98)00059-X.

Breckwoldt, M. O., Bode, J., Sahm, F., Krüwel, T., Solecki, G., Hahn, A., et al. (2019). Correlated MRI and ultramicroscopy (MR-UM) of brain tumors reveals vast heterogeneity of tumor infiltration and neoangiogenesis in preclinical models and human disease. *Front. Neurosci.* doi:10.3389/fnins.2018.01004.

Brennan, C. W., Verhaak, R. G. W., McKenna, A., Campos, B., Noushmehr, H., Salama, S. R., et al. (2013). The somatic genomic landscape of glioblastoma. *Cell*. doi:10.1016/j.cell.2013.09.034.

Brown, T. J., Brennan, M. C., Li, M., Church, E. W., Brandmeir, N. J., Rakszawski, K. L., et al. (2016). Association of the extent of resection with survival in glioblastoma a systematic review and meta-Analysis. *JAMA Oncol.* doi:10.1001/jamaoncol.2016.1373.

Buckanovich, R. J., Sasaroli, D., O'Brien-Jenkins, A., Botbyl, J., Conejo-Garcia, J. R., Benencia, F., et al. (2006). Use of immuno-LCM to identify the in situ expression profile of cellular constituents of the tumor microenvironment. *Cancer Biol. Ther.* doi:10.4161/cbt.5.6.2676.

Buckingham, S. C., Campbell, S. L., Haas, B. R., Montana, V., Robel, S., Ogunrinu, T., et al. (2011). Glutamate release by primary brain tumors induces epileptic activity. *Nat. Med.* 17, 1269–1274. doi:10.1038/nm.2453.

Buckingham, S. C., and Robel, S. (2013). Glutamate and tumor-associated epilepsy: Glial cell dysfunction in the peritumoral environment. *Neurochem. Int.* 63, 696–701. doi:10.1016/j.neuint.2013.01.027.

Burnet, N. G., Lynch, A. G., Jefferies, S. J., Price, S. J., Jones, P. H., Antoun, N. M., et al. (2007). High grade glioma: Imaging combined with pathological grade defines management and predicts prognosis. *Radiother. Oncol.* 85, 371–378. doi:10.1016/j.radonc.2007.10.008.

Busti, I., Allegra, M., Spalletti, C., Panzi, C., Restani, L., Billuart, P., et al. (2020). ROCK/PKA inhibition rescues hippocampal hyperexcitability and GABAergic neuron

alterations in Oligophrenin-1 Knock-out mouse model of X-linked intellectual disability. *J. Neurosci.* 40, 2776–2788. doi:10.1523/JNEUROSCI.0462-19.2020.

Butler, A. E., Matveyenko, A. V., Kirakossian, D., Park, J., Gurlo, T., and Butler, P. C. (2016). Recovery of high-quality RNA from laser capture microdissected human and rodent pancreas. *J. Histotechnol.* doi:10.1080/01478885.2015.1106073.

Buzsáki, G. (2009). *Rhythms of the Brain*. doi:10.1093/acprof:oso/9780195301069.001.0001.

Caleo, M., and Restani, L. (2018). Exploiting botulinum neurotoxins for the study of brain physiology and pathology. *Toxins (Basel).* doi:10.3390/toxins10050175.

Caleo, M., Restani, L., Gianfranceschi, L., Costantin, L., Rossi, C., Rossetto, O., et al. (2007). Transient Synaptic Silencing of Developing Striate Cortex Has Persistent Effects on Visual Function and Plasticity. *J. Neurosci.* doi:10.1523/jneurosci.0772-07.2007.

Caleo, M., Restani, L., and Hugh Perry, V. (2013). Silencing synapses: A route to understanding synapse degeneration in chronic neurodegenerative disease. *Prion*. doi:10.4161/pri.23327.

Caleo, M., Spinelli, M., Colosimo, F., Matak, I., Rossetto, O., Lackovic, Z., et al. (2018). Transynaptic Action of Botulinum Neurotoxin Type A at Central Cholinergic Boutons. *J. Neurosci.* doi:10.1523/jneurosci.0294-18.2018.

Campbell, S. L., Buckingham, S. C., and Sontheimer, H. (2012). Human glioma cells induce hyperexcitability in cortical networks. *Epilepsia*. doi:10.1111/j.1528-1167.2012.03557.x.

Campbell, S. L., Robel, S., Cuddapah, V. A., Robert, S., Buckingham, S. C., Kahle, K. T., et al. (2015). GABAergic disinhibition and impaired KCC2 cotransporter activity underlie tumor-associated epilepsy. *Glia* 63, 23–36. doi:10.1002/glia.22730.

Candolfi, M., Curtin, J. F., Nichols, W. S., Muhammad, A. K. M. G., King, G. D., Pluhar, G. E., et al. (2007). Intracranial glioblastoma models in preclinical neuro-oncology: Neuropathological characterization and tumor progression. *J. Neurooncol.* doi:10.1007/s11060-007-9400-9.

Candolfi, M., Kroeger, K., Muhammad, A., Yagiz, K., Farrokhi, C., Pechnick, R., et al. (2009). Gene Therapy for Brain Cancer: Combination Therapies Provide Enhanced Efficacy and Safety. *Curr. Gene Ther.* doi:10.2174/156652309789753301.

Caragher, S. P., Shireman, J. M., Huang, M., Miska, J., Atashi, F., Baisiwala, S., et al. (2019). Activation of dopamine receptor 2 prompts transcriptomic and metabolic plasticity in glioblastoma. *J. Neurosci.* doi:10.1523/JNEUROSCI.1589-18.2018.

Cardin, J. A., Carlén, M., Meletis, K., Knoblich, U., Zhang, F., Deisseroth, K., et al. (2009). Driving fast-spiking cells induces gamma rhythm and controls sensory responses. *Nature*. doi:10.1038/nature08002.

Caudill, J. S., Brown, P. D., Cerhan, J. H., and Rummans, T. A. (2011). Selective serotonin reuptake inhibitors, glioblastoma multiforme, and impact on toxicities and overall survival: The mayo clinic experience. *Am. J. Clin. Oncol. Cancer Clin. Trials*. doi:10.1097/COC.0b013e3181e8461a.

Ceccarelli, M., Barthel, F. P., Malta, T. M., Sabedot, T. S., Salama, S. R., Murray, B. A., et

al. (2016). Molecular Profiling Reveals Biologically Discrete Subsets and Pathways of Progression in Diffuse Glioma. *Cell*. doi:10.1016/j.cell.2015.12.028.

Cerri, C., Genovesi, S., Allegra, M., Pistillo, F., Püntener, U., Guglielmotti, A., et al. (2016). The Chemokine CCL2 Mediates the Seizure-enhancing Effects of Systemic Inflammation. *J. Neurosci.* 36, 3777–3788. doi:10.1523/jneurosci.0451-15.2016.

Chen, J., McKay, R. M., and Parada, L. F. (2012). Malignant glioma: Lessons from genomics, mouse models, and stem cells. *Cell*. doi:10.1016/j.cell.2012.03.009.

Cihoric, N., Tsikkinis, A., Minniti, G., Lagerwaard, F. J., Herrlinger, U., Mathier, E., et al. (2017). Current status and perspectives of interventional clinical trials for glioblastoma - analysis of ClinicalTrials.gov. *Radiat. Oncol.* doi:10.1186/s13014-016-0740-5.

Cohen, G., Burks, S. R., and Frank, J. A. (2018). Chlorotoxin—A multimodal imaging platform for targeting glioma tumors. *Toxins (Basel).* doi:10.3390/toxins10120496.

Cohen, S., Levi-Montalcini, R., and Hamburger, V. (1954). A NERVE GROWTH-STIMULATING FACTOR ISOLATED FROM SARCOM AS 37 AND 180. *Proc. Natl. Acad. Sci.* doi:10.1073/pnas.40.10.1014.

Colman, H., Berkey, B. A., Maor, M. H., Groves, M. D., Schultz, C. J., Vermeulen, S., et al. (2006). Phase II Radiation Therapy Oncology Group trial of conventional radiation therapy followed by treatment with recombinant interferon-β for supratentorial glioblastoma: Results of RTOG 9710. *Int. J. Radiat. Oncol. Biol. Phys.* doi:10.1016/j.ijrobp.2006.05.021.

Conti, L., Palma, E., Roseti, C., Lauro, C., Cipriani, R., De Groot, M., et al. (2011). Anomalous levels of Cl- transporters cause a decrease of GABAergic inhibition in human peritumoral epileptic cortex. *Epilepsia* 52, 1635–1644. doi:10.1111/j.1528-1167.2011.03111.x.

Cooke, S. F., and Bear, M. F. (2014). How the mechanisms of long-term synaptic potentiation and depression serve experience-dependent plasticity in primary visual cortex. *Philos. Trans. R. Soc. B Biol. Sci.* 369. doi:10.1098/rstb.2013.0284.

Corlew, R., Bosma, M. M., and Moody, W. J. (2004). Spontaneous, synchronous electrical activity in neonatal mouse cortical neurones. *J. Physiol.* doi:10.1113/jphysiol.2004.071621.

Corradini, I., Donzelli, A., Antonucci, F., Welzl, H., Loos, M., Martucci, R., et al. (2014). Epileptiform activity and cognitive deficits in SNAP-25+/- mice are normalized by antiepileptic drugs. *Cereb. Cortex* 24, 364–376. doi:10.1093/cercor/bhs316.

Corso, C. D., Bindra, R. S., and Mehta, M. P. (2017). The role of radiation in treating glioblastoma: here to stay. *J. Neurooncol.* doi:10.1007/s11060-016-2348-x.

Costantin, L. (2005). Antiepileptic Effects of Botulinum Neurotoxin E. *J. Neurosci.* doi:10.1523/jneurosci.4402-04.2005.

Cowie, C. J. A., and Cunningham, M. O. (2014). Peritumoral epilepsy: Relating form and function for surgical success. *Epilepsy Behav.* doi:10.1016/j.yebeh.2014.05.009.

D'Alessio, A., Proietti, G., Sica, G., and Scicchitano, B. M. (2019). Pathological and molecular features of glioblastoma and its peritumoral tissue. *Cancers (Basel).* 11. doi:10.3390/cancers11040469.

D'Urso, P. I., D'Urso, O. F., Storelli, C., Mallardo, M., Gianfreda, C. D., Montinaro, A., et al. (2012). miR-155 is up-regulated in primary and secondary glioblastoma and promotes tumour growth by inhibiting GABA receptors. *Int. J. Oncol.* 41, 228–234. doi:10.3892/ijo.2012.1420.

Danbolt, N. C. (2001). Glutamate uptake. *Prog. Neurobiol.* doi:10.1016/S0301-0082(00)00067-8.

de Groot, J., and Sontheimer, H. (2011). Glutamate and the biology of gliomas. *Glia*. doi:10.1002/glia.21113.

Deidda, G., Allegra, M., Cerri, C., Naskar, S., Bony, G., Zunino, G., et al. (2015). Early depolarizing GABA controls critical-period plasticity in the rat visual cortex. *Nat. Neurosci.* doi:10.1038/nn.3890.

Deisseroth, K., Singla, S., Toda, H., Monje, M., Palmer, T. D., and Malenka, R. C. (2004). Excitation-neurogenesis coupling in adult neural stem/progenitor cells. *Neuron*. doi:10.1016/S0896-6273(04)00266-1.

Di Angelantonio, S., Murana, E., Cocco, S., Scala, F., Bertollini, C., Molinari, M. G., et al. (2014). A role for intracellular zinc in glioma alteration of neuronal chloride equilibrium. *Cell Death Dis.* doi:10.1038/cddis.2014.437.

Dolma, S., Selvadurai, H. J., Lan, X., Lee, L., Kushida, M., Voisin, V., et al. (2016). Inhibition of Dopamine Receptor D4 Impedes Autophagic Flux, Proliferation, and Survival of Glioblastoma Stem Cells. *Cancer Cell*. doi:10.1016/j.ccell.2016.05.002.

Dong, H., Strome, S. E., Salomao, D. R., Tamura, H., Hirano, F., Flies, D. B., et al. (2002). Tumor-associated B7-H1 promotes T-cell apoptosis: A potential mechanism of immune evasion. *Nat. Med.* doi:10.1038/nm730.

Donovan, M. J., Hempstead, B. L., Horvath, C., Chao, M. V., and Schofield, D. (1993). Immunohistochemical localization of Trk receptor protein in pediatric small round blue cell tumors. *Am. J. Pathol.*

Douw, L., van Dellen, E., de Groot, M., Heimans, J. J., Klein, M., Stam, C. J., et al. (2010). Epilepsy is related to theta band brain connectivity and network topology in brain tumor patients. *BMC Neurosci.* 11. doi:10.1186/1471-2202-11-103.

Eberhart, C. G., Kaufman, W. E., Tihan, T., and Burger, P. C. (2001). Apoptosis, neuronal maturation, and neurotrophin expression within medulloblastoma nodules. *J. Neuropathol. Exp. Neurol.* doi:10.1093/jnen/60.5.462.

Edwards, R. H. (2007). The Neurotransmitter Cycle and Quantal Size. *Neuron*. doi:10.1016/j.neuron.2007.09.001.

Falsini, B., Chiaretti, A., Rizzo, D., Piccardi, M., Ruggiero, A., Manni, L., et al. (2016). Nerve growth factor improves visual loss in childhood optic gliomas: A randomized, double-blind, phase II clinical trial. *Brain*. doi:10.1093/brain/awv366.

Faraone, S. V., Perlis, R. H., Doyle, A. E., Smoller, J. W., Goralnick, J. J., Holmgren, M. A., et al. (2005). Molecular genetics of attention-deficit/hyperactivity disorder. *Biol. Psychiatry*. doi:10.1016/j.biopsych.2004.11.024.

Ferlay, J., Parkin, D. M., and Steliarova-Foucher, E. (2010). Estimates of cancer incidence and mortality in Europe in 2008. *Eur. J. Cancer*. doi:10.1016/j.ejca.2009.12.014.

Ferrari, E., Maywood, E. S., Restani, L., Caleo, M., Pirazzini, M., Rossetto, O., et al. (2011). Re-assembled botulinum neurotoxin inhibits CNS functions without systemic toxicity. *Toxins (Basel).* doi:10.3390/toxins3040345.

Fink, L., Kinfe, T., Stein, M. M., Ermert, L., Hänze, J., Kummer, W., et al. (2000). Immunostaining and laser-assisted cell picking for mRNA analysis. *Lab. Investig.* doi:10.1038/labinvest.3780037.

Fink, L., Kwapiszewska, G., Wilhelm, J., and Bohle, R. M. (2006). Laser-microdissection for cell type- and compartment-specific analyses on genomic and proteomic level. *Exp. Toxicol. Pathol.* doi:10.1016/j.etp.2006.02.010.

Fisher, J. L. (2004). A mutation in the GABAA receptor α1 subunit linked to human epilepsy affects channel gating properties. *Neuropharmacology*. doi:10.1016/j.neuropharm.2003.11.015.

Fisher, J. L., Palmisano, S., Schwartzbaum, J. A., Svensson, T., and Lönn, S. (2014). Comorbid conditions associated with glioblastoma. *J. Neurooncol.* doi:10.1007/s11060-013-1341-x.

Florell, S. R., Coffin, C. M., Holden, J. A., Zimmermann, J. W., Gerwels, J. W., Summers, B. K., et al. (2001). Preservation of RNA for functional genomic studies: A multidisciplinary tumor bank protocol. *Mod. Pathol.* doi:10.1038/modpathol.3880267.

Franceschi, S., Corsinovi, D., Lessi, F., Tantillo, E., Aretini, P., Menicagli, M., et al. (2018). Mitochondrial enzyme GLUD2 plays a critical role in glioblastoma progression. *EBioMedicine* 37. doi:10.1016/j.ebiom.2018.10.008.

Franceschi, S., Mazzanti, C. M., Lessi, F., Aretini, P., Carbone, F. G., La Ferla, M., et al. (2015). Investigating molecular alterations to profile short- and long-term recurrence-free survival in patients with primary glioblastoma. *Oncol. Lett.* doi:10.3892/ol.2015.3738.

Frenkel, M. Y., Sawtell, N. B., Diogo, A. C. M., Yoon, B., Neve, R. L., and Bear, M. F. (2006). Instructive Effect of Visual Experience in Mouse Visual Cortex. *Neuron*. doi:10.1016/j.neuron.2006.06.026.

Fresno Vara, J. Á., Casado, E., de Castro, J., Cejas, P., Belda-Iniesta, C., and González-Barón, M. (2004). P13K/Akt signalling pathway and cancer. *Cancer Treat. Rev.* doi:10.1016/j.ctrv.2003.07.007.

Fuchs, C., Abitbol, K., Burden, J. J., Mercer, A., Brown, L., Iball, J., et al. (2013). GABAA receptors can initiate the formation of functional inhibitory GABAergic synapses. *Eur. J. Neurosci.* doi:10.1111/ejn.12331.

Furnari, F. B., Fenton, T., Bachoo, R. M., Mukasa, A., Stommel, J. M., Stegh, A., et al. (2007). Malignant astrocytic glioma: Genetics, biology, and paths to treatment. *Genes Dev.* 21, 2683–2710. doi:10.1101/gad.1596707.

Gafarov, F. M. (2018). Neural electrical activity and neural network growth. *Neural Networks*. doi:10.1016/j.neunet.2018.02.001.

Galanopoulou, A. (2008). GABAA Receptors in Normal Development and Seizures: Friends or Foes? *Curr. Neuropharmacol.* 6, 1–20. doi:10.2174/157015908783769653.

Garofalo, S., D'Alessandro, G., Chece, G., Brau, F., Maggi, L., Rosa, A., et al. (2015). Enriched environment reduces glioma growth through immune and non-immune

mechanisms in mice. *Nat. Commun.* 6, 6623. doi:10.1038/ncomms7623.

Garofalo, S., Porzia, A., Mainiero, F., Di Angelantonio, S., Cortese, B., Basilico, B., et al. (2017). Environmental stimuli shape microglial plasticity in glioma. *Elife* 6. doi:10.7554/eLife.33415.

Gavrilovic, I. T., and Posner, J. B. (2005). Brain metastases: Epidemiology and pathophysiology. *J. Neurooncol.* doi:10.1007/s11060-004-8093-6.

Ge, S., Yang, C. hao, Hsu, K. sen, Ming, G. li, and Song, H. (2007). A Critical Period for Enhanced Synaptic Plasticity in Newly Generated Neurons of the Adult Brain. *Neuron*. doi:10.1016/j.neuron.2007.05.002.

Giachino, C., Boulay, J. L., Ivanek, R., Alvarado, A., Tostado, C., Lugert, S., et al. (2015). A Tumor Suppressor Function for Notch Signaling in Forebrain Tumor Subtypes. *Cancer Cell*. doi:10.1016/j.ccell.2015.10.008.

Gianfranceschi, L., Siciliano, R., Walls, J., Morales, B., Kirkwood, A., Huang, Z. J., et al. (2003). Visual cortex is rescued from the effects of dark rearing by overexpression of BDNF. *Proc. Natl. Acad. Sci.* doi:10.1073/pnas.1934836100.

Gibson, E. M., Purger, D., Mount, C. W., Goldstein, A. K., Lin, G. L., Wood, L. S., et al. (2014). Neuronal activity promotes oligodendrogenesis and adaptive myelination in the mammalian brain. *Science (80-.).* doi:10.1126/science.1252304.

Gielen, P. R., Schulte, B. M., Kers-Rebel, E. D., Verrijp, K., Petersen-Baltussen, H. M. J. M., Ter Laan, M., et al. (2015). Increase in Both CD14-Positive and CD15-Positive Myeloid-Derived Suppressor Cell Subpopulations in the Blood of Patients with Glioma but Predominance of CD15-Positive Myeloid-Derived Suppressor Cells in Glioma Tissue. *J. Neuropathol. Exp. Neurol.* doi:10.1097/NEN.0000000000000183.

Gips, B., van der Eerden, J. P. J. M., and Jensen, O. (2016). A biologically plausible mechanism for neuronal coding organized by the phase of alpha oscillations. *Eur. J. Neurosci.* doi:10.1111/ejn.13318.

Greenfield, L. J. (2013). Molecular mechanisms of antiseizure drug activity at GABAA receptors. *Seizure* 22, 589–600. doi:10.1016/j.seizure.2013.04.015.

Gururaj, A. E., Gibson, L., Panchabhai, S., Bai, M. H., Manyam, G., Lu, Y., et al. (2013). Access to the nucleus and functional association with c-Myc is required for the full oncogenic potential of ΔEGFR/EGFRvIII. *J. Biol. Chem.* doi:10.1074/jbc.M112.399352.

Haegens, S., Nácher, V., Luna, R., Romo, R., and Jensen, O. (2011). α-Oscillations in the monkey sensorimotor network influence discrimination performance by rhythmical inhibition of neuronal spiking. *Proc. Natl. Acad. Sci. U. S. A.* doi:10.1073/pnas.1117190108.

Hahn, A., Bode, J., Krüwel, T., Solecki, G., Heiland, S., Bendszus, M., et al. (2019). Glioblastoma multiforme restructures the topological connectivity of cerebrovascular networks. *Sci. Rep.* 9, 1–17. doi:10.1038/s41598-019-47567-w.

Haider, B., Häusser, M., and Carandini, M. (2013). Inhibition dominates sensory responses in the awake cortex. *Nature* 493, 97–102. doi:10.1038/nature11665.

Hanahan, D., and Coussens, L. M. (2012). Accessories to the Crime: Functions of Cells Recruited to the Tumor Microenvironment. *Cancer Cell* 21, 309–322.

doi:10.1016/j.ccr.2012.02.022.

Hanslmayr, S., Klimesch, W., Sauseng, P., Gruber, W., Doppelmayr, M., Freunberger, R., et al. (2005). Visual discrimination performance is related to decreased alpha amplitude but increased phase locking. *Neurosci. Lett.* doi:10.1016/j.neulet.2004.10.092.

Heinen, K., Bosman, L. W. J., Spijker, S., Van Pelt, J., Smit, A. B., Voorn, P., et al. (2004). Gabaa receptor maturation in relation to eye opening in the rat visual cortex. *Neuroscience*. doi:10.1016/j.neuroscience.2003.11.004.

Hellemans, J., Mortier, G., De Paepe, A., Speleman, F., and Vandesompele, J. (2008). qBase relative quantification framework and software for management and automated analysis of real-time quantitative PCR data. *Genome Biol.* doi:10.1186/gb-2007-8-2-r19.

Hengen, K. B., Torrado Pacheco, A., McGregor, J. N., Van Hooser, S. D., and Turrigiano, G. G. (2016). Neuronal Firing Rate Homeostasis Is Inhibited by Sleep and Promoted by Wake. *Cell*. doi:10.1016/j.cell.2016.01.046.

Hoelzinger, D. B., Demuth, T., and Berens, M. E. (2007). Autocrine factors that sustain glioma invasion and paracrine biology in the brain microenvironment. *J. Natl. Cancer Inst.* 99, 1583–1593. doi:10.1093/jnci/djm187.

Holland, E. C., Celestino, J., Dai, C., Schaefer, L., Sawaya, R. E., and Fuller, G. N. (2000). Combined activation of Ras and Akt in neural progenitors induces glioblastoma formation in mice. *Nat. Genet.* doi:10.1038/75596.

Holland, E. C., Hively, W. P., DePinho, R. A., and Varmus, H. E. (1998). A constitutively active epidermal growth factor receptor cooperates with disruption of G1 cell-cycle arrest pathways to induce glioma-like lesions in mice. *Genes Dev.* doi:10.1101/gad.12.23.3675.

Hong, E. J., McCord, A. E., and Greenberg, M. E. (2008). A Biological Function for the Neuronal Activity-Dependent Component of Bdnf Transcription in the Development of Cortical Inhibition. *Neuron*. doi:10.1016/j.neuron.2008.09.024.

Huberfeld, G., and Vecht, C. J. (2016). Seizures and gliomas - Towards a single therapeutic approach. *Nat. Rev. Neurol.* 12, 204–216. doi:10.1038/nrneurol.2016.26.

Ishiuchi, S., Yoshida, Y., Sugawara, K., Aihara, M., Ohtani, T., Watanabe, T., et al. (2007). Ca2+-permeable AMPA receptors regulate growth of human glioblastoma via Akt activation. *J. Neurosci.* doi:10.1523/JNEUROSCI.2180-07.2007.

Jahn, R., and Scheller, R. H. (2006). SNAREs - Engines for membrane fusion. *Nat. Rev. Mol. Cell Biol.* doi:10.1038/nrm2002.

Jain, K. K. (2018). A Critical Overview of Targeted Therapies for Glioblastoma. *Front. Oncol.* 8, 1–19. doi:10.3389/fonc.2018.00419.

Jiang, Y., Marinescu, V. D., Xie, Y., Jarvius, M., Maturi, N. P., Haglund, C., et al. (2017). Glioblastoma Cell Malignancy and Drug Sensitivity Are Affected by the Cell of Origin. *Cell Rep.* doi:10.1016/j.celrep.2017.01.003.

Johung, T., and Monje, M. (2017). Neuronal activity in the glioma microenvironment. *Curr. Opin. Neurobiol.* 47, 156–161. doi:10.1016/j.conb.2017.10.009.

Jones, C., Perryman, L., and Hargrave, D. (2012). Paediatric and adult malignant glioma: Close relatives or distant cousins? *Nat. Rev. Clin. Oncol.* doi:10.1038/nrclinonc.2012.87.

Jung, E., Alfonso, J., Osswald, M., Monyer, H., Wick, W., and Winkler, F. (2019). Emerging intersections between neuroscience and glioma biology. *Nat. Neurosci.* doi:10.1038/s41593-019-0540-y.

Kalemaki, K., Konstantoudaki, X., Tivodar, S., Sidiropoulou, K., and Karagogeos, D. (2018). Mice with decreased number of interneurons exhibit aberrant spontaneous and oscillatory activity in the cortex. *Front. Neural Circuits*. doi:10.3389/fncir.2018.00096.

Kamiya, A., Hayama, Y., Kato, S., Shimomura, A., Shimomura, T., Irie, K., et al. (2019). Genetic manipulation of autonomic nerve fiber innervation and activity and its effect on breast cancer progression. *Nat. Neurosci.* 22, 1289–1305. doi:10.1038/s41593-019-0430-3.

Kantz, H., and Schreiber, T. (2003). *Nonlinear Time Series Analysis*. 2nd ed. Cambridge University Press doi:10.1017/CBO9780511755798.

Kegelman, T. P., Hu, B., Emdad, L., Das, S. K., Sarkar, D., and Fisher, P. B. (2014). “In vivo modeling of malignant Glioma: The road to effective therapy,” in *Advances in Cancer Research* doi:10.1016/B978-0-12-800249-0.00007-X.

Keke, F., Hongyang, Z., Hui, Q., Jixiao, L., and Jian, C. (2004). A combination of flk1-based DNA vaccine and an immunomodulatory gene (IL-12) in the treatment of murine cancer. *Cancer Biother. Radiopharm.* doi:10.1089/1084978042484795.

Kerlin, A. M., Andermann, M. L., Berezovskii, V. K., and Reid, R. C. (2010). Broadly Tuned Response Properties of Diverse Inhibitory Neuron Subtypes in Mouse Visual Cortex. *Neuron* 67, 858–871. doi:10.1016/j.neuron.2010.08.002.

Kersten, K., Visser, K. E., Miltenburg, M. H., and Jonkers, J. (2017). Genetically engineered mouse models in oncology research and cancer medicine. *EMBO Mol. Med.* doi:10.15252/emmm.201606857.

Kim, J. A., Averbook, B. J., Chambers, K., Rothchild, K., Kjaergaard, J., and Shu, S. (2001). Divergent effects of 4-1BB antibodies on antitumor immunity and on tumor-reactive T-cell generation. *Cancer Res.*

Kim, S. S., Harford, J. B., Pirollo, K. F., and Chang, E. H. (2015). Effective treatment of glioblastoma requires crossing the blood-brain barrier and targeting tumors including cancer stem cells: The promise of nanomedicine. *Biochem. Biophys. Res. Commun.* doi:10.1016/j.bbrc.2015.06.137.

Kimura, S., Yoshino, A., Katayama, Y., Watanabe, T., and Fukushima, T. (2002). Growth control of C6 glioma in vivo by nerve growth factor. *J. Neurooncol.* 59, 199–205. doi:10.1023/A:1019919019497.

Klimesch, W. (2012). Alpha-band oscillations, attention, and controlled access to stored information. *Trends Cogn. Sci.* doi:10.1016/j.tics.2012.10.007.

Klimesch, W., Sauseng, P., and Hanslmayr, S. (2007). EEG alpha oscillations: The inhibition-timing hypothesis. *Brain Res. Rev.* doi:10.1016/j.brainresrev.2006.06.003.

Köhling, R., Senner, V., Paulus, W., and Speckmann, E. J. (2006). Epileptiform activity

preferentially arises outside tumor invasion zone in glioma xenotransplants. *Neurobiol. Dis.* doi:10.1016/j.nbd.2005.10.001.

Kuki, T., Fujihara, K., Miwa, H., Tamamaki, N., Yanagawa, Y., and Mushiake, H. (2015). Contribution of parvalbumin and somatostatin-expressing gabaergic neurons to slow oscillations and the balance in beta-gamma oscillations across cortical layers. *Front. Neural Circuits*. doi:10.3389/fncir.2015.00006.

Kulick, C., Gutherz, S., Kondratyev, A., and Forcelli, P. A. (2014). Ontogenic profile of seizures evoked by the beta-carboline DMCM (methyl-6,7-dimethoxy-4-ethyl-β-carboline-3-carboxylate) in rats. *Eur. J. Pharmacol.* doi:10.1016/j.ejphar.2014.06.012.

Labrakakis, C., Patt, S., Hartmann, J., and Kettenmann, H. (1998). Functional GABA A receptors on human glioma cells . *Eur. J. Neurosci.* doi:10.1046/j.1460-9568.1998.00036.x.

Lane, R., Simon, T., Vintu, M., Solkin, B., Koch, B., Stewart, N., et al. (2019). Cell-derived extracellular vesicles can be used as a biomarker reservoir for glioblastoma tumor subtyping. *Commun. Biol.* doi:10.1038/s42003-019-0560-x.

Langford, D. J., Bailey, A. L., Chanda, M. L., Clarke, S. E., Drummond, T. E., Echols, S., et al. (2010). Coding of facial expressions of pain in the laboratory mouse. *Nat. Methods* 7, 447–449. doi:10.1038/nmeth.1455.

Laub, C. K., Stefanik, J., and Doherty, L. (2018). Approved Treatments for Patients with Recurrent High-grade Gliomas. *Semin. Oncol. Nurs.* 34, 486–493. doi:10.1016/j.soncn.2018.10.005.

Lee, J. H., Lee, J. E., Kahng, J. Y., Kim, S. H., Park, J. S., Yoon, S. J., et al. (2018). Human glioblastoma arises from subventricular zone cells with low-level driver mutations. *Nature*. doi:10.1038/s41586-018-0389-3.

Lenting, K., Verhaak, R., ter Laan, M., Wesseling, P., and Leenders, W. (2017). Glioma: experimental models and reality. *Acta Neuropathol.* doi:10.1007/s00401-017-1671-4.

Li, M., Han, S., and Shi, X. (2016). In situ dendritic cell vaccination for the treatment of glioma and literature review. *Tumor Biol.* doi:10.1007/s13277-015-3958-1.

Lichtor, T., Glick, R. P., Tae Sung Kim, Hand, R., and Cohen, E. P. (1995). Prolonged survival of mice with glioma injected intracerebrally with double cytokine-secreting cells. *J. Neurosurg.* doi:10.3171/jns.1995.83.6.1038.

Lim, L., Mi, D., Llorca, A., and Marín, O. (2018). Development and Functional Diversification of Cortical Interneurons. *Neuron* 100, 294–313. doi:10.1016/j.neuron.2018.10.009.

Lin, K. W., Liao, A., and Qutub, A. A. (2015). Simulation predicts IGFBP2-HIF1α interaction drives glioblastoma growth. *PLoS Comput. Biol.* doi:10.1371/journal.pcbi.1004169.

Liu, Y., Carlsson, R., Ambjorn, M., Hasan, M., Badn, W., Darabi, A., et al. (2013). PD-L1 Expression by Neurons Nearby Tumors Indicates Better Prognosis in Glioblastoma Patients. *J. Neurosci.* doi:10.1523/jneurosci.5812-12.2013.

Llaguno, S. R. A., and Parada, L. F. (2016). Cell of origin of glioma: Biological and clinical implications. *Br. J. Cancer*. doi:10.1038/bjc.2016.354.

Lorincz, M. L., Kékesi, K. A., Juhász, G., Crunelli, V., and Hughes, S. W. (2009). Temporal Framing of Thalamic Relay-Mode Firing by Phasic Inhibition during the Alpha Rhythm. *Neuron*. doi:10.1016/j.neuron.2009.08.012.

Louis, D. N. (2006). Molecular pathology of malignant gliomas. *Annu. Rev. Pathol. Mech. Dis.* doi:10.1146/annurev.pathol.1.110304.100043.

Louis, D. N., Ohgaki, H., Wiestler, O. D., Cavenee, W. K., Burger, P. C., Jouvet, A., et al. (2007). The 2007 WHO classification of tumours of the central nervous system. *Acta Neuropathol.* 114, 97–109. doi:10.1007/s00401-007-0243-4.

Louis, D. N., Perry, A., Reifenberger, G., von Deimling, A., Figarella-Branger, D., Cavenee, W. K., et al. (2016). The 2016 World Health Organization Classification of Tumors of the Central Nervous System: a summary. *Acta Neuropathol.* 131, 803–820. doi:10.1007/s00401-016-1545-1.

Lundstrom, B. N., Boly, M., Duckrow, R., Zaveri, H. P., and Blumenfeld, H. (2019). Slowing less than 1 Hz is decreased near the seizure onset zone. *Sci. Rep.*, 1–10. doi:10.1038/s41598-019-42347-y.

MacKenzie, G., O'Toole, K., K., Moss, J., S., and Maguire, J. (2017). Compromised GABAergic inhibition contributes to tumor-associated epilepsy. *Physiol. Behav.* 176, 139–148. doi:10.1016/j.physbeh.2017.03.040.

Maffei, A., and Turrigiano, G. G. (2008). Multiple modes of network homeostasis in visual cortical layer 2/3. *J. Neurosci.* doi:10.1523/JNEUROSCI.5298-07.2008.

Mahé, C., Bernhard, M., Bobirnac, I., Keser, C., Loetscher, E., Feuerbach, D., et al. (2004). Functional expression of the serotonin 5-HT 7 receptor in human glioblastoma cell lines. *Br. J. Pharmacol.* doi:10.1038/sj.bjp.0705936.

Mainardi, M., Pietrasanta, M., Vannini, E., Rossetto, O., and Caleo, M. (2012). Tetanus neurotoxin-induced epilepsy in mouse visual cortex. *Epilepsia* 53, 132–136. doi:10.1111/j.1528-1167.2012.03510.x.

Mancino, M., Ametller, E., Gascón, P., and Almendro, V. (2011). The neuronal influence on tumor progression. *Biochim. Biophys. Acta - Rev. Cancer*. doi:10.1016/j.bbcan.2011.04.005.

Marco, P., Sola, R. G., Cajal, S. R. Y., and DeFelipe, J. (1997). Loss of inhibitory synapses on the soma and axon initial segment of pyramidal cells in human epileptic peritumoural neocortex: Implications for epilepsy. *Brain Res. Bull.* 44, 47–66. doi:10.1016/S0361-9230(97)00090-7.

Marcus, H. J., Carpenter, K. L. H., Price, S. J., and Hutchinson, P. J. (2010). In vivo assessment of high-grade glioma biochemistry using microdialysis: A study of energy-related molecules, growth factors and cytokines. *J. Neurooncol.* 97, 11–23. doi:10.1007/s11060-009-9990-5.

Mariotti, L., Losi, G., Lia, A., Melone, M., Chiavegato, A., Gómez-Gonzalo, M., et al. (2018). Interneuron-specific signaling evokes distinctive somatostatin-mediated responses in adult cortical astrocytes. *Nat. Commun.* 9. doi:10.1038/s41467-017-02642-6.

Martin-Villalba, A., Okuducu, A. F., and Von Deimling, A. (2008). The evolution of our understanding on glioma. *Brain Pathol.* doi:10.1111/j.1750-3639.2008.00136.x.

Matarredona, E. R., and Pastor, A. M. (2019). Extracellular Vesicle-Mediated Communication between the Glioblastoma and Its Microenvironment. *Cells*. doi:10.3390/cells9010096.

Maurel, P., and Salzer, J. L. (2000). Axonal regulation of Schwann cell proliferation and survival and the initial events of myelination requires PI 3-kinase activity. *J. Neurosci.* doi:10.1523/jneurosci.20-12-04635.2000.

McClelland, S., Sosanya, O., Mitin, T., Degnin, C., Chen, Y., Attia, A., et al. (2018). Application of tumor treating fields for newly diagnosed glioblastoma: understanding of nationwide practice patterns. *J. Neurooncol.* doi:10.1007/s11060-018-2945-y.

McLendon, R., Friedman, A., Bigner, D., Van Meir, E. G., Brat, D. J., Mastrogianakis, G. M., et al. (2008). Comprehensive genomic characterization defines human glioblastoma genes and core pathways. *Nature*. doi:10.1038/nature07385.

Meeker, R. B., and Williams, K. S. (2015). The p75 neurotrophin receptor: At the crossroad of neural repair and death. *Neural Regen. Res.* doi:10.4103/1673-5374.156967.

Miller, K. J., Sorensen, L. B., Ojemann, J. G., and Den Nijs, M. (2009). Power-law scaling in the brain surface electric potential. *PLoS Comput. Biol.* doi:10.1371/journal.pcbi.1000609.

Miyai, M., Tomita, H., Soeda, A., Yano, H., Iwama, T., and Hara, A. (2017). Current trends in mouse models of glioblastoma. *J. Neurooncol.* 135, 423–432. doi:10.1007/s11060-017-2626-2.

Morandi, L., Franceschi, E., de Biase, D., Marucci, G., Tosoni, A., Ermani, M., et al. (2010). Promoter methylation analysis of O6-methylguanine-DNA methyltransferase in glioblastoma: Detection by locked nucleic acid based quantitative PCR using an imprinted gene (SNURF) as a reference. *BMC Cancer*. doi:10.1186/1471-2407-10-48.

Morton, J. J., Bird, G., Refaeli, Y., and Jimeno, A. (2016). Humanized mouse xenograft models: Narrowing the tumor-microenvironment gap. *Cancer Res.* doi:10.1158/0008-5472.CAN-16-1260.

Mrsic-Flogel, T. D., Hofer, S. B., Ohki, K., Reid, R. C., Bonhoeffer, T., and Hübener, M. (2007). Homeostatic Regulation of Eye-Specific Responses in Visual Cortex during Ocular Dominance Plasticity. *Neuron*. doi:10.1016/j.neuron.2007.05.028.

Munteanu, R. M., Eva, L., Dobrovăţ, B. I., Iordache, A. C., Pendefunda, L., Dumitrescu, N., et al. (2017). Longer survival of a patient with glioblastoma resected with 5-aminolevulinic acid (5-ALA)-guided surgery and foreign body reaction to polyglycolic acid (PGA) suture. *Rom. J. Morphol. Embryol.*

Nakagawara, A., Arima-Nakagawara, M., Scavarda, N. J., Azar, C. G., Cantor, A. B., and Brodeur, G. M. (1993). Association between High Levels of Expression of the TRK Gene and Favorable Outcome in Human Neuroblastoma. *N. Engl. J. Med.* doi:10.1056/NEJM199303253281205.

Negro, S., Lessi, F., Duregotti, E., Aretini, P., La Ferla, M., Franceschi, S., et al. (2017). CXCL 12α/ SDF -1 from perisynaptic Schwann cells promotes regeneration of injured motor axon terminals . *EMBO Mol. Med.* doi:10.15252/emmm.201607257.

Nelson, S. B., and Turrigiano, G. G. (1998). Synaptic depression: A key player in the cortical balancing act. *Nat. Neurosci.* doi:10.1038/2775.

Newcomb, E. W., and Zagzag, D. (2009). “The Murine GL261 Glioma Experimental Model to Assess Novel Brain Tumor Treatments,” in *CNS Cancer* doi:10.1007/978-1-60327-553-8_12.

O’Rourke, D. M., Nasrallah, M. P., Desai, A., Melenhorst, J. J., Mansfield, K., Morrissette, J. J. D., et al. (2017). A single dose of peripherally infused EGFRvIII-directed CAR T cells mediates antigen loss and induces adaptive resistance in patients with recurrent glioblastoma. *Sci. Transl. Med.* doi:10.1126/scitranslmed.aaa0984.

Oh, T., Fakurnejad, S., Sayegh, E. T., Clark, A. J., Ivan, M. E., Sun, M. Z., et al. (2014). Immunocompetent murine models for the study of glioblastoma immunotherapy. *J. Transl. Med.* doi:10.1186/1479-5876-12-107.

Okino, S. T., Kong, M., Sarras, H., and Wang, Y. (2016). Evaluation of bias associated with high-multiplex, target-specific pre-amplification. *Biomol. Detect. Quantif.* doi:10.1016/j.bdq.2015.12.001.

Okun, M., Steinmetz, N. A., Cossell, L., Iacaruso, M. F., Ko, H., Barthó, P., et al. (2015). Diverse coupling of neurons to populations in sensory cortex. *Nature* 521, 511–515. doi:10.1038/nature14273.

Oldrini, B., Curiel-García, Á., Marques, C., Matia, V., Uluçkan, Ö., Graña-Castro, O., et al. (2018). Somatic genome editing with the RCAS-TVA-CRISPR-Cas9 system for precision tumor modeling. *Nat. Commun.* doi:10.1038/s41467-018-03731-w.

Osswald, M., Jung, E., Sahm, F., Solecki, G., Venkataramani, V., Blaes, J., et al. (2015). Brain tumour cells interconnect to a functional and resistant network. *Nature*. doi:10.1038/nature16071.

Ostrom, Q. T., Cioffi, G., Gittleman, H., Patil, N., Waite, K., Kruchko, C., et al. (2019). CBTRUS Statistical Report: Primary Brain and Other Central Nervous System Tumors Diagnosed in the United States in 2012-2016. *Neuro. Oncol.* doi:10.1093/neuonc/noz150.

Ostrom, Q. T., Gittleman, H., Xu, J., Kromer, C., Wolinsky, Y., Kruchko, C., et al. (2016). CBTRUS statistical report: Primary brain and other central nervous system tumors diagnosed in the United States in 2009-2013. *Neuro. Oncol.* 17, v1–v75. doi:10.1093/neuonc/nov189.

Otto-Meyer, S., DeFaccio, R., Dussold, C., Ladomersky, E., Zhai, L., Lauing, K. L., et al. (2020). A retrospective survival analysis of Glioblastoma patients treated with selective serotonin reuptake inhibitors. *Brain, Behav. Immun. - Heal.* 2, 100025. doi:10.1016/J.BBIH.2019.100025.

Ozdemir-Kaynak, E., Qutub, A. A., and Yesil-Celiktas, O. (2018). Advances in glioblastoma multiforme treatment: New models for nanoparticle therapy. *Front. Physiol.* 9, 170. doi:10.3389/fphys.2018.00170.

Paez-Gonzalez, P., Asrican, B., Rodriguez, E., and Kuo, C. T. (2014). Identification of distinct ChAT+ neurons and activity-dependent control of postnatal SVZ neurogenesis. *Nat. Neurosci.* doi:10.1038/nn.3734.

Pallud, J., Le Van Quyen, M., Bielle, F., Pellegrino, C., Varlet, P., Labussiere, M., et al. (2014). Cortical GABAergic excitation contributes to epileptic activities around human glioma. *Sci. Transl. Med.* 6, 244ra89-244ra89. doi:10.1126/scitranslmed.3008065.

Park, H., and Poo, M. M. (2013). Neurotrophin regulation of neural circuit development and function. *Nat. Rev. Neurosci.* doi:10.1038/nrn3379.

Park, J. C., Chang, I. B., Ahn, J. H., Kim, J. H., Song, J. H., Moon, S. M., et al. (2018). Nerve growth factor stimulates glioblastoma proliferation through Notch1 receptor signaling. *J. Korean Neurosurg. Soc.* 61, 441–449. doi:10.3340/jkns.2017.0219.

Parsa, A. T., Waldron, J. S., Panner, A., Crane, C. A., Parney, I. F., Barry, J. J., et al. (2007). Loss of tumor suppressor PTEN function increases B7-H1 expression and immunoresistance in glioma. *Nat. Med.* doi:10.1038/nm1517.

Patel, A. P., Tirosh, I., Trombetta, J. J., Shalek, A. K., Gillespie, S. M., Wakimoto, H., et al. (2014). Single-cell RNA-seq highlights intratumoral heterogeneity in primary glioblastoma. *Science (80-.).* doi:10.1126/science.1254257.

Pathania, M., De Jay, N., Maestro, N., Harutyunyan, A. S., Nitarska, J., Pahlavan, P., et al. (2017). H3.3K27M Cooperates with Trp53 Loss and PDGFRA Gain in Mouse Embryonic Neural Progenitor Cells to Induce Invasive High-Grade Gliomas. *Cancer Cell*. doi:10.1016/j.ccell.2017.09.014.

Patt, S., Steenbeck, J., Hochstetter, A., Kraft, R., Huonker, R., Haueisen, J., et al. (2000). Source localization and possible causes of interictal epileptic activity in tumor-associated epilepsy. *Neurobiol. Dis.* doi:10.1006/nbdi.2000.0288.

Pellegrino, G., Tombini, M., Curcio, G., Campana, C., Di Pino, G., Assenza, G., et al. (2017). Slow Activity in Focal Epilepsy during Sleep and Wakefulness. *Clin. EEG Neurosci.* doi:10.1177/1550059416652055.

Perry, A., Ellison, D. W., Reifenberger, G., Kleihues, P., von Deimling, A., Figarella-Branger, D., et al. (2016). The 2016 World Health Organization Classification of Tumors of the Central Nervous System: a summary. *Acta Neuropathol.* 131, 803–820. doi:10.1007/s00401-016-1545-1.

Perry, A., and Wesseling, P. (2016). “Histologic classification of gliomas,” in *Handbook of Clinical Neurology* doi:10.1016/B978-0-12-802997-8.00005-0.

Peterson, D. L., Sheridan, P. J., and Brown, W. E. (1994). Animal models for brain tumors: historical perspectives and future directions. *J. Neurosurg.* doi:10.3171/jns.1994.80.5.0865.

Peterson, E. J., and Voytek, B. (2017). Alpha oscillations control cortical gain by modulating excitatory- inhibitory background activity. *bioRxiv*. doi:10.1101/185074.

Pizzorusso, T., Medini, P., Berardi, N., Chierzi, S., Fawcett, J. W., and Maffei, L. (2002). Reactivation of ocular dominance plasticity in the adult visual cortex. *Science (80-.).* 298, 1248–1251. doi:10.1126/science.1072699.

Plautz, G. E., Touhalisky, J. E., and Shu, S. (1997). Treatment of murine gliomas by adoptive transfer of ex vivo activated tumor-draining lymph node cells. *Cell. Immunol.* doi:10.1006/cimm.1997.1140.

Porciatti, V., Pizzorusso, T., and Maffei, L. (1999). The visual physiology of the wild type mouse determined with pattern VEPs. *Vision Res.* 39, 3071–3081. doi:10.1016/S0042-6989(99)00022-X.

Portela, M., Venkataramani, V., Fahey-Lozano, N., Seco, E., Losada-Perez, M., Winkler, F., et al. (2019). Glioblastoma cells vampirize WNT from neurons and trigger a

JNK/MMP signaling loop that enhances glioblastoma progression and neurodegeneration. *PLoS Biol.* doi:10.1371/journal.pbio.3000545.

Puia, G., Vicini, S., Seeburg, P. H., and Costa, E. (1991). Influence of recombinant γ-aminobutyric acid-(A) receptor subunit composition on the action of allosteric modulators of γ-aminobutyric acid-gated Cl- currents. *Mol. Pharmacol.*

Quail, D. F., and Joyce, J. A. (2017). The Microenvironmental Landscape of Brain Tumors. *Cancer Cell*. doi:10.1016/j.ccell.2017.02.009.

Rabin, S. J., Tornatore, C., Baker-Cairns, B., Spiga, G., and Mocchetti, I. (1998). TrkA receptors delay C6-2B glioma cell growth in rat striatum. *Mol. Brain Res.* doi:10.1016/S0169-328X(98)00020-5.

Radin, D. P., and Patel, P. (2017). BDNF: An oncogene or tumor suppressor? *Anticancer Res.* doi:10.21873/anticanres.11783.

Reardon, D. A., Omuro, A., Brandes, A. A., Rieger, J., Wick, A., Sepulveda, J., et al. (2017). OS10.3 Randomized Phase 3 Study Evaluating the Efficacy and Safety of Nivolumab vs Bevacizumab in Patients With Recurrent Glioblastoma: CheckMate 143. *Neuro. Oncol.* doi:10.1093/neuonc/nox036.071.

Reilly, K. M., and Jacks, T. (2001). Genetically engineered mouse models of astrocytoma: GEMs in the rough? *Semin. Cancer Biol.* doi:10.1006/scbi.2000.0375.

Reitman, Z. J., Winkler, F., and Elia, A. E. H. (2018). New Directions in the Treatment of Glioblastoma. *Semin. Neurol.* 38, 50–61. doi:10.1055/s-0038-1623534.

Restani, L., Cerri, C., Pietrasanta, M., Gianfranceschi, L., Maffei, L., and Caleo, M. (2009). Functional Masking of Deprived Eye Responses by Callosal Input during Ocular Dominance Plasticity. *Neuron* 64, 707–718. doi:10.1016/j.neuron.2009.10.019.

Restani, L., Giribaldi, F., Manich, M., Bercsenyi, K., Menendez, G., Rossetto, O., et al. (2012a). Botulinum Neurotoxins A and E Undergo Retrograde Axonal Transport in Primary Motor Neurons. *PLoS Pathog.* doi:10.1371/journal.ppat.1003087.

Restani, L., Novelli, E., Bottari, D., Leone, P., Barone, I., Galli-Resta, L., et al. (2012b). Botulinum Neurotoxin A Impairs Neurotransmission Following Retrograde Transynaptic Transport. *Traffic* 13, 1083–1089. doi:10.1111/j.1600-0854.2012.01369.x.

Rieu, I., and Powers, S. J. (2009). Real-time quantitative RT-PCR: Design, calculations, and statistics. *Plant Cell*. doi:10.1105/tpc.109.066001.

Righes Marafiga, J., Vendramin Pasquetti, M., and Calcagnotto, M. E. (2020). GABAergic interneurons in epilepsy: More than a simple change in inhibition. *Epilepsy Behav.* doi:10.1016/j.yebeh.2020.106935.

Robert, S. M., and Sontheimer, H. (2014). Glutamate transporters in the biology of malignant gliomas. *Cell. Mol. Life Sci.* doi:10.1007/s00018-013-1521-z.

Robertson, F. L., Marqués-Torrejón, M. A., Morrison, G. M., and Pollard, S. M. (2019). Experimental models and tools to tackle glioblastoma. *DMM Dis. Model. Mech.* doi:10.1242/dmm.040386.

Robinson, C. G., Palomo, J. M., Rahmathulla, G., McGraw, M., Donze, J., Liu, L., et al. (2010). Effect of alternative temozolomide schedules on glioblastoma O 6-

methylguanine-DNA methyltransferase activity and survival. *Br. J. Cancer* 103, 498–504. doi:10.1038/sj.bjc.6605792.

Rohena, L., Neidich, J., Truitt Cho, M., Gonzalez, K. D., Tang, S., Devinsky, O., et al. (2013). Mutation in SNAP25 as a novel genetic cause of epilepsy and intellectual disability . *Rare Dis.* doi:10.4161/rdis.26314.

Rossetto, O., Morbiato, L., Caccin, P., Rigoni, M., and Montecucco, C. (2006). Presynaptic enzymatic neurotoxins. *J. Neurochem.* doi:10.1111/j.1471-4159.2006.03965.x.

Roy, S., Lahiri, D., Maji, T., and Biswas, J. (2015). Recurrent Glioblastoma: Where we stand. *South Asian J. Cancer*. doi:10.4103/2278-330x.175953.

Rzeski, W., Turski, L., and Ikonomidou, C. (2001). Glutamate antagonists limit tumor growth. *PNAS* 98, 6372–6377. doi:10.1016/S0006-2952(02)01218-2.

Samarut, É., Swaminathan, A., Riché, R., Liao, M., Hassan-Abdi, R., Renault, S., et al. (2018). γ-Aminobutyric acid receptor alpha 1 subunit loss of function causes genetic generalized epilepsy by impairing inhibitory network neurodevelopment. *Epilepsia*. doi:10.1111/epi.14576.

Savaskan, N. E., Heckel, A., Hahnen, E., Engelhorn, T., Doerfler, A., Ganslandt, O., et al. (2008). Small interfering RNA-mediated xCT silencing in gliomas inhibits neurodegeneration and alleviates brain edema. *Nat. Med.* doi:10.1038/nm1772.

Schiavo, G., Matteoli, M., and Montecucco, C. (2000). Neurotoxins affecting neuroexocytosis. *Physiol. Rev.* doi:10.1152/physrev.2000.80.2.717.

Schiavo, G., and Montecucco, C. (1995). Tetanus and Botulism Neurotoxins: Isolation and Assay. *Methods Enzymol.* doi:10.1016/0076-6879(95)48041-2.

Scholz, J., Klein, M. C., Behrens, T. E. J., and Johansen-Berg, H. (2009). Training induces changes in white-matter architecture. *Nat. Neurosci.* doi:10.1038/nn.2412.

Schönherr, M., Stefan, H., Hamer, H. M., Rössler, K., Buchfelder, M., and Rampp, S. (2017). The delta between postoperative seizure freedom and persistence: Automatically detected focal slow waves after epilepsy surgery. *NeuroImage Clin.* 13, 256–263. doi:10.1016/j.nicl.2016.12.001.

Schroeder, A., Mueller, O., Stocker, S., Salowsky, R., Leiber, M., Gassmann, M., et al. (2006). The RIN: An RNA integrity number for assigning integrity values to RNA measurements. *BMC Mol. Biol.* doi:10.1186/1471-2199-7-3.

Seano, G., Nia, H. T., Emblem, K. E., Datta, M., Ren, J., Krishnan, S., et al. (2019). Solid stress in brain tumours causes neuronal loss and neurological dysfunction and can be reversed by lithium. *Nat. Biomed. Eng.* 3, 230–245. doi:10.1038/s41551-018-0334-7.

Seligman, A. M., and Shear, M. J. (1939). Experimental Production of Brain Tumors in Mice with Methylcholanthrene. *Cancer Res.* doi:10.1158/ajc.1939.364.

Sessolo, M., Marcon, I., Bovetti, S., Losi, G., Cammarota, M., Ratto, G. M., et al. (2015). Parvalbumin-positive inhibitory interneurons oppose propagation but favor generation of focal epileptiform activity. *J. Neurosci.* doi:10.1523/JNEUROSCI.5117-14.2015.

Sharrack, S., Joannides, A. J., Sage, W., and Price, S. (2018). The impact of visual impairment on Health-Related Quality of Life (HRQoL) scores in brain tumour patients. *Neuro. Oncol.* 20, i6–i6. doi:10.1093/neuonc/nox237.026.

Shinojima, N., Tada, K., Shiraishi, S., Kamiryo, T., Kochi, M., Nakamura, H., et al. (2003). Prognostic Value of Epidermal Growth Factor Receptor in Patients with Glioblastoma Multiforme. *Cancer Res.*

Sidransky, D., Mikkelsen, T., Schwechheimer, K., Rosenblum, M. L., Cavanee, W., and Vogelstein, B. (1992). Clonal expansion of p53 mutant cells is associated with brain tumour progression. *Nature*. doi:10.1038/355846a0.

Soeda, A., Hara, A., Kunisada, T., Yoshimura, S. I., Iwama, T., and Park, D. M. (2015). The evidence of glioblastoma heterogeneity. *Sci. Rep.* doi:10.1038/srep07979.

Sofroniew, M. V, Howe, C. L., and Mobley, W. C. (2001). Nerve Growth Factor Signaling, Neuroprotection, and Neural Repair. *Annu. Rev. Neurosci.* doi:10.1146/annurev.neuro.24.1.1217.

Sontheimer, H. (2008a). A role for glutamate in growth and invasion of primary brain tumors. *J. Neurochem.* 105, 287–295. doi:10.1111/j.1471-4159.2008.05301.x.

Sontheimer, H. (2008b). A role for glutamate in growth and invasion of primary brain tumors. 29, 61–71. doi:10.1111/j.1471-4159.2008.05301.x.A.

Spalletti, C., Alia, C., Lai, S., Panarese, A., Conti, S., Micera, S., et al. (2017). Combining robotic training and inactivation of the healthy hemisphere restores pre-stroke motor patterns in mice. *Elife* 6, 1–31. doi:10.7554/eLife.28662.

Stine, R. A., and Abarbanel, H. D. I. (1997). Analysis of Observed Chaotic Data. *Technometrics*. doi:10.2307/1271140.

Stoecklein, V. M., Stoecklein, S., Galiè, F., Ren, J., Schmutzer, M., Unterrainer, M., et al. (2020). Resting-state fMRI Detects Alterations in Whole Brain Connectivity Related to Tumor Biology in Glioma Patients. *Neuro. Oncol.* doi:10.1093/neuonc/noaa044.

Stummer, W., Pichlmeier, U., Meinel, T., Wiestler, O. D., Zanella, F., and Reulen, H. J. (2006). Fluorescence-guided surgery with 5-aminolevulinic acid for resection of malignant glioma: a randomised controlled multicentre phase III trial. *Lancet Oncol.* doi:10.1016/S1470-2045(06)70665-9.

Stupp, R., Taillibert, S., Kanner, A., Read, W., Steinberg, D. M., Lhermitte, B., et al. (2017). Effect of tumor-treating fields plus maintenance temozolomide vs maintenance temozolomide alone on survival in patients with glioblastoma a randomized clinical trial. *JAMA - J. Am. Med. Assoc.* doi:10.1001/jama.2017.18718.

Sugiyama, S., Di Nardo, A. A., Aizawa, S., Matsuo, I., Volovitch, M., Prochiantz, A., et al. (2008). Experience-Dependent Transfer of Otx2 Homeoprotein into the Visual Cortex Activates Postnatal Plasticity. *Cell* 134, 508–520. doi:10.1016/j.cell.2008.05.054.

Synowitz, M., Ahmann, P., Matyash, M., Kuhn, S. A., Hofmann, B., Zimmer, C., et al. (2001). GABAA-receptor expression in glioma cells is triggered by contact with neuronal cells. *Eur. J. Neurosci.* doi:10.1046/j.0953-816X.2001.01764.x.

Szatmári, T., Lumniczky, K., Désaknai, S., Trajcevski, S., Hídvégi, E. J., Hamada, H., et al. (2006). Detailed characterization of the mouse glioma 261 tumor model for experimental glioblastoma therapy. *Cancer Sci.* 97, 546–553. doi:10.1111/j.1349-7006.2006.00208.x.

Takeuchi, H., Sekiguchi, A., Taki, Y., Yokoyama, S., Yomogida, Y., Komuro, N., et al. (2010). Training of working memory impacts structural connectivity. *J. Neurosci.*

doi:10.1523/JNEUROSCI.4611-09.2010.

Tanahira, C., Higo, S., Watanabe, K., Tomioka, R., Ebihara, S., Kaneko, T., et al. (2009). Parvalbumin neurons in the forebrain as revealed by parvalbumin-Cre transgenic mice. *Neurosci. Res.* 63, 213–223. doi:10.1016/j.neures.2008.12.007.

Taphoorn, M. J. B., Sizoo, E. M., and Bottomley, A. (2010). Review on Quality of Life Issues in Patients with Primary Brain Tumors. *Oncologist*. doi:10.1634/theoncologist.2009-0291.

Terunuma, M., Vargas, K. J., Wilkins, M. E., Ramírez, O. A., Jaureguiberry-Bravo, M., Pangalos, M. N., et al. (2010). Prolonged activation of NMDA receptors promotes dephosphorylation and alters postendocytic sorting of GABAB receptors. *Proc. Natl. Acad. Sci. U. S. A.* doi:10.1073/pnas.1000853107.

Tewari, B. P., Chaunsali, L., Campbell, S. L., Patel, D. C., Goode, A. E., and Sontheimer, H. (2018). Perineuronal nets decrease membrane capacitance of peritumoral fast spiking interneurons in a model of epilepsy. *Nat. Commun.* 9. doi:10.1038/s41467-018-07113-0.

Tononi, G., and Cirelli, C. (2012). Time to be SHY? Some comments on sleep and synaptic homeostasis. *Neural Plast.* doi:10.1155/2012/415250.

Trent, J., Meltzer, P., Rosenblum, M., Harsh, G., Kinzler, K., Mashal, R., et al. (1986). Evidence for rearrangement, amplification, and expression of c-myc in a human glioblastoma. *Proc. Natl. Acad. Sci. U. S. A.* doi:10.1073/pnas.83.2.470.

Tsiatas, M., Mountzios, G., and Curigliano, G. (2016). Future perspectives in cancer immunotherapy. *Ann. Transl. Med.* doi:10.21037/atm.2016.07.14.

Turrigiano, G. (2012). Homeostatic synaptic plasticity: Local and global mechanisms for stabilizing neuronal function. *Cold Spring Harb. Perspect. Biol.* doi:10.1101/cshperspect.a005736.

Turton, K., Chaddock, J. A., and Acharya, K. R. (2002). Botulinum and tetanus neurotoxins: Structure, function and therapeutic utility. *Trends Biochem. Sci.* doi:10.1016/S0968-0004(02)02177-1.

Vallone, F., Lai, S., Spalletti, C., Panarese, A., Alia, C., Micera, S., et al. (2016). Post-stroke longitudinal alterations of inter-hemispheric correlation and hemispheric dominance in mouse pre-motor cortex. *PLoS One* 11, 1–26. doi:10.1371/journal.pone.0146858.

van Breemen, M. S., Wilms, E. B., and Vecht, C. J. (2007). Epilepsy in patients with brain tumours: epidemiology, mechanisms, and management. *Lancet Neurol.* doi:10.1016/S1474-4422(07)70103-5.

van Kessel, E., Baumfalk, A. E., van Zandvoort, M. J. E., Robe, P. A., and Snijders, T. J. (2017). Tumor-related neurocognitive dysfunction in patients with diffuse glioma: a systematic review of neurocognitive functioning prior to anti-tumor treatment. *J. Neurooncol.* 134, 9–18. doi:10.1007/s11060-017-2503-z.

Vanhoutte, N., and Hermans, E. (2008). Glutamate-induced glioma cell proliferation is prevented by functional expression of the glutamate transporter GLT-1. *FEBS Lett.* doi:10.1016/j.febslet.2008.04.053.

Vannini, E., Maltese, F., Olimpico, F., Fabbri, A., Costa, M., Caleo, M., et al. (2017).

Progression of motor deficits in glioma-bearing mice: impact of CNF1 therapy at symptomatic stages. *Oncotarget* 8, 23539–23550. doi:10.18632/oncotarget.15328.

Vannini, E., Olimpico, F., Middei, S., Ammassari-Teule, M., De Graaf, E. L., McDonnell, L., et al. (2016a). Electrophysiology of glioma: a Rho GTPase-activating protein reduces tumor growth and spares neuron structure and function. *Neuro. Oncol.* 18, 1634–1643. doi:10.1093/neuonc/now114.

Vannini, E., Restani, L., Pietrasanta, M., Panarese, A., Mazzoni, A., Rossetto, O., et al. (2016b). Altered sensory processing and dendritic remodeling in hyperexcitable visual cortical networks. *Brain Struct. Funct.* 221, 2919–2936. doi:10.1007/s00429-015-1080-1.

Vega, J. A., García-Suárez, O., Hannestad, J., Pérez-Pérez, M., and Germanà, A. (2003). Neurotrophins and the immune system. *J. Anat.* doi:10.1046/j.1469-7580.2003.00203.x.

Venkataramani, V., Tanev, D. I., Strahle, C., Studier-Fischer, A., Fankhauser, L., Kessler, T., et al. (2019). Glutamatergic synaptic input to glioma cells drives brain tumour progression. *Nature* 573, 532–538. doi:10.1038/s41586-019-1564-x.

Venkatesh, H., and Monje, M. (2017). Neuronal Activity in Ontogeny and Oncology. *Trends in Cancer*. doi:10.1016/j.trecan.2016.12.008.

Venkatesh, H. S., Johung, T. B., Caretti, V., Noll, A., Tang, Y., Nagaraja, S., et al. (2015). Neuronal activity promotes glioma growth through neuroligin-3 secretion. *Cell* 161, 803–816. doi:10.1016/j.cell.2015.04.012.

Venkatesh, H. S., Morishita, W., Geraghty, A. C., Silverbush, D., Gillespie, S. M., Arzt, M., et al. (2019). Electrical and synaptic integration of glioma into neural circuits. *Nature* 573, 539–545. doi:10.1038/s41586-019-1563-y.

Venkatesh, H. S., Tam, L. T., Woo, P. J., Lennon, J., Nagaraja, S., Gillespie, S. M., et al. (2017). Targeting neuronal activity-regulated neuroligin-3 dependency in high-grade glioma. *Nature* 549, 533–537. doi:10.1038/nature24014.

Verhaak, R. G. W., Hoadley, K. A., Purdom, E., Wang, V., Qi, Y., Wilkerson, M. D., et al. (2010). Integrated Genomic Analysis Identifies Clinically Relevant Subtypes of Glioblastoma Characterized by Abnormalities in PDGFRA, IDH1, EGFR, and NF1. *Cancer Cell*. doi:10.1016/j.ccr.2009.12.020.

Wadhwa, S., Nag, T. C., Jindal, A., Kushwaha, R., Mahapatra, A. K., and Sarkar, C. (2003). Expression of the neurotrophin receptors Trk A and Trk B in adult human astrocytoma and glioblastoma. *J. Biosci.* doi:10.1007/BF02706217 LK - http://utah-primoprod.hosted.exlibrisgroup.com/openurl/UTAH/UTAH-S?sid=EMBASE&issn=02505991&id=doi:10.1007%2FBF02706217&atitle=Expression+of+the+neurotrophin+receptors+Trk+A+and+Trk+B+in+adult+human+astrocytoma+and+glioblastoma&stitle=J.+Biosci.&title=Journal+of+Biosciences&volume=28&issue=2&spage=181&epage=188&aulast=Wadhwa&aufirst=Shashi&auinit=S.&aufull=Wadhwa+S.&coden=JOBSD&isbn=&pages=181-188&date=2003&auinit1=S&auinitm=.

Wainwright, D. A., Horbinski, C. M., Hashizume, R., and James, C. D. (2017). Therapeutic Hypothesis Testing With Rodent Brain Tumor Models. *Neurotherapeutics*. doi:10.1007/s13311-017-0523-1.

Walsh, P., Kane, N., and Butler, S. (2005). The clinical role of evoked potentials. *Neurol.*

Pract. doi:10.1136/jnnp.2005.068130.

Wang, H., Peca, J., Matsuzaki, M., Matsuzaki, K., Noguchi, J., Qiu, L., et al. (2007). High-speed mapping of synaptic connectivity using photostimulation in Channelrhodopsin-2 transgenic mice. *Proc. Natl. Acad. Sci. U. S. A.* 104, 8143–8148. doi:10.1073/pnas.0700384104.

Wang, W., Dong, B., Ittmann, M., and Yang, F. (2016). A Versatile Gene Delivery System for Efficient and Tumor Specific Gene Manipulation in vivo. *Discoveries* 4, e58. doi:10.15190/d.2016.5.

Weil, S., Osswald, M., Solecki, G., Grosch, J., Jung, E., Lemke, D., et al. (2017). Tumor microtubes convey resistance to surgical lesions and chemotherapy in gliomas. *Neuro. Oncol.* doi:10.1093/neuonc/nox070.

Weller, M., Wick, W., Aldape, K., Brada, M., Berger, M., Pfister, S. M., et al. (2015). Glioma. *Nat. Rev. Dis. Prim.* 1. doi:10.1038/nrdp.2015.17.

Wen, P. Y., and Kesari, S. (2008). Malignant gliomas in adults. *N. Engl. J. Med.* doi:10.1056/NEJMra0708126.

Wesseling, P., and Capper, D. (2018). WHO 2016 Classification of gliomas. *Neuropathol. Appl. Neurobiol.* 44, 139–150. doi:10.1111/nan.12432.

Wesseling, P., Kros, J. M., and Jeuken, J. W. M. (2011). The pathological diagnosis of diffuse gliomas: Towards a smart synthesis of microscopic and molecular information in a multidisciplinary context. *Diagnostic Histopathol.* doi:10.1016/j.mpdhp.2011.08.005.

Wick, W., Osswald, M., Wick, A., and Winkler, F. (2018). Treatment of glioblastoma in adults. *Ther. Adv. Neurol. Disord.* 11, 1–13. doi:10.1177/1756286418790452.

Wick, W., Weller, M., Van Den Bent, M., Sanson, M., Weiler, M., Von Deimling, A., et al. (2014). MGMT testing - The challenges for biomarker-based glioma treatment. *Nat. Rev. Neurol.* doi:10.1038/nrneurol.2014.100.

Wong, R. O. L., Chernjavsky, A., Smith, S. J., and Shatz, C. J. (1995). Early functional neural networks in the developing retina. *Nature*. doi:10.1038/374716a0.

Wood, M. D., Halfpenny, A. M., and Moore, S. R. (2019). Applications of molecular neuro-oncology - A review of diffuse glioma integrated diagnosis and emerging molecular entities. *Diagn. Pathol.* 14, 1–16. doi:10.1186/s13000-019-0802-8.

Wu, A., Wiesner, S., Xiao, J., Ericson, K., Chen, W., Hall, W. A., et al. (2007). Expression of MHC I and NK ligands on human CD133+ glioma cells: possible targets of immunotherapy. *J. Neurooncol.* doi:10.1007/s11060-006-9265-3.

Xiong, J., Zhou, L., Lim, Y., Yang, M., Zhu, Y. H., Li, Z. W., et al. (2013). Mature BDNF promotes the growth of glioma cells in vitro. *Oncol. Rep.* doi:10.3892/or.2013.2746.

Yan, H., Parsons, D. W., Jin, G., McLendon, R., Rasheed, B. A., Yuan, W., et al. (2009). IDH1 and IDH2 mutations in gliomas. *N. Engl. J. Med.* doi:10.1056/NEJMoa0808710.

Ye, Z. C., Rothstein, J. D., and Sontheimer, H. (1999). Compromised glutamate transport in human glioma cells: Reduction- mislocalization of sodium-dependent glutamate transporters and enhanced activity of cystine-glutamate exchange. *J. Neurosci.* doi:10.1523/jneurosci.19-24-10767.1999.

You, G., Sha, Z., and Jiang, T. (2012a). The pathogenesis of tumor-related epilepsy and its implications for clinical treatment. *Seizure*. doi:10.1016/j.seizure.2011.12.016.

You, Y., Klistorner, A., Thie, J., Gupta, V., and Graham, S. (2012b). Axonal loss in a rat model of optic neuritis is closely correlated with visual evoked potential amplitudes using electroencephalogram-based scaling. *Investig. Ophthalmol. Vis. Sci.* doi:10.1167/iovs.12-9843.

Young, S. Z., and Bordey, A. (2009). GABA's control of stem and cancer cell proliferation in adult neural and peripheral niches. *Physiology* 24, 171–185. doi:10.1152/physiol.00002.2009.

Yu, J., Gutnisky, D. A., Hires, S. A., and Svoboda, K. (2016). Layer 4 fast-spiking interneurons filter thalamocortical signals during active somatosensation. *Nat. Neurosci.* 19, 1647–1657. doi:10.1038/nn.4412.

Yu, K., Lin, C. C. J., Hatcher, A., Lozzi, B., Kong, K., Huang-Hobbs, E., et al. (2020). PIK3CA variants selectively initiate brain hyperactivity during gliomagenesis. *Nature* 578, 166–171. doi:10.1038/s41586-020-1952-2.

Zagzag, D., Amirnovin, R., Greco, M. A., Yee, H., Holash, J., Wiegand, S. J., et al. (2000). Vascular apoptosis and involution in gliomas precede neovascularization: A novel concept for glioma growth and angiogenesis. *Lab. Investig.* doi:10.1038/labinvest.3780088.

Zagzag, D., Salnikow, K., Chiriboga, L., Yee, H., Lan, L., Ali, M. A., et al. (2005). Downregulation of major histocompatibility complex antigens in invading glioma cells: Stealth invasion of the brain. *Lab. Investig.* doi:10.1038/labinvest.3700233.

Zeng, W., Tang, Z., Li, Y., Yin, G., Liu, Z., Gao, J., et al. (2020). Patient-derived xenografts of different grade gliomas retain the heterogeneous histological and genetic features of human gliomas. *Cancer Cell Int.* doi:10.1186/s12935-019-1086-5.